NASA/CR—2009-215269

Coupled Thermo-Electro-Magneto-Elastic Response of Smart Stiffened Panels

Brett A. Bednarcyk
Ohio Aerospace Institute, Brook Park, Ohio

Phillip W. Yarrington
Collier Research Corporation, Hampton, Virginia

July 2009

NASA STI Program . . . in Profile

Since its founding, NASA has been dedicated to the advancement of aeronautics and space science. The NASA Scientific and Technical Information (STI) program plays a key part in helping NASA maintain this important role.

The NASA STI Program operates under the auspices of the Agency Chief Information Officer. It collects, organizes, provides for archiving, and disseminates NASA's STI. The NASA STI program provides access to the NASA Aeronautics and Space Database and its public interface, the NASA Technical Reports Server, thus providing one of the largest collections of aeronautical and space science STI in the world. Results are published in both non-NASA channels and by NASA in the NASA STI Report Series, which includes the following report types:

- TECHNICAL PUBLICATION. Reports of completed research or a major significant phase of research that present the results of NASA programs and include extensive data or theoretical analysis. Includes compilations of significant scientific and technical data and information deemed to be of continuing reference value. NASA counterpart of peer-reviewed formal professional papers but has less stringent limitations on manuscript length and extent of graphic presentations.

- TECHNICAL MEMORANDUM. Scientific and technical findings that are preliminary or of specialized interest, e.g., quick release reports, working papers, and bibliographies that contain minimal annotation. Does not contain extensive analysis.

- CONTRACTOR REPORT. Scientific and technical findings by NASA-sponsored contractors and grantees.

- CONFERENCE PUBLICATION. Collected papers from scientific and technical conferences, symposia, seminars, or other meetings sponsored or cosponsored by NASA.

- SPECIAL PUBLICATION. Scientific, technical, or historical information from NASA programs, projects, and missions, often concerned with subjects having substantial public interest.

- TECHNICAL TRANSLATION. English-language translations of foreign scientific and technical material pertinent to NASA's mission.

Specialized services also include creating custom thesauri, building customized databases, organizing and publishing research results.

For more information about the NASA STI program, see the following:

- Access the NASA STI program home page at *http://www.sti.nasa.gov*

- E-mail your question via the Internet to *help@sti.nasa.gov*

- Fax your question to the NASA STI Help Desk at 443–757–5803

- Telephone the NASA STI Help Desk at 443–757–5802

- Write to:
  NASA Center for AeroSpace Information (CASI)
  7115 Standard Drive
  Hanover, MD 21076–1320

NASA/CR—2009-215269

Coupled Thermo-Electro-Magneto-Elastic Response of Smart Stiffened Panels

Brett A. Bednarcyk
Ohio Aerospace Institute, Brook Park, Ohio

Phillip W. Yarrington
Collier Research Corporation, Hampton, Virginia

Prepared under Cooperative Agreement NCC3–878

National Aeronautics and
Space Administration

Glenn Research Center
Cleveland, Ohio 44135

July 2009

Level of Review: This material has been technically reviewed by expert reviewer(s).

Available from

NASA Center for Aerospace Information
7115 Standard Drive
Hanover, MD 21076–1320

National Technical Information Service
5285 Port Royal Road
Springfield, VA 22161

Available electronically at http://gltrs.grc.nasa.gov

Coupled Thermo-Electro-Magneto-Elastic Response of Smart Stiffened Panels

Brett A. Bednarcyk
Ohio Aerospace Institute
Brook Park, Ohio 44142

Phillip W. Yarrington
Collier Research Corporation
Hampton, Virginia 23666

Abstract

This report documents the procedures developed for incorporating smart laminate and panel analysis capabilities within the HyperSizer aerospace structural sizing software package. HyperSizer analyzes stiffened panels composed of arbitrary composite laminates through stiffener homogenization, or "smearing", techniques. The result is an effective constitutive equation for the stiffened panel that is suitable for use in a full vehicle-scale finite element analysis via MSC/NASTRAN. The existing thermo-elastic capabilities of HyperSizer have herein been extended to include coupled thermo-electro-magneto-elastic analysis capabilities. This represents a significant step toward realization of design tools capable of guiding the development of the next generation of smart aerospace structures. Verification results are presented that compare the developed smart HyperSizer capability with an ABAQUS piezoelectric finite element solution for a facesheet-flange combination. These results show good agreement between HyperSizer and ABAQUS, but highlight a limitation of the HyperSizer formulation in that constant electric field components are assumed.

1. Introduction

Adaptive structures show a great deal of promise for future aerospace applications. The envisioned structure's adaptive capabilities will rely on so-called "smart" (or "intelligent") materials, which have properties that enable them to sense various stimuli and react in some way. Incorporating these intelligent materials has the potential to remove fundamental design constraints and transform aerospace structures into life-like responsive systems, enabling optimum performance, reliability, and weight throughout a changing mission profile. The work presented herein focuses on the structural application of one type of smart material: piezo-electro-magnetic materials (i.e., piezoelectric and piezomagnetic ceramics). Piezo-electro-magnetic materials are those that exhibit coupling among their electric, magnetic, mechanical, and thermal responses. That is, for example, in response to an applied voltage or current, a piezoelectric material (such as lead zirconium titanate, or PZT) will respond mechanically with a change in strain or stress. Conversely, if piezoelectric materials are loaded mechanically or thermally, a change in their electric field or flux results. Thus, piezoelectric materials can serve as both actuators and sensors and have the potential to perform tasks passively through utilization of an induced field/flux to cause a desired mechanical response. Piezomagnetic materials (such as $CoFe_2O_4$) exhibit similar coupling between their magnetic and mechanical behaviors, and by forming a composite of piezoelectric and piezomagnetic materials, a fully coupled piezo-electro-magnetic material can be produced. Piezo-electro-magnetic materials are characterized by their fast response times to applied (or sensed) stimuli (on the order of 10^{-2} to 10^{1} milliseconds) and thus have found significant application as vibration dampers. Reviews of piezo-electro-magnetic concepts and materials are available in references 1 to 4.

In order to realize the potential embodied by smart materials and structures, advances in modeling and simulation technologies are needed. The standard tools for structural design are finite element analysis (FEA) models (e.g., ANSYS, NASTRAN, ABAQUS). However, FEA models are ill-suited

(i.e., inefficient, subject to operator error) for rapid design and sizing (i.e., trade studies) for structural components. Further, the lack of well-developed and robust capabilities related to intelligent materials underscores the shortcomings of the FEA approach when it comes to adaptive structures. There is thus a need for physics-based design, analysis, and sizing tools are needed that capture the essential characteristics of piezo-electro-magnetic materials and enable the analysis of structures composed of these materials.

Major investments have been made by NASA over the last decade that laid the groundwork for such design tools. The work described herein has resulted from the research project entitled "Multi-Scale Sizing of Lightweight Multifunctional Spacecraft Structural Components." This project, funded by NASA Headquarters, has brought together NASA Glenn Research Center's Micromechanical Analysis Code with Generalized Method of Cells (MAC/GMC) (refs. 5 and 6), which simulates the nonlinear behavior of smart and composite materials, and HyperSizer (ref. 7), a commercial structural sizing software package originating from NASA Langley technology. Both MAC/GMC and HyperSizer have been enhanced to simulate piezo-electro-magnetic materials and seamlessly linked such that MAC/GMC provides the ply-level behavior of a traditional or smart composite (or monolithic) within a stiffened structure modeled by HyperSizer. In addition, HyperSizer has been enhanced to enable consideration of time-dependent loading, allowing simulation of an entire mission profile. As such, the software can now consider many points from a structure's operating envelope, rather than simply sizing based on a single load level. HyperSizer also links with FEA to enable automatic application of higher-scale structural loads on the structural components that are optimized by the software. Thus the integrated HyperSizer—MAC/GMC product now represents a unique multi-scale tool for the analysis of advance lightweight aerospace structures. Through its linkage with FEA, the software can consider a truly integrated vehicle structural design rather than an isolated design of each component.

This report describes the methods and procedures that have been developed to enable the analysis of piezo-electro-magnetic materials within HyperSizer. Starting with the analysis of a piezo-electro-magnetic laminate, new laminate level matrices that account for the electric, magnetic, thermo-electric and thermo-magnetic effects are developed. These then can be treated in a way analogous to the HyperSizer treatment of the laminate thermal matrix, enabling use of homogenization, or "smearing" techniques to develop stiffened panel level electric, magnetic, thermo-electric, and thermo-magnetic terms. The developed methods are based on a classical lamination theory treatment of the laminates comprising a given stiffened panel, and the homogenization of the stiffened panel so it can be represented with classical lamination theory terms. It is this simplicity that provides the methods with the level of efficiency needed to consider many design cases rapidly while still capturing the dominant first-order effects. A good body of work exists for the analysis of piezoelectric laminates, using both analytical (refs. 8 to 17) and finite element (refs. 18 to 22) approaches. The piezomagnetic laminates have also received some attention (refs. 23 to 25). The work most closely related to the methods developed herein involve the extension of classical lamination theory to include piezoelectric plies by Lee (ref. 8), Crawley and Lazarus (ref. 9) and Tauchert (ref. 10), and to include piezomagnetic and inelastic behavior by Bednarcyk (ref. 26).

2. Reference Plane Shifting Procedure for a Thermo-Electro-Magneto-Elastic Laminate

Because a stiffened panel is, in general, composed of a number of laminates, each of which has properties that are typically calculated with respect to its own midplane, a first step in calculating properties of the panel as a whole involves shifting the reference plane of a given laminate. As will be shown, if the reference plane of each laminate comprising a stiffened panel can be shifted to a common reference plane, the homogenization of the laminate properties to form the properties of the stiffened panel properties becomes straightforward.

Consider and arbitrary number of composite laminates, each of which has its constitutive behavior defined with respect to its midplane via the standard thermo-elastic lamination theory equation (refs. 27 and 28),

$$\begin{bmatrix} \mathbf{N} \\ \mathbf{M} \end{bmatrix} = \begin{bmatrix} \mathbf{A}^0 & \mathbf{B}^0 \\ \mathbf{B}^0 & \mathbf{D}^0 \end{bmatrix} \begin{bmatrix} \boldsymbol{\varepsilon}^0 \\ \boldsymbol{\kappa}^0 \end{bmatrix} - \begin{bmatrix} \mathbf{N}_0^T \\ \mathbf{M}_0^T \end{bmatrix} \tag{1}$$

In this equation, **N** and **M** are the force and moment resultant vectors, which are related to the midplane strain and curvature vectors, $\boldsymbol{\varepsilon}^0$ and $\boldsymbol{\kappa}^0$, by the laminate extensional, coupling, and bending stiffness matrices (measured with respect to the midplane), $\mathbf{A}^0$, $\mathbf{B}^0$, and $\mathbf{D}^0$, and the thermal force and moment resultant vectors (measured with respect to the midplane), $\mathbf{N}_0^T$ and $\mathbf{M}_0^T$. The laminate midplane stiffness matrices and thermal resultants are given by,

$$\mathbf{A}^0 = \sum_k \bar{\mathbf{Q}}_k \left[z_{k-1}^0 - z_k^0 \right] \qquad \mathbf{B}^0 = -\frac{1}{2} \sum_k \bar{\mathbf{Q}}_k \left[\left(z_{k-1}^0 \right)^2 - \left(z_k^0 \right)^2 \right] \qquad \mathbf{D}^0 = \frac{1}{3} \sum_k \bar{\mathbf{Q}}_k \left[\left(z_{k-1}^0 \right)^3 - \left(z_k^0 \right)^3 \right] \tag{2}$$

$$\begin{aligned} \mathbf{N}_0^T &= \sum_k \bar{\mathbf{Q}}_k \boldsymbol{\alpha}_k \left[z_{k-1}^0 - z_k^0 \right] \Delta T_0 + \frac{1}{2} \sum_k \bar{\mathbf{Q}}_k \boldsymbol{\alpha}_k \left[\left(z_{k-1}^0 \right)^2 - \left(z_k^0 \right)^2 \right] \Delta G \\ \mathbf{M}_0^T &= -\frac{1}{2} \sum_k \bar{\mathbf{Q}}_k \boldsymbol{\alpha}_k \left[\left(z_{k-1}^0 \right)^2 - \left(z_k^0 \right)^2 \right] \Delta T_0 - \frac{1}{3} \sum_k \bar{\mathbf{Q}}_k \boldsymbol{\alpha}_k \left[\left(z_{k-1}^0 \right)^3 - \left(z_k^0 \right)^3 \right] \Delta G \end{aligned} \tag{3}$$

where $\bar{\mathbf{Q}}_k$ is the reduced stiffness matrix of ply k, $\boldsymbol{\alpha}_k$ is the coefficient of thermal expansion vector of ply k, z_k^0 is the z-coordinate position of the top of ply k measured with respect to the laminate midplane, ΔT_0 is the temperature change from reference temperature at the laminate midplane, and ΔG is the linear laminate through-thickness temperature gradient, i.e., $T(z) - T_{\text{ref}} = \Delta T_0 + z\,\Delta G$, with $T(z)$ being the temperature at any z-coordinate location and T_{ref} being the reference temperature.

We now consider a shift of the reference plane from the laminate midplane to an arbitrary z-coordinate position and seek to determine the effect on the quantities given in eqs. (2) and (3). This arbitrary reference plane shift is depicted in figure 1. Considering point A, in the original, laminate midplane coordinate system, this point is located at $z_A^0 = -h/2$, whereas, in the new shifted coordinate system, this point is located at $z_A^{\text{new}} = -h/2 - \Delta z$. Thus, for an arbitrary shift of reference plane we have

$$z^{\text{new}} = z^0 - \Delta z \tag{4}$$

where Δz measures the distance in the positive z-direction from original laminate reference plane to the new laminate reference plane. The temperature change from reference temperature at the new reference plane is given based on the linear through-thickness temperature gradient as,

$$\Delta T_{\text{new}} = \Delta T_0 + \Delta G\ \Delta z \tag{5}$$

The laminate stiffness matrices, measured with respect to the new shifted reference plane are given by,

$$\mathbf{A}^{\text{new}} = \sum_k \bar{\mathbf{Q}}_k \left[z_{k-1}^{\text{new}} - z_k^{\text{new}} \right] \tag{6}$$

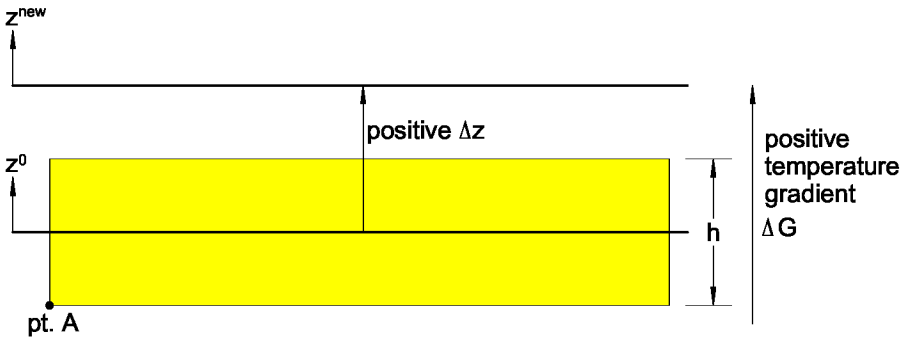

Figure 1.—Arbitrary reference plane shift from the laminate midplane.

$$\mathbf{B}^{\text{new}} = -\frac{1}{2}\sum_k \bar{\mathbf{Q}}_k \left[\left(z_{k-1}^{\text{new}}\right)^2 - \left(z_k^{\text{new}}\right)^2 \right] \tag{7}$$

$$\mathbf{D}^{\text{new}} = \frac{1}{3}\sum_k \bar{\mathbf{Q}}_k \left[\left(z_{k-1}^{\text{new}}\right)^3 - \left(z_k^{\text{new}}\right)^3 \right] \tag{8}$$

Substituting for z^{new} in eqs. (6) to (8) using eq. (4) we arrive at,

$$\mathbf{A}^{\text{new}} = \sum_k \bar{\mathbf{Q}}_k \left[z_{k-1}^{\text{new}} - z_k^{\text{new}} \right] = \sum_k \bar{\mathbf{Q}}_k \left[\left(z_{k-1}^0 - \Delta z\right) - \left(z_k^0 - \Delta z\right) \right] = \sum_k \bar{\mathbf{Q}}_k \left[z_{k-1}^0 - z_k^0 \right] = \mathbf{A}^0$$

$$\mathbf{A}^{\text{new}} = \mathbf{A}^0 \tag{9}$$

$$\begin{aligned}
\mathbf{B}^{\text{new}} &= -\frac{1}{2}\sum_k \bar{\mathbf{Q}}_k \left[\left(z_{k-1}^{\text{new}}\right)^2 - \left(z_k^{\text{new}}\right)^2 \right] = -\frac{1}{2}\sum_k \bar{\mathbf{Q}}_k \left[\left(z_{k-1}^0 - \Delta z\right)^2 - \left(z_k^0 - \Delta z\right)^2 \right] \\
&= -\frac{1}{2}\sum_k \bar{\mathbf{Q}}_k \left[\left(z_{k-1}^0\right)^2 - 2\, z_{k-1}^0\, \Delta z + \Delta z^2 - \left(z_k^0\right)^2 + 2\, z_k^0\, \Delta z - \Delta z^2 \right] \\
&= -\frac{1}{2}\sum_k \bar{\mathbf{Q}}_k \left[\left(z_{k-1}^0\right)^2 - \left(z_k^0\right)^2 - 2\Delta z \left(z_{k-1}^0 - z_k^0\right) \right] \\
&= -\frac{1}{2}\sum_k \bar{\mathbf{Q}}_k \left[\left(z_{k-1}^0\right)^2 - \left(z_k^0\right)^2 \right] - \frac{1}{2}\sum_k \bar{\mathbf{Q}}_k \left[-2\Delta z \left(z_{k-1}^0 - z_k^0\right) \right] \\
&= -\frac{1}{2}\sum_k \bar{\mathbf{Q}}_k \left[\left(z_{k-1}^0\right)^2 - \left(z_k^0\right)^2 \right] + \Delta z \sum_k \bar{\mathbf{Q}}_k \left[z_{k-1}^0 - z_k^0 \right] \\
&= \mathbf{B}^0 + \Delta z\, \mathbf{A}^0
\end{aligned}$$

$$\mathbf{B}^{\text{new}} = \mathbf{B}^0 + \Delta z\, \mathbf{A}^0 \tag{10}$$

$$\begin{aligned}
\mathbf{D}^{\text{new}} &= \frac{1}{3}\sum_k \bar{\mathbf{Q}}_k \left[\left(z_{k-1}^{\text{new}}\right)^3 - \left(z_k^{\text{new}}\right)^3 \Big|_{\rfloor} \right] = \frac{1}{3}\sum_k \bar{\mathbf{Q}}_k \left[\left(z_{k-1}^0 - \Delta z\right)^3 - \left(z_k^0 - \Delta z\right)^3 \Big|_{\rfloor} \right] \\
&= \frac{1}{3}\sum_k \bar{\mathbf{Q}}_k \left\{ \left[\left(z_{k-1}^0\right)^3 - 3\Delta z \left(z_{k-1}^0\right)^2 + 3\Delta z^2 z_{k-1}^0 - \Delta z^3 \Big|_{\rfloor} \right] - \left[\left(z_k^0\right)^3 - 3\Delta z \left(z_k^0\right)^2 + 3\Delta z^2 z_k^0 - \Delta z^3 \Big|_{\rfloor} \right] \right\} \\
&= \frac{1}{3}\sum_k \bar{\mathbf{Q}}_k \left[\left(z_{k-1}^0\right)^3 - \left(z_k^0\right)^3 \Big|_{\rfloor} \right] + \frac{1}{3}\sum_k \bar{\mathbf{Q}}_k \left(-3\Delta z\right) \left[\left(z_{k-1}^0\right)^2 - \left(z_k^0\right)^2 \Big|_{\rfloor} \right] + \frac{1}{3}\sum_k \bar{\mathbf{Q}}_k \left(3\Delta z^2\right) \left[z_{k-1}^0 - z_k^0 \right] \\
&= \frac{1}{3}\sum_k \bar{\mathbf{Q}}_k \left[\left(z_{k-1}^0\right)^3 - \left(z_k^0\right)^3 \Big|_{\rfloor} \right] - \Delta z \sum_k \bar{\mathbf{Q}}_k \left[\left(z_{k-1}^0\right)^2 - \left(z_k^0\right)^2 \Big|_{\rfloor} \right] + \Delta z^2 \sum_k \bar{\mathbf{Q}}_k \left[z_{k-1}^0 - z_k^0 \right] \\
&= \mathbf{D}^0 + 2\ \Delta z\, \mathbf{B}^0 + \Delta z^2\, \mathbf{A}^0
\end{aligned}$$

$$\mathbf{D}^{\text{new}} = \mathbf{D}^0 + 2\ \Delta z\, \mathbf{B}^0 + \Delta z^2\, \mathbf{A}^0 \tag{11}$$

Likewise, for the thermal force and moment resultants measured with respect to the new shifted reference plane, we have,

$$\begin{aligned}
\mathbf{N}_{\text{new}}^T &= \sum_k \bar{\mathbf{Q}}_k \boldsymbol{\alpha}_k \left[z_{k-1}^{\text{new}} - z_k^{\text{new}} \right] \Delta T_{\text{new}} + \frac{1}{2}\sum_k \bar{\mathbf{Q}}_k \boldsymbol{\alpha}_k \left[\left(z_{k-1}^{\text{new}}\right)^2 - \left(z_k^{\text{new}}\right)^2 \Big|_{\rfloor} \right] \Delta G \\
\mathbf{M}_{\text{new}}^T &= -\frac{1}{2}\sum_k \bar{\mathbf{Q}}_k \boldsymbol{\alpha}_k \left[\left(z_{k-1}^{\text{new}}\right)^2 - \left(z_k^{\text{new}}\right)^2 \Big|_{\rfloor} \right] \Delta T_{\text{new}} - \frac{1}{3}\sum_k \bar{\mathbf{Q}}_k \boldsymbol{\alpha}_k \left[\left(z_{k-1}^{\text{new}}\right)^3 - \left(z_k^{\text{new}}\right)^3 \Big|_{\rfloor} \right] \Delta G
\end{aligned} \tag{12}$$

Substituting for z^{new} in eq. (12) using eq. (4) and for ΔT_{new} using eq. (5), we arrive at,

$$
\begin{aligned}
\mathbf{N}_{\text{new}}^{T} &= \sum_k \bar{\mathbf{Q}}_k \boldsymbol{\alpha}_k \left[z_{k-1}^0 - \Delta z - z_k^0 + \Delta z \right] \left(\Delta T_0 + \Delta G \; \Delta z \right) \\
&\quad + \frac{1}{2} \sum_k \bar{\mathbf{Q}}_k \boldsymbol{\alpha}_k \left[\left(z_{k-1}^0 - \Delta z \right)^2 - \left(z_k^0 - \Delta z \right)^2 \right] \Delta G \\
&= \sum_k \bar{\mathbf{Q}}_k \boldsymbol{\alpha}_k \left[z_{k-1}^0 - z_k^0 \right] \left(\Delta T_0 + \Delta G \; \Delta z \right) \\
&\quad + \frac{1}{2} \sum_k \bar{\mathbf{Q}}_k \boldsymbol{\alpha}_k \left[\left(z_{k-1}^0 \right)^2 - 2 \; z_{k-1}^0 \, \Delta z + \Delta z^2 - \left(z_k^0 \right)^2 + 2 \; z_k^0 \, \Delta z - \Delta z^2 \right] \Delta G \\
&= \sum_k \bar{\mathbf{Q}}_k \boldsymbol{\alpha}_k \left[z_{k-1}^0 - z_k^0 \right] \Delta T_0 + \sum_k \bar{\mathbf{Q}}_k \boldsymbol{\alpha}_k \left[z_{k-1}^0 - z_k^0 \right] \Delta G \; \Delta z \\
&\quad + \frac{1}{2} \sum_k \bar{\mathbf{Q}}_k \boldsymbol{\alpha}_k \left[\left(z_{k-1}^0 \right)^2 - \left(z_k^0 \right)^2 - 2 \Delta z \left(z_{k-1}^0 - z_k^0 \right) \right] \Delta G \\
&= \sum_k \bar{\mathbf{Q}}_k \boldsymbol{\alpha}_k \left[z_{k-1}^0 - z_k^0 \right] \Delta T_0 + \frac{1}{2} \sum_k \bar{\mathbf{Q}}_k \boldsymbol{\alpha}_k \left[\left(z_{k-1}^0 \right)^2 - \left(z_k^0 \right)^2 \right] \Delta G \\
&\quad + \sum_k \bar{\mathbf{Q}}_k \boldsymbol{\alpha}_k \left[z_{k-1}^0 - z_k^0 \right] \Delta G \; \Delta z - \sum_k \bar{\mathbf{Q}}_k \boldsymbol{\alpha}_k \left[z_{k-1}^0 - z_k^0 \right] \Delta G \Delta z \\
&= \sum_k \bar{\mathbf{Q}}_k \boldsymbol{\alpha}_k \left[z_{k-1}^0 - z_k^0 \right] \Delta T_0 + \frac{1}{2} \sum_k \bar{\mathbf{Q}}_k \boldsymbol{\alpha}_k \left[\left(z_{k-1}^0 \right)^2 - \left(z_k^0 \right)^2 \right] \Delta G \\
&= \mathbf{N}_0^T
\end{aligned}
$$

$$
\mathbf{N}_{\text{new}}^{T} = \mathbf{N}_0^T \tag{13}
$$

$$
\begin{aligned}
\mathbf{M}_{\text{new}}^{T} &= -\frac{1}{2} \sum_k \bar{\mathbf{Q}}_k \boldsymbol{\alpha}_k \left[\left(z_{k-1}^0 - \Delta z \right)^2 - \left(z_k^0 - \Delta z \right)^2 \right] \left(\Delta T_0 + \Delta G \; \Delta z \right) \\
&\quad - \frac{1}{3} \sum_k \bar{\mathbf{Q}}_k \boldsymbol{\alpha}_k \left[\left(z_{k-1}^0 - \Delta z \right)^3 - \left(z_k^0 - \Delta z \right)^3 \right] \Delta G \\
&= -\frac{1}{2} \sum_k \bar{\mathbf{Q}}_k \boldsymbol{\alpha}_k \left[\left(z_{k-1}^0 \right)^2 - 2 \; z_{k-1}^0 \, \Delta z + \Delta z^2 - \left(z_k^0 \right)^2 + 2 \; z_k^0 \, \Delta z - \Delta z^2 \right] \left(\Delta T_0 + \Delta G \; \Delta z \right) \\
&\quad - \frac{1}{3} \sum_k \bar{\mathbf{Q}}_k \boldsymbol{\alpha}_k \left[\left[\left(z_{k-1}^0 \right)^3 - 3 \Delta z \left(z_{k-1}^0 \right)^2 + 3 \Delta z^2 \, z_{k-1}^0 - \Delta z^3 \right] \right. \\
&\quad \left. - \left[\left(z_k^0 \right)^3 - 3 \Delta z \left(z_k^0 \right)^2 + 3 \Delta z^2 \, z_k^0 - \Delta z^3 \right] \right] \Delta G
\end{aligned}
$$

$$
\begin{aligned}
&= -\frac{1}{2}\sum_k \bar{\mathbf{Q}}_k \boldsymbol{\alpha}_k \left[\left(z_{k-1}^0\right)^2 - \left(z_k^0\right)^2 \right] (\Delta T_0 + \Delta G\ \Delta z) - \frac{1}{2}\sum_k \bar{\mathbf{Q}}_k \boldsymbol{\alpha}_k \left[-2\Delta z \left(z_{k-1}^0 - z_k^0\right) \right] (\Delta T_0 + \Delta G\ \Delta z) \\
&\quad -\frac{1}{3}\sum_k \bar{\mathbf{Q}}_k \boldsymbol{\alpha}_k \left[\left(z_{k-1}^0\right)^3 - \left(z_k^0\right)^3 \right] \Delta G - \frac{1}{3}\sum_k \bar{\mathbf{Q}}_k \boldsymbol{\alpha}_k \left[-3\Delta z \left[\left(z_{k-1}^0\right)^2 - \left(z_k^0\right)^2 \right] \right] \Delta G \\
&\quad -\frac{1}{3}\sum_k \bar{\mathbf{Q}}_k \boldsymbol{\alpha}_k \left[3\Delta z^2 \left(z_{k-1}^0 - z_k^0\right) \right] \Delta G \\
&= -\frac{1}{2}\sum_k \bar{\mathbf{Q}}_k \boldsymbol{\alpha}_k \left[\left(z_{k-1}^0\right)^2 - \left(z_k^0\right)^2 \right] \Delta T_0 - \frac{1}{2}\sum_k \bar{\mathbf{Q}}_k \boldsymbol{\alpha}_k \left[\left(z_{k-1}^0\right)^2 - \left(z_k^0\right)^2 \right] \Delta G\ \Delta z \\
&\quad + \sum_k \bar{\mathbf{Q}}_k \boldsymbol{\alpha}_k \left[z_{k-1}^0 - z_k^0 \right] \Delta T_0 \Delta z + \sum_k \bar{\mathbf{Q}}_k \boldsymbol{\alpha}_k \left[z_{k-1}^0 - z_k^0 \right] \Delta G\, \Delta z^2 \\
&\quad -\frac{1}{3}\sum_k \bar{\mathbf{Q}}_k \boldsymbol{\alpha}_k \left[\left(z_{k-1}^0\right)^3 - \left(z_k^0\right)^3 \right] \Delta G + \sum_k \bar{\mathbf{Q}}_k \boldsymbol{\alpha}_k \left[\left(z_{k-1}^0\right)^2 - \left(z_k^0\right)^2 \right] \Delta G \Delta z \\
&\quad - \sum_k \bar{\mathbf{Q}}_k \boldsymbol{\alpha}_k \left[z_{k-1}^0 - z_k^0 \right] \Delta G \Delta z^2 \\
&= -\frac{1}{2}\sum_k \bar{\mathbf{Q}}_k \boldsymbol{\alpha}_k \left[\left(z_{k-1}^0\right)^2 - \left(z_k^0\right)^2 \right] \Delta T_0 - \frac{1}{3}\sum_k \bar{\mathbf{Q}}_k \boldsymbol{\alpha}_k \left[\left(z_{k-1}^0\right)^3 - \left(z_k^0\right)^3 \right] \Delta G \\
&\quad + \frac{1}{2}\sum_k \bar{\mathbf{Q}}_k \boldsymbol{\alpha}_k \left[\left(z_{k-1}^0\right)^2 - \left(z_k^0\right)^2 \right] \Delta G\ \Delta z + \sum_k \bar{\mathbf{Q}}_k \boldsymbol{\alpha}_k \left[z_{k-1}^0 - z_k^0 \right] \Delta T_0 \Delta z \\
&= \mathbf{M}_0^T + \Delta z\, \mathbf{N}_0^T
\end{aligned}
$$

$$
\mathbf{M}_{\text{new}}^T = \mathbf{M}_0^T + \Delta z\, \mathbf{N}_0^T \tag{14}
$$

HyperSizer employs an alternate non-classical form of the laminate constitutive eq. (1) in which the thermal effects are accounted for using "thermal ABD" terms (ref. 29). In this case, the laminate constitutive equation is written as,

$$
\begin{bmatrix} \mathbf{N} \\ \mathbf{M} \end{bmatrix} = \begin{bmatrix} \mathbf{A}^0 & \mathbf{B}^0 \\ \mathbf{B}^0 & \mathbf{D}^0 \end{bmatrix} \begin{bmatrix} \boldsymbol{\varepsilon}^0 \\ \boldsymbol{\kappa}^0 \end{bmatrix} - \begin{bmatrix} \mathbf{A}_0^\alpha & \mathbf{B}_0^\alpha \\ \mathbf{B}_0^\alpha & \mathbf{D}_0^\alpha \end{bmatrix} \begin{bmatrix} \Delta T_0 \\ -\Delta G \end{bmatrix} \tag{15}
$$

where,

$$
\mathbf{A}_0^\alpha = \sum_k \bar{\mathbf{Q}}_k \boldsymbol{\alpha}_k \left[z_{k-1}^0 - z_k^0 \right] \tag{15a}
$$

$$
\mathbf{B}_0^\alpha = -\frac{1}{2}\sum_k \bar{\mathbf{Q}}_k \boldsymbol{\alpha}_k \left[\left(z_{k-1}^0\right)^2 - \left(z_k^0\right)^2 \right] \tag{15b}
$$

$$\mathbf{D}_0^{\alpha} = \frac{1}{3}\sum_k \bar{\mathbf{Q}}_k \boldsymbol{\alpha}_k \left[\left(z_{k-1}^0\right)^3 - \left(z_k^0\right)^3 \right] \tag{15c}$$

the thermal force and moment resultants are related to the thermal ABD terms by,

$$\mathbf{N}_0^T = \mathbf{A}_0^{\alpha}\, \Delta T_0 - \mathbf{B}_0^{\alpha}\, \Delta G \tag{16}$$

$$\mathbf{M}_0^T = \mathbf{B}_0^{\alpha}\, \Delta T_0 - \mathbf{D}_0^{\alpha}\, \Delta G \tag{17}$$

With respect to the new shifted reference plane, we have,

$$\mathbf{N}_{\text{new}}^T = \mathbf{A}_{\text{new}}^{\alpha}\, \Delta T_{\text{new}} - \mathbf{B}_{\text{new}}^{\alpha}\, \Delta G \tag{18}$$

$$\mathbf{M}_{\text{new}}^T = \mathbf{B}_{\text{new}}^{\alpha}\, \Delta T_{\text{new}} - \mathbf{D}_{\text{new}}^{\alpha}\, \Delta G \tag{19}$$

Substituting eq. (5) into eq. (18) yields,

$$\begin{aligned} \mathbf{N}_{\text{new}}^T &= \mathbf{A}_{\text{new}}^{\alpha} \left(\Delta T_0 + \Delta G\ \Delta z\right) - \mathbf{B}_{\text{new}}^{\alpha}\, \Delta G = \mathbf{A}_{\text{new}}^{\alpha} \Delta T_0 + \mathbf{A}_{\text{new}}^{\alpha} \Delta G\ \Delta z - \mathbf{B}_{\text{new}}^{\alpha}\, \Delta G \\ &= \mathbf{A}_{\text{new}}^{\alpha} \Delta T_0 - \left(\mathbf{B}_{\text{new}}^{\alpha} - \mathbf{A}_{\text{new}}^{\alpha} \Delta z\right) \Delta G \end{aligned} \tag{20}$$

Using eq. (13) and comparing the terms present in eq. (20) with those in eq. (16) gives,

$$\mathbf{A}_{\text{new}}^{\alpha} = \mathbf{A}_0^{\alpha} \tag{21}$$

and,

$$\mathbf{B}_0^{\alpha} = \mathbf{B}_{\text{new}}^{\alpha} - \mathbf{A}_{\text{new}}^{\alpha} \Delta z \tag{22}$$

Substituting using eq. (21) and rearranging yields,

$$\mathbf{B}_{\text{new}}^{\alpha} = \mathbf{B}_0^{\alpha} + \Delta z\, \mathbf{A}_0^{\alpha} \tag{23}$$

Substituting eq. (5) into (18) gives,

$$\begin{aligned} \mathbf{M}_{\text{new}}^T &= \mathbf{B}_{\text{new}}^{\alpha} \left(\Delta T_0 + \Delta G\ \Delta z\right) - \mathbf{D}_{\text{new}}^{\alpha}\, \Delta G = \mathbf{B}_{\text{new}}^{\alpha} \Delta T_0 + \mathbf{B}_{\text{new}}^{\alpha} \Delta G\ \Delta z - \mathbf{D}_{\text{new}}^{\alpha}\, \Delta G \\ &= \mathbf{B}_{\text{new}}^{\alpha} \Delta T_0 - \left(\mathbf{D}_{\text{new}}^{\alpha} - \mathbf{B}_{\text{new}}^{\alpha} \Delta z\right) \Delta G \end{aligned} \tag{24}$$

Using eq. (14) and substituting using eqs. (16) to (17) yields,

$$\begin{aligned} \mathbf{M}_{\text{new}}^T &= \mathbf{B}_0^{\alpha}\, \Delta T_0 - \mathbf{D}_0^{\alpha}\, \Delta G + \Delta z \left(\mathbf{A}_0^{\alpha}\, \Delta T_0 - \mathbf{B}_0^{\alpha}\, \Delta G\right) \\ &= \left(\mathbf{B}_0^{\alpha} + \Delta z\, \mathbf{A}_0^{\alpha}\right) \Delta T_0 - \left(\mathbf{D}_0^{\alpha} + \mathbf{B}_0^{\alpha} \Delta z\right) \Delta G \end{aligned} \tag{25}$$

Comparing the terms in eq. (25) with those in eq. (24), we confirm eq. (23) and also have,

$$\mathbf{D}^{\alpha}_{\text{new}} - \mathbf{B}^{\alpha}_{\text{new}}\Delta z = \mathbf{D}^{\alpha}_{0} + \mathbf{B}^{\alpha}_{0}\Delta z \tag{26}$$

Rearranging eq. (26) and substituting using eq. (23) then yields,

$$\mathbf{D}^{\alpha}_{\text{new}} = \mathbf{D}^{\alpha}_{0} + 2\Delta z\mathbf{B}^{\alpha}_{0} + \Delta z^{2}\,\mathbf{A}^{\alpha}_{0} \tag{27}$$

Equations (9) to (11), (13), (14), (21), (23), and (27) thus enable the determination of the thermo-elastic laminate constitutive equation terms with respect to an arbitrary reference plane from the reference plane thermo-elastic laminate constitutive equation terms and the reference plane shift, Δz.

Thermo-piezo-electro-magnetic effects can be included within the midplane laminate constitutive eq. (1) (see ref. 26 for details) as,

$$\begin{bmatrix}\mathbf{N}\\ \mathbf{M}\end{bmatrix} = \begin{bmatrix}\mathbf{A}^{0} & \mathbf{B}^{0}\\ \mathbf{B}^{0} & \mathbf{D}^{0}\end{bmatrix}\begin{bmatrix}\boldsymbol{\varepsilon}^{0}\\ \boldsymbol{\kappa}^{0}\end{bmatrix} - \begin{bmatrix}\mathbf{N}^{T}_{0}\\ \mathbf{M}^{T}_{0}\end{bmatrix} - \begin{bmatrix}\mathbf{N}^{E}_{0}\\ \mathbf{M}^{E}_{0}\end{bmatrix} - \begin{bmatrix}\mathbf{N}^{ET}_{0}\\ \mathbf{M}^{ET}_{0}\end{bmatrix} - \begin{bmatrix}\mathbf{N}^{M}_{0}\\ \mathbf{M}^{M}_{0}\end{bmatrix} - \begin{bmatrix}\mathbf{N}^{MT}_{0}\\ \mathbf{M}^{MT}_{0}\end{bmatrix} \tag{28}$$

where $\mathbf{N}^{E}_{0}$ and $\mathbf{M}^{E}_{0}$ are the electric force an moment resultant vectors, $\mathbf{N}^{ET}_{0}$ and $\mathbf{M}^{ET}_{0}$ are the thermo-electric force and moment resultant vectors, $\mathbf{N}^{M}_{0}$ and $\mathbf{M}^{M}_{0}$ are the magnetic force and moment resultant vectors, and $\mathbf{N}^{MT}_{0}$ and $\mathbf{M}^{MT}_{0}$ are the thermo-magnetic force and moment resultant vectors, all determined with respect to the laminate midplane. These thermo-piezo-electro-magnetic force and moment resultant vectors are given by,

$$\mathbf{N}^{E}_{0} = \begin{bmatrix}N^{E}_{x}\\ N^{E}_{y}\\ N^{E}_{xy}\end{bmatrix}_{0} = \sum_{k=1}^{N}[\hat{\mathbf{e}}_{k}]\begin{bmatrix}E_{x}\\ E_{y}\\ E_{z}\end{bmatrix}_{k}(z_{k}-z_{k-1}) \qquad \mathbf{M}^{E}_{0} = \begin{bmatrix}M^{E}_{x}\\ M^{E}_{y}\\ M^{E}_{xy}\end{bmatrix}_{0} = -\frac{1}{2}\sum_{k=1}^{N}[\hat{\mathbf{e}}_{k}]\begin{bmatrix}E_{x}\\ E_{y}\\ E_{z}\end{bmatrix}_{k}\left(z_{k}^{2}-z_{k-1}^{2}\right) \tag{29}$$

$$\mathbf{N}^{ET}_{0} = \begin{bmatrix}N^{ET}_{x}\\ N^{ET}_{y}\\ N^{ET}_{xy}\end{bmatrix}_{0} = \sum_{k=1}^{N}[\hat{\mathbf{e}}_{k}]\int_{z_{k-1}}^{z_{k}}\begin{bmatrix}E^{T}_{x}\\ E^{T}_{y}\\ E^{T}_{z}\end{bmatrix}_{k}dz \qquad \mathbf{M}^{ET}_{0} = \begin{bmatrix}M^{ET}_{x}\\ M^{ET}_{y}\\ M^{ET}_{xy}\end{bmatrix}_{0} = -\sum_{k=1}^{N}[\hat{\mathbf{e}}_{k}]\int_{z_{k-1}}^{z_{k}}\begin{bmatrix}E^{T}_{x}\\ E^{T}_{y}\\ E^{T}_{z}\end{bmatrix}_{k}z\,dz \tag{30}$$

$$\mathbf{N}^{M}_{0} = \begin{bmatrix}N^{M}_{x}\\ N^{M}_{y}\\ N^{M}_{xy}\end{bmatrix}_{0} = \sum_{k=1}^{N}[\hat{\mathbf{q}}_{k}]\int_{z_{k-1}}^{z_{k}}\begin{bmatrix}H_{x}\\ H_{y}\\ H_{z}\end{bmatrix}_{k}dz \qquad \mathbf{M}^{E}_{0} = \begin{bmatrix}M^{M}_{x}\\ M^{M}_{y}\\ M^{M}_{xy}\end{bmatrix}_{0} = -\frac{1}{2}\sum_{k=1}^{N}[\hat{\mathbf{q}}_{k}]\begin{bmatrix}H_{x}\\ H_{y}\\ H_{z}\end{bmatrix}_{k}\left(z_{k}^{2}-z_{k-1}^{2}\right) \tag{31}$$

$$\mathbf{N}_0^{MT} = \left[\begin{matrix} N_x^{MT} \\ N_y^{MT} \\ N_{xy}^{MT} \end{matrix}\right]_0 = \sum_{k=1}^{N} [\hat{\mathbf{q}}_k] \int_{z_{k-1}}^{z_k} \left[\begin{matrix} H_x^T \\ H_y^T \\ H_z^T \end{matrix}\right]_k dz \qquad \mathbf{M}_0^{MT} = \left[\begin{matrix} M_x^{MT} \\ M_y^{MT} \\ M_{xy}^{MT} \end{matrix}\right]_0 = -\sum_{k=1}^{N} [\hat{\mathbf{q}}_k] \int_{z_{k-1}}^{z_k} \left[\begin{matrix} H_x^T \\ H_y^T \\ H_z^T \end{matrix}\right]_k z\, dz \quad (32)$$

where E_i are the electric field components, E_i^T are the thermo-electric field components, H_i are the magnetic field components, H_i^T are the thermo-magnetic field components, $\hat{\mathbf{e}}_k$ is the 3×3 reduced piezoelectric coefficient matrix (for layer *k*),

$$[\hat{\mathbf{e}}_k] = \left[\begin{matrix} \hat{e}_{11} & \hat{e}_{21} & \hat{e}_{31} \\ \hat{e}_{12} & \hat{e}_{22} & \hat{e}_{32} \\ \hat{e}_{16} & \hat{e}_{26} & \hat{e}_{36} \end{matrix}\right]_k \quad (33)$$

and $\hat{\mathbf{q}}_k$ is the 3×3 reduced piezomagnetic matrix (for layer *k*),

$$[\hat{\mathbf{q}}_k] = \left[\begin{matrix} \hat{\mathbf{q}}_{11} & \hat{\mathbf{q}}_{21} & \hat{\mathbf{q}}_{31} \\ \hat{\mathbf{q}}_{12} & \hat{\mathbf{q}}_{22} & \hat{\mathbf{q}}_{32} \\ \hat{\mathbf{q}}_{16} & \hat{\mathbf{q}}_{26} & \hat{\mathbf{q}}_{36} \end{matrix}\right]_k \quad (34)$$

(see ref. 26 for details). It should be noted that the minus signs present in the above moment resultant eqs. (29) to (32) are due to the coordinate system employed shown in figure 1. This coordinate system differs from that used by Bednarcyk (ref. 26), in which the aforementioned minus signs do not appear.

For consistency, we now develop an alternative representation of these force and moment resultants that by introducing terms analogous to the thermal ABD terms present in eq. (15). Restricting the applied electric field components to the case in which they are constant throughout the laminate, eq. (29) can be written as,

$$\mathbf{N}_0^E = \left[\sum_{k=1}^{N} [\hat{\mathbf{e}}_k](z_{k-1} - z_k)\right] \left[\begin{matrix} E_x \\ E_y \\ E_z \end{matrix}\right] \qquad \mathbf{M}_0^E = \left[-\frac{1}{2}\sum_{k=1}^{N} [\hat{\mathbf{e}}_k]\left(z_{k-1}^2 - z_k^2\right)\right] \left[\begin{matrix} E_x \\ E_y \\ E_z \end{matrix}\right] \quad (33)$$

Combining eq. (33),

$$\left[\begin{matrix} \mathbf{N}_0^E \\ \mathbf{M}_0^E \end{matrix}\right] = \left[\begin{matrix} \sum_{k=1}^{N} [\hat{\mathbf{e}}_k](z_{k-1} - z_k) \\ -\frac{1}{2}\sum_{k=1}^{N} [\hat{\mathbf{e}}_k]\left(z_{k-1}^2 - z_k^2\right) \end{matrix}\right] \left[\begin{matrix} E_x \\ E_y \\ E_z \end{matrix}\right] \quad (34)$$

or,

$$\underbrace{\begin{bmatrix}\mathbf{N}_0^E\\ \mathbf{M}_0^E\end{bmatrix}}_{6\times1}=\underbrace{\begin{bmatrix}\mathbf{A}_0^E\\ \mathbf{B}_0^E\end{bmatrix}}_{6\times3}\underbrace{\begin{bmatrix}E_x\\ E_y\\ E_z\end{bmatrix}}_{3\times1} \tag{35}$$

where,

$$\mathbf{A}_0^E=\sum_{k=1}^{N}[\hat{e}_k](z_{k-1}-z_k)\qquad \mathbf{B}_0^E=-\frac{1}{2}\sum_{k=1}^{N}[\hat{e}_k]\left(z_{k-1}^2-z_k^2\right) \tag{36}$$

Here $\mathbf{A}_0^E$ and $\mathbf{B}_0^E$ are each 3×3 matrices and combine to form the laminate electric AB matrix, as shown in eq. (35).

Similarly, restricting the applied magnetic field components to the case in which they are constant throughout the laminate, we can write eq. (31) as,

$$\underbrace{\begin{bmatrix}\mathbf{N}_0^M\\ \mathbf{M}_0^M\end{bmatrix}}_{6\times1}=\underbrace{\begin{bmatrix}\mathbf{A}_0^M\\ \mathbf{B}_0^M\end{bmatrix}}_{6\times3}\underbrace{\begin{bmatrix}H_x\\ H_y\\ H_z\end{bmatrix}}_{3\times1} \tag{37}$$

where,

$$\mathbf{A}_0^M=\sum_{k=1}^{N}[\hat{q}_k](z_{k-1}-z_k)\qquad \mathbf{B}_0^M=-\frac{1}{2}\sum_{k=1}^{N}[\hat{q}_k]\left(z_{k-1}^2-z_k^2\right) \tag{38}$$

Here $\mathbf{A}_0^M$ and $\mathbf{B}_0^M$ are each 3×3 matrices and combine to form the laminate magnetic AB matrix, as shown in eq. (37).

The temperature change from reference at any point within a ply is given by $T(z) - T_{\text{ref}} = \Delta T_0 + z\,\Delta G$, and the thermo-electric and thermo-magnetic field components, appearing in eqs. (30) and (32), are related to this temperature change by,

$$\begin{bmatrix}E_x^T\\ E_y^T\\ E_z^T\end{bmatrix}_k=\boldsymbol{\zeta}_k^*\left(\Delta T_0+z\;\Delta G\right)\qquad \begin{bmatrix}H_x^T\\ H_y^T\\ H_z^T\end{bmatrix}_k=\boldsymbol{\psi}_k^*\left(\Delta T_0+z\;\Delta G\right) \tag{39}$$

where $\boldsymbol{\zeta}_k^*$ is the effective pyroelectric constant vector of ply k and $\boldsymbol{\psi}_k^*$ is the effective pyromagnetic constant vector for ply k, both in the global laminate coordinate system. Note that the relations between the thermal field quantities and the pyroelectric and pyromagnetic constants in eq. (39) is analogous to that of the thermal strain and the coefficient of thermal expansion. Substituting eq. (39) into eqs. (30) and (32) yields,

$$\mathbf{N}_0^{ET} = \sum_{k=1}^{N} [\hat{\mathbf{e}}_k] \int_{z_{k-1}}^{z_k} \zeta_k^* (\Delta T_0 + z\ \Delta G)\, dz \qquad \mathbf{M}_0^{ET} = -\sum_{k=1}^{N} [\hat{\mathbf{e}}_k] \int_{z_{k-1}}^{z_k} \zeta_k^* (\Delta T_0 + z\ \Delta G)\, z\, dz \tag{40}$$

$$\mathbf{N}_0^{MT} = \sum_{k=1}^{N} [\hat{\mathbf{q}}_k] \int_{z_{k-1}}^{z_k} \psi_k^* (\Delta T_0 + z\ \Delta G)\, dz \qquad \mathbf{M}_0^{MT} = -\sum_{k=1}^{N} [\hat{\mathbf{q}}_k] \int_{z_{k-1}}^{z_k} \psi_k^* (\Delta T_0 + z\ \Delta G)\, z\, dz \tag{41}$$

or,

$$\begin{bmatrix} \mathbf{N}_0^{ET} \\ \mathbf{M}_0^{ET} \end{bmatrix} = \begin{bmatrix} \sum_{k=1}^{N} [\hat{\mathbf{e}}_k] \zeta_k^* (z_{k-1} - z_k) \Delta T_0 + \frac{1}{2} \sum_{k=1}^{N} [\hat{\mathbf{e}}_k] \zeta_k^* \left(z_{k-1}^2 - z_k^2 \right) \Delta G \\ -\frac{1}{2} \sum_{k=1}^{N} [\hat{\mathbf{e}}_k] \zeta_k^* \left(z_{k-1}^2 - z_k^2 \right) \Delta T_0 - \frac{1}{3} \sum_{k=1}^{N} [\hat{\mathbf{e}}_k] \zeta_k^* \left(z_{k-1}^3 - z_k^3 \right) \Delta G \end{bmatrix} \tag{42}$$

$$\begin{bmatrix} \mathbf{N}_0^{MT} \\ \mathbf{M}_0^{MT} \end{bmatrix} = \begin{bmatrix} \sum_{k=1}^{N} [\hat{\mathbf{q}}_k] \psi_k^* (z_{k-1} - z_k) \Delta T_0 + \frac{1}{2} \sum_{k=1}^{N} [\hat{\mathbf{q}}_k] \psi_k^* \left(z_{k-1}^2 - z_k^2 \right) \Delta G \\ -\frac{1}{2} \sum_{k=1}^{N} [\hat{\mathbf{q}}_k] \psi_k^* \left(z_{k-1}^2 - z_k^2 \right) \Delta T_0 - \frac{1}{3} \sum_{k=1}^{N} [\hat{\mathbf{q}}_k] \psi_k^* \left(z_{k-1}^3 - z_k^3 \right) \Delta G \end{bmatrix} \tag{43}$$

or,

$$\underbrace{\begin{bmatrix} \mathbf{N}_0^{ET} \\ \mathbf{M}_0^{ET} \end{bmatrix}}_{6\times1} = \underbrace{\begin{bmatrix} \mathbf{A}_0^{ET} & \mathbf{B}_0^{ET} \\ \mathbf{B}_0^{ET} & \mathbf{D}_0^{ET} \end{bmatrix}}_{6\times2} \underbrace{\begin{bmatrix} \Delta T_0 \\ -\Delta G \end{bmatrix}}_{2\times1} \qquad \underbrace{\begin{bmatrix} \mathbf{N}_0^{MT} \\ \mathbf{M}_0^{MT} \end{bmatrix}}_{6\times1} = \underbrace{\begin{bmatrix} \mathbf{A}_0^{MT} & \mathbf{B}_0^{MT} \\ \mathbf{B}_0^{MT} & \mathbf{D}_0^{MT} \end{bmatrix}}_{6\times2} \underbrace{\begin{bmatrix} \Delta T_0 \\ -\Delta G \end{bmatrix}}_{2\times1} \tag{44}$$

where,

$$\mathbf{A}_0^{ET} = \sum_{k=1}^{N} [\hat{\mathbf{e}}_k] \zeta_k^* (z_{k-1} - z_k) \quad \mathbf{B}_0^{ET} = -\frac{1}{2} \sum_{k=1}^{N} [\hat{\mathbf{e}}_k] \zeta_k^* \left(z_{k-1}^2 - z_k^2 \right) \quad \mathbf{D}_0^{ET} = \frac{1}{3} \sum_{k=1}^{N} [\hat{\mathbf{e}}_k] \zeta_k^* \left(z_{k-1}^3 - z_k^3 \right) \tag{45}$$

$$\mathbf{A}_0^{MT} = \sum_{k=1}^{N} [\hat{\mathbf{q}}_k] \psi_k^* (z_{k-1} - z_k) \quad \mathbf{B}_0^{MT} = -\frac{1}{2} \sum_{k=1}^{N} [\hat{\mathbf{q}}_k] \psi_k^* \left(z_{k-1}^2 - z_k^2 \right) \quad \mathbf{D}_0^{MT} = \frac{1}{3} \sum_{k=1}^{N} [\hat{\mathbf{q}}_k] \psi_k^* \left(z_{k-1}^3 - z_k^3 \right) \tag{46}$$

Note that each of the above thermo-electric and thermo-magnetic ABD terms is a 3×1 matrix. We can now write the laminate constitutive eqs. (15) and (28) as,

$$\begin{bmatrix}\mathbf{N}\\ \mathbf{M}\end{bmatrix}=\begin{bmatrix}\mathbf{A}^0 & \mathbf{B}^0\\ \mathbf{B}^0 & \mathbf{D}^0\end{bmatrix}\begin{bmatrix}\boldsymbol{\varepsilon}^0\\ \boldsymbol{\kappa}^0\end{bmatrix}-\begin{bmatrix}\mathbf{A}_0^{\alpha} & \mathbf{B}_0^{\alpha}\\ \mathbf{B}_0^{\alpha} & \mathbf{D}_0^{\alpha}\end{bmatrix}\begin{bmatrix}\Delta T_0\\ -\Delta G\end{bmatrix}-\begin{bmatrix}\mathbf{A}_0^{E} & \mathbf{B}_0^{E}\\ \mathbf{B}_0^{E} & \mathbf{D}_0^{E}\end{bmatrix}\begin{bmatrix}E_x\\ E_y\\ E_z\end{bmatrix}-\begin{bmatrix}\mathbf{A}_0^{M} & \mathbf{B}_0^{M}\\ \mathbf{B}_0^{M} & \mathbf{D}_0^{M}\end{bmatrix}\begin{bmatrix}H_x\\ H_y\\ H_z\end{bmatrix}$$
$$-\begin{bmatrix}\mathbf{A}_0^{ET} & \mathbf{B}_0^{ET}\\ \mathbf{B}_0^{ET} & \mathbf{D}_0^{ET}\end{bmatrix}\begin{bmatrix}\Delta T_0\\ -\Delta G\end{bmatrix}-\begin{bmatrix}\mathbf{A}_0^{MT} & \mathbf{B}_0^{MT}\\ \mathbf{B}_0^{MT} & \mathbf{D}_0^{MT}\end{bmatrix}\begin{bmatrix}\Delta T_0\\ -\Delta G\end{bmatrix} \tag{47}$$

Comparing the electric, magnetic, thermo-electric, and thermo-magnetic terms in eq. (47) with the thermal terms in eq. (47) (see eqs. (15a) to (15c), (36), (38), and (45) to (46), it is clear that there is a direct analogy among all $\mathbf{A}_0^j$ matrices, among all $\mathbf{B}_0^j$ matrices, and among all $\mathbf{D}_0^j$ matrices. Since the z_k functionality in all of these thermo-electro-magnetic ABD terms is the same as that of the thermal ABD terms, it can be shown that these thermo-electro-magnetic ABD terms will shift reference plane (see fig. 1) in a way analogous to the shift in the thermal ABD terms given in eqs. (21), (23), and (27). Thus, for a reference plane shift of Δz, we have,

$$\mathbf{A}_{\text{new}}^j=\mathbf{A}_0^j \quad \mathbf{B}_{\text{new}}^j=\mathbf{B}_0^j+\Delta z\,\mathbf{A}_0^j \lhd, \quad j=E,\ M,\ ET,\ MT \tag{48}$$

$$\mathbf{D}_{\text{new}}^j=\mathbf{D}_0^j+2\Delta z\mathbf{B}_0^j+\Delta z^2\,\mathbf{A}_0^j, \quad j=ET,\ MT \tag{49}$$

In terms of the thermo-electro-magnetic force and moment resultants (eqs. (33), (38), (42), and (43)), we have,

$$\mathbf{N}_{\text{new}}^j=\mathbf{N}_0^j,\ j=E,\ M,\ ET,\ MT \tag{50}$$

$$\mathbf{M}_{\text{new}}^j=\mathbf{M}_0^j+\Delta z\,\mathbf{N}_0^j,\ j=E,\ M,\ ET,\ MT \tag{51}$$

A simple procedure has thus been established for shifting all elements of the thermo-electro-magneto-elastic laminate constitutive eq. (47) from the laminate midplane to an arbitrary reference plane. This new laminate constitutive equation is given by,

$$\begin{bmatrix}\mathbf{N}\\ \mathbf{M}\end{bmatrix}=\begin{bmatrix}\mathbf{A}^{\text{new}} & \mathbf{B}^{\text{new}}\\ \mathbf{B}^{\text{new}} & \mathbf{D}^{\text{new}}\end{bmatrix}\begin{bmatrix}\boldsymbol{\varepsilon}^{\text{new}}\\ \boldsymbol{\kappa}^{\text{new}}\end{bmatrix}-\begin{bmatrix}\mathbf{A}_{\text{new}}^{\alpha} & \mathbf{B}_{\text{new}}^{\alpha}\\ \mathbf{B}_{\text{new}}^{\alpha} & \mathbf{D}_{\text{new}}^{\alpha}\end{bmatrix}\begin{bmatrix}\Delta T_{\text{new}}\\ -\Delta G\end{bmatrix}-\begin{bmatrix}\mathbf{A}_{\text{new}}^{E} & \mathbf{B}_{\text{new}}^{E}\\ \mathbf{B}_{\text{new}}^{E} & \mathbf{D}_{\text{new}}^{E}\end{bmatrix}\begin{bmatrix}E_x\\ E_y\\ E_z\end{bmatrix}-\begin{bmatrix}\mathbf{A}_{\text{new}}^{M} & \mathbf{B}_{\text{new}}^{M}\\ \mathbf{B}_{\text{new}}^{M} & \mathbf{D}_{\text{new}}^{M}\end{bmatrix}\begin{bmatrix}H_x\\ H_y\\ H_z\end{bmatrix}$$
$$-\begin{bmatrix}\mathbf{A}_{\text{new}}^{ET} & \mathbf{B}_{\text{new}}^{ET}\\ \mathbf{B}_{\text{new}}^{ET} & \mathbf{D}_{\text{new}}^{ET}\end{bmatrix}\begin{bmatrix}\Delta T_{\text{new}}\\ -\Delta G\end{bmatrix}-\begin{bmatrix}\mathbf{A}_{\text{new}}^{MT} & \mathbf{B}_{\text{new}}^{MT}\\ \mathbf{B}_{\text{new}}^{MT} & \mathbf{D}_{\text{new}}^{MT}\end{bmatrix}\begin{bmatrix}\Delta T_{\text{new}}\\ -\Delta G\end{bmatrix} \tag{52}$$

3.0 Homogenization Procedure for a Group of Laminates

Now that a reference plane shifting procedure has been established, it is possible to develop a simple methodology for homogenizing the constitutive equations of a group of laminates to arrive at an effective laminate constitutive equation of the laminate constituted by the group. Because each term in the laminate constitutive eq. (47) is determined via summation of ply-level quantities, provided that the constitutive equations of all laminates in the group are determined with respect to the same reference plane (eq. (52)), the constitutive equation of the group can be determined via a simple summation. Thus, given a number

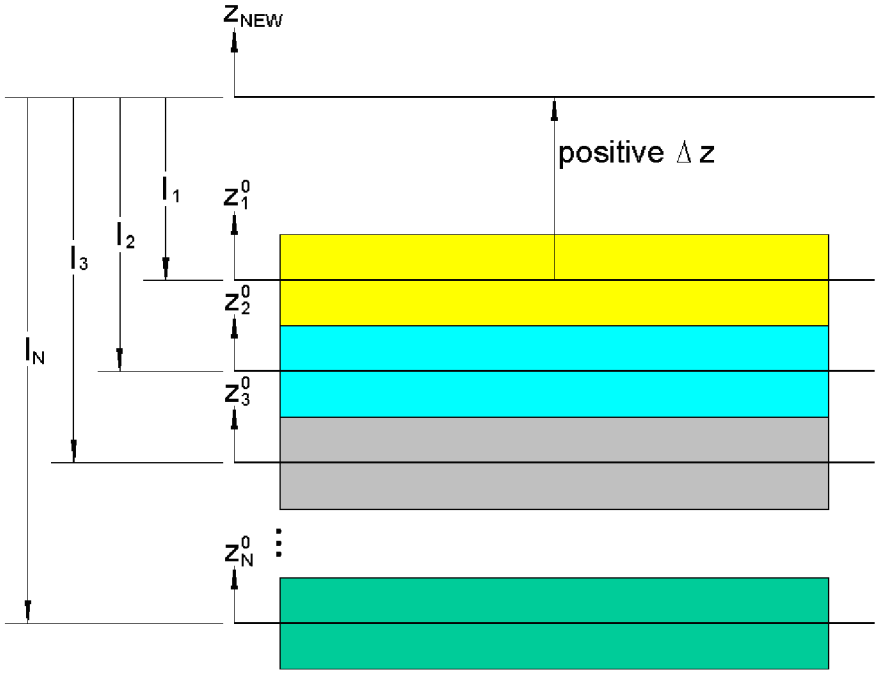

Figure 2.—A group of laminates whose constitutive equation terms have been determined with respect to a common reference plane, defined by the origin of the coordinate z_{new}. This allows determination of effective constitutive equation terms (with respect to the common reference plane) for the laminate constituted by the group.

of laminates and the z_{new} coordinate of the original reference plane of each laminate (given by l_k, see fig. 2), we can shift the reference plane of each laminate to the common z_{new} reference plane and then sum the resulting ABD_p matrices to determine the new homogenized ABD of the entire group of laminates.

For each laminate (denoted by the subscript p) in figure 2 the reference plane shift is given by, $\Delta z_p^0 = -l_p$ because Δz_p^0 is measured from a laminate's original reference plane to the new reference plane, while l_p is measured in the opposite direction, from the new reference plane to the laminate's original reference plane. Considering first the standard laminate ABD matrix terms,

$$\mathbf{A}_{\text{Group}} = \sum_p \mathbf{A}_p^{\text{new}} = \sum_p \mathbf{A}_p^0 \rightarrow \mathbf{A}_{\text{Group}} = \sum_p \mathbf{A}_p^0 \tag{53}$$

$$\mathbf{B}_{\text{Group}} = \sum_k \mathbf{B}_p^{\text{new}} = \sum_p \left(\mathbf{B}_p^0 + \Delta z_p\, \mathbf{A}_p^0\right) = \sum_p \left(\mathbf{B}_p^0 - l_p\, \mathbf{A}_p^0\right) \rightarrow \mathbf{B}_{\text{Group}} = \sum_p \left(\mathbf{B}_p^0 - l_p\, \mathbf{A}_p^0\right) \tag{54}$$

$$\begin{aligned} \mathbf{D}_{\text{Group}} &= \sum_p \mathbf{D}_p^{\text{new}} = \sum_p \left(\mathbf{D}_p^0 + 2\,\Delta z_p\, \mathbf{B}_p^0 + \Delta z_p{}^2\, \mathbf{A}_p^0\right) \\ &= \sum_k \left(\mathbf{D}_p^0 - 2\, l_p\, \mathbf{B}_p^0 + l_p{}^2\, \mathbf{A}_p^0\right) \end{aligned} \qquad \rightarrow \mathbf{D}_{\text{Group}} = \sum_p \left(\mathbf{D}_p^0 - 2\, l_p\, \mathbf{B}_p^0 + l_p{}^2\, \mathbf{A}_p^0\right) \tag{55}$$

Similarly, the homogenized thermal terms are given by,

$$\mathbf{A}_{\text{Group}}^{\alpha} = \sum_p \left(\mathbf{A}_{\text{new}}^{\alpha}\right)_p = \sum_p \left(\mathbf{A}_0^{\alpha}\right)_p \rightarrow \mathbf{A}_{\text{Group}}^{\alpha} = \sum_p \left(\mathbf{A}_0^{\alpha}\right)_p \tag{56}$$

$$\mathbf{B}^{\alpha}_{\text{Group}} = \sum_{p}\left(\mathbf{B}^{\alpha}_{\text{new}}\right)_p = \sum_{p}\left[\left(\mathbf{B}^{\alpha}_{0}\right)_p + \Delta z_p \left(\mathbf{A}^{\alpha}_{0}\right)_p\right] = \sum_{p}\left[\left(\mathbf{B}^{\alpha}_{0}\right)_p - l_p \left(\mathbf{A}^{\alpha}_{0}\right)_p\right] \rightarrow \mathbf{B}^{\alpha}_{\text{Group}} = \sum_{p}\left[\left(\mathbf{B}^{\alpha}_{0}\right)_p - l_p \left(\mathbf{A}^{\alpha}_{0}\right)_p\right] \quad (57)$$

$$\mathbf{D}^{\alpha}_{\text{Group}} = \sum_{p}\left(\mathbf{D}^{\alpha}_{\text{new}}\right)_p = \sum_{k}\left[\left(\mathbf{D}^{\alpha}_{0}\right)_p + 2\,\Delta z_p \left(\mathbf{B}^{\alpha}_{0}\right)_p + \Delta z_p{}^2 \left(\mathbf{A}^{\alpha}_{0}\right)_p\right] \rightarrow = \sum_{p}\left[\left(\mathbf{D}^{\alpha}_{0}\right)_p - 2\,l_p \left(\mathbf{B}^{\alpha}_{0}\right)_p + l_p{}^2 \left(\mathbf{A}^{\alpha}_{0}\right)_p\right] \quad (58)$$

$$\mathbf{D}^{\alpha}_{\text{Group}} = \sum_{p}\left[\left(\mathbf{D}^{\alpha}_{0}\right)_p - 2\,l_p \left(\mathbf{B}^{\alpha}_{0}\right)_p + l_p{}^2 \left(\mathbf{A}^{\alpha}_{0}\right)_p\right]$$

$$\mathbf{N}^{T}_{\text{Group}} = \sum_{p}\left(\mathbf{N}^{T}_{\text{new}}\right)_p = \sum_{p}\left(\mathbf{N}^{T}_{0}\right)_p \rightarrow \mathbf{N}^{T}_{\text{Group}} = \sum_{p}\left(\mathbf{N}^{T}_{0}\right)_p \quad (59)$$

$$\mathbf{M}^{T}_{\text{Group}} = \sum_{p}\left(\mathbf{M}^{T}_{\text{new}}\right)_p = \sum_{p}\left(\mathbf{N}^{T}_{0} + \Delta z\ \mathbf{M}^{T}_{0}\right)_p = \sum_{p}\left(\mathbf{N}^{T}_{0} - l_k\ \mathbf{M}^{T}_{0}\right)_p \rightarrow \mathbf{M}^{T}_{\text{Group}} = \sum_{p}\left(\mathbf{M}^{T}_{0} - l_k\ \mathbf{N}^{T}_{0}\right)_p \quad (60)$$

Finally, the homogenized thermo-electro-magnetic terms are given by,

$$\mathbf{A}^{j}_{\text{Group}} = \sum_{p}\left(\mathbf{A}^{j}_{0}\right)_p,\ j = E,\ M,\ ET,\ MT \quad (61)$$

$$\mathbf{B}^{j}_{\text{Group}} = \sum_{p}\left[\left(\mathbf{B}^{j}_{0}\right)_p - l_p \left(\mathbf{A}^{j}_{0}\right)_p\right],\ j = E,\ M,\ ET,\ MT \quad (62)$$

$$\mathbf{D}^{j}_{\text{Group}} = \sum_{p}\left[\left(\mathbf{D}^{j}_{0}\right)_p - 2\,l_p \left(\mathbf{B}^{j}_{0}\right)_p + l_p{}^2 \left(\mathbf{A}^{j}_{0}\right)_p\right],\ j = ET,\ MT \quad (63)$$

$$\mathbf{N}^{j}_{\text{Group}} = \sum_{p}\left(\mathbf{N}^{j}_{0}\right)_p,\ j = E,\ M,\ ET,\ MT \quad (64)$$

$$\mathbf{M}^{j}_{\text{Group}} = \sum_{p}\left(\mathbf{M}^{j}_{0} - l_p\ \mathbf{N}^{j}_{0}\right)_p,\ j = E,\ M,\ ET,\ MT \quad (65)$$

The homogenized constitutive equation for the group of laminates with respect to the reference plane defined by the origin of the z_{new} coordinate in figure 2 is given by,

$$\begin{bmatrix}\mathbf{N}\\ \mathbf{M}\end{bmatrix}=\begin{bmatrix}\mathbf{A}_{\text{Group}} & \mathbf{B}_{\text{Group}}\\ \mathbf{B}_{\text{Group}} & \mathbf{D}_{\text{Group}}\end{bmatrix}\begin{bmatrix}\boldsymbol{\varepsilon}^{\text{new}}\\ \boldsymbol{\kappa}^{\text{new}}\end{bmatrix}-\begin{bmatrix}\mathbf{A}^{\alpha}_{\text{Group}} & \mathbf{B}^{\alpha}_{\text{Group}}\\ \mathbf{B}^{\alpha}_{\text{Group}} & \mathbf{D}^{\alpha}_{\text{Group}}\end{bmatrix}\begin{bmatrix}\Delta T_{\text{new}}\\ -\Delta G\end{bmatrix}-\begin{bmatrix}\mathbf{A}^{E}_{\text{Group}}\\ \mathbf{B}^{E}_{\text{Group}}\end{bmatrix}\begin{bmatrix}E_x\\ E_y\\ E_z\end{bmatrix}-\begin{bmatrix}\mathbf{A}^{M}_{\text{Group}}\\ \mathbf{B}^{M}_{\text{Group}}\end{bmatrix}\begin{bmatrix}H_x\\ H_y\\ H_z\end{bmatrix}$$
$$-\begin{bmatrix}\mathbf{A}^{ET}_{\text{Group}} & \mathbf{B}^{ET}_{\text{Group}}\\ \mathbf{B}^{ET}_{\text{Group}} & \mathbf{D}^{ET}_{\text{Group}}\end{bmatrix}\begin{bmatrix}\Delta T_{\text{new}}\\ -\Delta G\end{bmatrix}-\begin{bmatrix}\mathbf{A}^{MT}_{\text{Group}} & \mathbf{B}^{MT}_{\text{Group}}\\ \mathbf{B}^{MT}_{\text{Group}} & \mathbf{D}^{MT}_{\text{Group}}\end{bmatrix}\begin{bmatrix}\Delta T_{\text{new}}\\ -\Delta G\end{bmatrix} \tag{66}$$

4. Analysis of Blade Stiffened Panels

The geometry of a blade stiffened panel is shown in figure 3. The face sheet can be an arbitrary composite laminate that is oriented as shown in the x, y, z coordinate system such that the z-direction is the laminate through-thickness direction. This coordinate system is also used for the stiffened panel as a whole. The blade stiffener can also be an arbitrary laminate, but, as shown, it is oriented in the x_B, y_B, z_B coordinate system with the blade through-thickness direction, z_B, corresponding to the panel y-direction. Note that the x_B-direction for the blade corresponds to the x-direction of the face sheet and panel as a whole.

The key assumption made in incorporating the blade contribution to the overall behavior of the stiffened panel is that the contribution is largely decoupled from the face sheet contribution. That is, the response of the blade in its own y_B-direction is assumed not to affect the panel and face sheet response due to the small contact region between the components. Considering first the panel mechanical behavior, the decoupling assumption is embodied by assigning the blade the following effective in-plane properties (in the local blade coordinate system),

$$\bar{E}^B_x \neq 0, \quad \bar{E}^B_y = 0, \quad \bar{\nu}^B_{xy} = 0, \quad \bar{G}^B_{xy} = 0 \tag{67}$$

Thus, in terms of its effect on the panel response, the blade will have a contribution to the axial stiffness (x-direction), but no direct stiffness contribution and no Poisson contribution in the y_B-direction (panel z-direction), and no shear contribution. $\bar{E}^B_x$ is the effective (homogenized) axial stiffness of the blade. It can be calculated from the inverse of the blade laminate extensional stiffness matrix, $\mathbf{A}^{-1}$, as,

$$\bar{E}^B_x = \frac{1}{t_B \; AI^B_{11}} \tag{68}$$

where t_B is the thickness of the blade (see fig. 3) and AI^B_{11} is the 11 component of the inverse of the blade laminate extensional stiffness matrix. Based on the effective properties given in eq. (67), the uncoupled reduced stiffness matrix of the blade is,

$$\bar{\mathbf{Q}}^u_B = \begin{bmatrix}\bar{E}^B_x & 0 & 0\\ 0 & 0 & 0\\ 0 & 0 & 0\end{bmatrix} \tag{69}$$

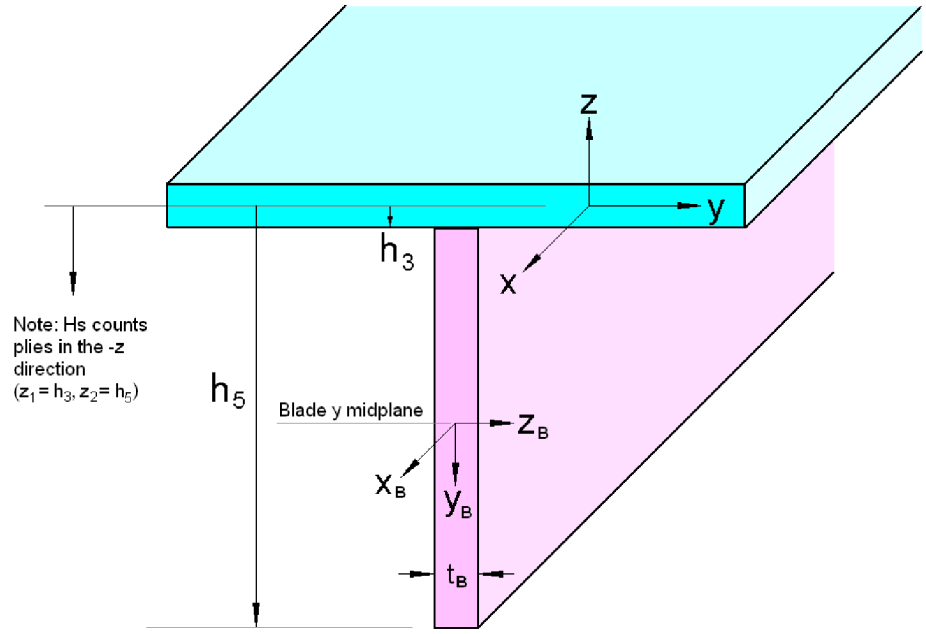

Figure 3.—Geometry of a blade stiffened panel. The face sheet is shown in blue, while the blade stiffener is shown in pink.

In the panel coordinate system (see fig. 3), the blade stiffness contribution is taken to be the volume-weighted sum of the blade uncoupled reduced stiffness matrix and the empty space between the blades along the panel y-direction. If the blade spacing (i.e., distance between adjacent blades) is denoted as S, this blade contribution is given by,

$$\bar{\mathbf{Q}}_B^{\text{cont}} = \frac{t_B \bar{\mathbf{Q}}_B^u}{S} = \frac{t_B}{S}\begin{bmatrix} \bar{E}_x^B & 0 & 0 \\ 0 & 0 & 0 \\ 0 & 0 & 0 \end{bmatrix} = \frac{1}{S\ AI_B^{11}}\begin{bmatrix} 1 & 0 & 0 \\ 0 & 0 & 0 \\ 0 & 0 & 0 \end{bmatrix} \tag{70}$$

Employing eq. (2), the blade contributions to the ABD terms with respect to the blade's midplane (see fig. 3) are given by,

$$\mathbf{A}_B^0 = \bar{\mathbf{Q}}_B^{\text{cont}}\left[-\frac{h_5 - h_3}{2} - \frac{h_5 - h_3}{2}\right] = \bar{\mathbf{Q}}_B^{\text{cont}}\left(h_3 - h_5\right) \tag{71}$$

$$\mathbf{B}_B^0 = -\frac{1}{2}\bar{\mathbf{Q}}_B^{\text{cont}}\left[\left(-\frac{h_5 - h_3}{2}\right)^2 - \left(\frac{h_5 - h_3}{2}\right)^2\right] = 0 \tag{72}$$

$$\mathbf{D}_B^0 = \frac{1}{3}\bar{\mathbf{Q}}_B^{\text{cont}}\left[\left(-\frac{h_5 - h_3}{2}\right)^3 - \left(\frac{h_5 - h_3}{2}\right)^3\right] = \frac{1}{12}\bar{\mathbf{Q}}_B^{\text{cont}}\left(h_3 - h_5\right)^3 \tag{73}$$

Shifting these terms to the midplane of the face sheet, which serves as the reference plane for the panel, using eqs. (9) to (11) with $\Delta z = \frac{h_5 + h_3}{2}$ yields,

$$\mathbf{A}_B^{\text{cont}} = \bar{\mathbf{Q}}_B^{\text{cont}} \left(h_3 - h_5 \right) \tag{74}$$

$$\mathbf{B}_B^{\text{cont}} = \frac{h_3 + h_5}{2} \bar{\mathbf{Q}}_B^{\text{cont}} \left(h_3 - h_5 \right) = \frac{1}{2} \bar{\mathbf{Q}}_B^{\text{cont}} \left(h_3^2 - h_5^2 \right) \tag{75}$$

$$\mathbf{D}_B^{\text{cont}} = \frac{1}{12} \bar{\mathbf{Q}}_B^{\text{cont}} \left(h_3 - h_5 \right)^3 + \left(\frac{h_3 + h_5}{2} \right)^2 \bar{\mathbf{Q}}_B^{\text{cont}} \left(h_3 - h_5 \right) = \frac{1}{3} \bar{\mathbf{Q}}_B^{\text{cont}} \left(h_3^3 - h_5^3 \right) \tag{76}$$

Then, as discussed in section 3, the contributions of the blade and the face sheet to the panel ABD terms can be added to yield the effective panel ABD terms (since the blade and face sheet terms are now known with respect to the same reference plane). Thus,

$$\mathbf{A}_{\text{panel}} = \mathbf{A}_{\text{FS}} + \bar{\mathbf{Q}}_B^{\text{cont}} \left(h_3 - h_5 \right) \tag{77}$$

$$\mathbf{B}_{\text{panel}} = \mathbf{B}_{\text{FS}} + \frac{1}{2} \bar{\mathbf{Q}}_B^{\text{cont}} \left(h_3^2 - h_5^2 \right) \tag{78}$$

$$\mathbf{D}_{\text{panel}} = \mathbf{D}_{\text{FS}} + \frac{1}{3} \bar{\mathbf{Q}}_B^{\text{cont}} \left(h_3^3 - h_5^3 \right) \tag{79}$$

where $\mathbf{A}_{\text{FS}}$, $\mathbf{B}_{\text{FS}}$, and $\mathbf{D}_{\text{FS}}$ are the face sheet laminate extensional, coupling, and bending stiffnesses, respectively.

Considering the thermal response of the blade stiffened panel, the decoupling of the blade from the panel thermal response indicates that only the x-direction thermal expansion of the blade will have an effect. Thus, the effective coefficients of thermal expansion (in the blade coordinate system, fig. 3) assigned to the blade for its thermal contribution are,

$$\bar{\alpha}_x^B \neq 0, \quad \bar{\alpha}_y^B = 0, \quad \bar{\alpha}_{xy}^B = 0 \tag{80}$$

$\bar{\alpha}_x^B$ is the effective thermal expansion coefficient in the x-direction. This term can be calculated by considering the inverted form of the general laminate constitutive eq. (47),

$$\begin{aligned}
\begin{bmatrix} \boldsymbol{\varepsilon}^0 \\ \boldsymbol{\kappa} \end{bmatrix} = & \begin{bmatrix} \mathbf{A}^0 & \mathbf{B}^0 \\ \mathbf{B}^0 & \mathbf{D}^0 \end{bmatrix}^{-1} \begin{bmatrix} \mathbf{N} \\ \mathbf{M} \end{bmatrix} - \begin{bmatrix} \mathbf{A}^0 & \mathbf{B}^0 \\ \mathbf{B}^0 & \mathbf{D}^0 \end{bmatrix}^{-1} \begin{bmatrix} \mathbf{A}_0^{\alpha} & \mathbf{B}_0^{\alpha} \\ \mathbf{B}_0^{\alpha} & \mathbf{D}_0^{\alpha} \end{bmatrix} \begin{bmatrix} \Delta T_0 \\ -\Delta G \end{bmatrix} \\
& - \begin{bmatrix} \mathbf{A}^0 & \mathbf{B}^0 \\ \mathbf{B}^0 & \mathbf{D}^0 \end{bmatrix}^{-1} \begin{bmatrix} \mathbf{A}_0^{E} \\ \mathbf{B}_0^{E} \end{bmatrix} \begin{bmatrix} E_x \\ E_y \\ E_z \end{bmatrix} - \begin{bmatrix} \mathbf{A}^0 & \mathbf{B}^0 \\ \mathbf{B}^0 & \mathbf{D}^0 \end{bmatrix}^{-1} \begin{bmatrix} \mathbf{A}_0^{M} \\ \mathbf{B}_0^{M} \end{bmatrix} \begin{bmatrix} H_x \\ H_y \\ H_z \end{bmatrix} \\
& - \begin{bmatrix} \mathbf{A}^0 & \mathbf{B}^0 \\ \mathbf{B}^0 & \mathbf{D}^0 \end{bmatrix}^{-1} \begin{bmatrix} \mathbf{A}_0^{ET} & \mathbf{B}_0^{ET} \\ \mathbf{B}_0^{ET} & \mathbf{D}_0^{ET} \end{bmatrix} \begin{bmatrix} \Delta T_0 \\ -\Delta G \end{bmatrix} - \begin{bmatrix} \mathbf{A}^0 & \mathbf{B}^0 \\ \mathbf{B}^0 & \mathbf{D}^0 \end{bmatrix}^{-1} \begin{bmatrix} \mathbf{A}_0^{MT} & \mathbf{B}_0^{MT} \\ \mathbf{B}_0^{MT} & \mathbf{D}_0^{MT} \end{bmatrix} \begin{bmatrix} \Delta T_0 \\ -\Delta G \end{bmatrix}
\end{aligned} \tag{81}$$

Clearly, a thermal matrix can be identified as "CTE-like", and, as identified by Collier (1993) (ref. 29),

$$\begin{bmatrix} \mathbf{A}^0 & \mathbf{B}^0 \\ \mathbf{B}^0 & \mathbf{D}^0 \end{bmatrix}^{-1} \begin{bmatrix} \mathbf{A}_0^\alpha & \mathbf{B}_0^\alpha \\ \mathbf{B}_0^\alpha & \mathbf{D}_0^\alpha \end{bmatrix} = \begin{bmatrix} \boldsymbol{\alpha}_{\text{lam}} & \boldsymbol{\delta}_{\text{lam}}^{\text{coupling}} \\ \boldsymbol{\alpha}_{\text{lam}}^{\text{coupling}} & \boldsymbol{\delta}_{\text{lam}} \end{bmatrix} \tag{82}$$

where $\boldsymbol{\alpha}_{\text{lam}}$ is a 3×1 vector relating strain to temperature change, $\boldsymbol{\alpha}_{\text{lam}}^{\text{coupling}}$ is a 3×1 vector relating curvature to temperature change, $\boldsymbol{\delta}_{\text{lam}}^{\text{coupling}}$ is a 3×1 vector relating strain to through-thickness temperature gradient, and $\boldsymbol{\delta}_{\text{lam}}$ is a 3×1 vector relating curvature to through-thickness temperature gradient. The x-direction effective thermal expansion coefficient for the laminate is then simply the first component of $\boldsymbol{\alpha}_{\text{lam}}$, that is,

$$\bar{\alpha}_x^B = \left(\alpha_{\text{lam}}\right)_1 \tag{83}$$

where $\left(\alpha_{\text{lam}}\right)_1$ is the 1,1 component of the 6×2 matrix formed by eq. (82), and the blade CTE vector is given by,

$$\bar{\boldsymbol{\alpha}}_B = \begin{bmatrix} \bar{\alpha}_x^B \\ 0 \\ 0 \end{bmatrix} \tag{84}$$

Employing eq. (15), the blade contributions to the panel thermal ABD terms with respect to the blade's midplane (see fig. 3) are given by,

$$\left(\mathbf{A}_B^\alpha\right)^0 = \bar{\mathbf{Q}}_B^{\text{cont}}\,\bar{\boldsymbol{\alpha}}_B \left[-\frac{h_5 - h_3}{2} \quad -\frac{h_5 - h_3}{2}\right] = \bar{\mathbf{Q}}_B^{\text{cont}}\,\bar{\boldsymbol{\alpha}}_B \left(h_3 - h_5\right) \tag{85}$$

$$\left(\mathbf{B}_B^\alpha\right)^0 = -\frac{1}{2}\bar{\mathbf{Q}}_B^{\text{cont}}\,\bar{\boldsymbol{\alpha}}_B \left[\left(-\frac{h_5 - h_3}{2}\right)^2 - \left(\frac{h_5 - h_3}{2}\right)^2\right] = 0 \tag{86}$$

$$\left(\mathbf{D}_B^\alpha\right)^0 = \frac{1}{3}\bar{\mathbf{Q}}_B^{\text{cont}}\,\bar{\boldsymbol{\alpha}}_B \left[\left(-\frac{h_5 - h_3}{2}\right)^3 - \left(\frac{h_5 - h_3}{2}\right)^3\right] = \frac{1}{12}\bar{\mathbf{Q}}_B^{\text{cont}}\,\bar{\boldsymbol{\alpha}}_B \left(h_3 - h_5\right)^3 \tag{87}$$

Shifting these terms to the midplane of the face sheet, which serves as the reference plane for the panel, using eqs. (21), (23), and (27) with $\Delta z = \dfrac{h_5 + h_3}{2}$ yields,

$$\left(\mathbf{A}_B^\alpha\right)^{\text{cont}} = \bar{\mathbf{Q}}_B^{\text{cont}}\,\bar{\boldsymbol{\alpha}}_B \left(h_3 - h_5\right) \tag{88}$$

$$\left(\mathbf{B}_B^\alpha\right)^{\text{cont}} = \frac{h_3 + h_5}{2}\bar{\mathbf{Q}}_B^{\text{cont}}\,\bar{\boldsymbol{\alpha}}_B \left(h_3 - h_5\right) = \frac{1}{2}\bar{\mathbf{Q}}_B^{\text{cont}}\,\bar{\boldsymbol{\alpha}}_B \left(h_3^2 - h_5^2\right) \tag{89}$$

$$\left(\mathbf{D}_B^{\alpha}\right)^{\text{cont}} = \frac{1}{12}\bar{\mathbf{Q}}_B^{\text{cont}}\,\bar{\boldsymbol{\alpha}}_B\left(h_3 - h_5\right)^3 + \left(\frac{h_3 + h_5}{2}\right)^2 \bar{\mathbf{Q}}_B^{\text{cont}}\,\bar{\boldsymbol{\alpha}}_B\left(h_3 - h_5\right) = \frac{1}{3}\bar{\mathbf{Q}}_B^{\text{cont}}\,\bar{\boldsymbol{\alpha}}_B\left(h_3^3 - h_5^3\right) \tag{90}$$

Then, as discussed in section 3, the contributions of the blade and the face sheet to the panel thermal ABD terms can be added to yield the effective panel thermal ABD terms (since the blade and face sheet terms are now known with respect to the same reference plane). Thus,

$$\mathbf{A}_{\text{panel}}^{\alpha} = \mathbf{A}_{\text{FS}}^{\alpha} + \bar{\mathbf{Q}}_B^{\text{cont}}\,\bar{\boldsymbol{\alpha}}_B\left(h_3 - h_5\right) \tag{91}$$

$$\mathbf{B}_{\text{panel}}^{\alpha} = \mathbf{B}_{\text{FS}}^{\alpha} + \frac{1}{2}\bar{\mathbf{Q}}_B^{\text{cont}}\,\bar{\boldsymbol{\alpha}}_B\left(h_3^2 - h_5^2\right) \tag{92}$$

$$\mathbf{D}_{\text{panel}}^{\alpha} = \mathbf{D}_{\text{FS}}^{\alpha} + \frac{1}{3}\bar{\mathbf{Q}}_B^{\text{cont}}\,\bar{\boldsymbol{\alpha}}_B\left(h_3^3 - h_5^3\right) \tag{93}$$

where $\mathbf{A}_{\text{FS}}^{\alpha}$, $\mathbf{B}_{\text{FS}}^{\alpha}$, and $\mathbf{D}_{\text{FS}}^{\alpha}$ are the face sheet laminate thermal ABD matrices.

A similar treatment applies to the thermo-electro-magnetic terms. The decoupling of the blade from the panel thermo-electro-magnetic response indicates that only the *x*-direction electric, magnetic, thermo-electric, and thermo-magnetic expansion of the blade will have an effect. Thus, the effective piezoelectric, piezomagnetic, pyroelectric and pyromagnetic coefficients (in the blade coordinate system, fig. 3) assigned to the blade for its thermo-electro-magnetic contributions are,

$$\bar{\mathbf{e}}_B = \begin{bmatrix} \bar{e}_{11}^B & \bar{e}_{21}^B & \bar{e}_{31}^B \\ 0 & 0 & 0 \\ 0 & 0 & 0 \\ 0 & 0 & 0 \\ 0 & 0 & 0 \\ 0 & 0 & 0 \end{bmatrix} \tag{94}$$

$$\bar{\mathbf{q}}_B = \begin{bmatrix} \bar{q}_{11}^B & \bar{q}_{21}^B & \bar{q}_{31}^B \\ 0 & 0 & 0 \\ 0 & 0 & 0 \\ 0 & 0 & 0 \\ 0 & 0 & 0 \\ 0 & 0 & 0 \end{bmatrix} \tag{95}$$

$$\bar{\boldsymbol{\zeta}}_B = \begin{bmatrix} \bar{\zeta}_1^B \\ 0 \\ 0 \end{bmatrix} \tag{96}$$

$$\bar{\Psi}_B = \begin{bmatrix} \bar{\Psi}_1^B \\ 0 \\ 0 \end{bmatrix} \tag{97}$$

where $\bar{e}_{ij}^B$, $\bar{q}_{ij}^B$, $\bar{\zeta}_1^B$, and $\bar{\Psi}_1^B$ are the effective piezoelectric, piezomagnetic, pyroelectric, and pyromagnetic coefficients, respectively, that influence the x-direction. In eq. (81) the following identifications can be made,

$$\begin{bmatrix} \mathbf{A}^0 & \mathbf{B}^0 \\ \mathbf{B}^0 & \mathbf{D}^0 \end{bmatrix}^{-1} \begin{bmatrix} \mathbf{A}_0^E \\ \mathbf{B}_0^E \end{bmatrix} = \begin{bmatrix} \mathbf{e}_{\text{lam}} \\ \mathbf{e}_{\text{lam}}^{\text{coupling}} \end{bmatrix} \tag{98}$$

$$\begin{bmatrix} \mathbf{A}^0 & \mathbf{B}^0 \\ \mathbf{B}^0 & \mathbf{D}^0 \end{bmatrix}^{-1} \begin{bmatrix} \mathbf{A}_0^M \\ \mathbf{B}_0^M \end{bmatrix} = \begin{bmatrix} \mathbf{q}_{\text{lam}} \\ \mathbf{q}_{\text{lam}}^{\text{coupling}} \end{bmatrix} \tag{99}$$

$$\begin{bmatrix} \mathbf{A}^0 & \mathbf{B}^0 \\ \mathbf{B}^0 & \mathbf{D}^0 \end{bmatrix}^{-1} \begin{bmatrix} \mathbf{A}_0^{ET} & \mathbf{B}_0^{ET} \\ \mathbf{B}_0^{ET} & \mathbf{D}_0^{ET} \end{bmatrix} = \begin{bmatrix} \boldsymbol{\alpha}\mathbf{e}_{\text{lam}} & \boldsymbol{\delta}\mathbf{e}_{\text{lam}}^{\text{coupling}} \\ \boldsymbol{\alpha}\mathbf{e}_{\text{lam}}^{\text{coupling}} & \boldsymbol{\delta}\mathbf{e}_{\text{lam}} \end{bmatrix} \tag{100}$$

$$\begin{bmatrix} \mathbf{A}^0 & \mathbf{B}^0 \\ \mathbf{B}^0 & \mathbf{D}^0 \end{bmatrix}^{-1} \begin{bmatrix} \mathbf{A}_0^{MT} & \mathbf{B}_0^{MT} \\ \mathbf{B}_0^{MT} & \mathbf{D}_0^{MT} \end{bmatrix} = \begin{bmatrix} \boldsymbol{\alpha}\mathbf{q}_{\text{lam}} & \boldsymbol{\delta}\mathbf{q}_{\text{lam}}^{\text{coupling}} \\ \boldsymbol{\alpha}\mathbf{q}_{\text{lam}}^{\text{coupling}} & \boldsymbol{\delta}\mathbf{q}_{\text{lam}} \end{bmatrix} \tag{101}$$

where $\mathbf{e}_{\text{lam}}$ and $\mathbf{q}_{\text{lam}}$ are 3×3 matrices relating strain to electric and magnetic field, respectively, $\mathbf{e}_{\text{lam}}^{\text{coupling}}$ and $\mathbf{q}_{\text{lam}}^{\text{coupling}}$ are 3×3 matrices relating curvature to electric and magnetic field, respectively, $\boldsymbol{\alpha}\mathbf{e}_{\text{lam}}$ and $\boldsymbol{\alpha}\mathbf{q}_{\text{lam}}$ are 3×1 vectors relating strain to temperature changes (due to thermo-electric and thermo-magnetic coupling, respectively), $\boldsymbol{\alpha}\mathbf{e}_{\text{lam}}^{\text{coupling}}$ and $\boldsymbol{\alpha}\mathbf{q}_{\text{lam}}^{\text{coupling}}$ are 3×1 matrices relating curvature to temperature change (due to thermo-electric and thermo-magnetic coupling, respectively), $\boldsymbol{\delta}\mathbf{e}_{\text{lam}}^{\text{coupling}}$ and $\boldsymbol{\delta}\mathbf{q}_{\text{lam}}^{\text{coupling}}$ are 3×1 matrices relating strain to through-thickness temperature gradient (due to thermo-electric and thermo-magnetic coupling, respectively), and $\boldsymbol{\delta}\mathbf{e}_{\text{lam}}$ and $\boldsymbol{\delta}\mathbf{q}_{\text{lam}}$ are 3×1 matrices relating curvature to through-thickness temperature gradient (due to thermo-electric and thermo-magnetic coupling, respectively).

As was the case for the blade thermal expansion coefficients, the thermo-electro-magnetic coefficients present in eqs. (94) to (97) can be extracted from eqs. (98) to (101). The $\bar{e}_{ij}^B$ and $\bar{q}_{ij}^B$ terms are simply the first rows of the $\mathbf{e}_{\text{lam}}$ matrix and the $\mathbf{q}_{\text{lam}}$ matrix, respectively, while $\bar{\zeta}_1^B$, and $\bar{\Psi}_1^B$ are simply the first term in the $\boldsymbol{\alpha}\mathbf{e}_{\text{lam}}$ and $\boldsymbol{\alpha}\mathbf{q}_{\text{lam}}$ vectors.

Employing eqs. (36), (38), (45), and (46), the blade contributions to the panel electric, magnetic, thermo-electric, and thermo-magnetic ABD terms with respect to the blade's midplane (see fig. 3) are given by,

$$\left(\mathbf{A}_B^E\right)^0 = \bar{\mathbf{Q}}_B^{\text{cont}}\,\bar{\mathbf{e}}_B\left[-\frac{h_5-h_3}{2}-\frac{h_5-h_3}{2}\right]_{\rfloor}^{\lceil} = \bar{\mathbf{Q}}_B^{\text{cont}}\,\bar{\mathbf{e}}_B\left(h_3-h_5\right) \tag{102}$$

$$\left(\mathbf{B}_B^E\right)^0 = -\frac{1}{2}\bar{\mathbf{Q}}_B^{\text{cont}}\,\bar{\mathbf{e}}_B\left[\left(-\frac{h_5-h_3}{2}\right)^2-\left(\frac{h_5-h_3}{2}\right)^2\right]_{\rfloor}^{\lceil} = 0 \tag{103}$$

$$\left(\mathbf{A}_B^M\right)^0 = \bar{\mathbf{Q}}_B^{\text{cont}}\,\bar{\mathbf{q}}_B\left[-\frac{h_5-h_3}{2}-\frac{h_5-h_3}{2}\right]_{\rfloor}^{\lceil} = \bar{\mathbf{Q}}_B^{\text{cont}}\,\bar{\mathbf{q}}_B\left(h_3-h_5\right) \tag{104}$$

$$\left(\mathbf{B}_B^M\right)^0 = -\frac{1}{2}\bar{\mathbf{Q}}_B^{\text{cont}}\,\bar{\mathbf{q}}_B\left[\left(-\frac{h_5-h_3}{2}\right)^2-\left(\frac{h_5-h_3}{2}\right)^2\right]_{\rfloor}^{\lceil} = 0 \tag{105}$$

$$\left(\mathbf{A}_B^{ET}\right)^0 = \bar{\mathbf{Q}}_B^{\text{cont}}\,\bar{\boldsymbol{\zeta}}_B\left[-\frac{h_5-h_3}{2}-\frac{h_5-h_3}{2}\right]_{\rfloor}^{\lceil} = \bar{\mathbf{Q}}_B^{\text{cont}}\,\bar{\boldsymbol{\zeta}}_B\left(h_3-h_5\right) \tag{106}$$

$$\left(\mathbf{B}_B^{ET}\right)^0 = -\frac{1}{2}\bar{\mathbf{Q}}_B^{\text{cont}}\,\bar{\boldsymbol{\zeta}}_B\left[\left(-\frac{h_5-h_3}{2}\right)^2-\left(\frac{h_5-h_3}{2}\right)^2\right]_{\rfloor}^{\lceil} = 0 \tag{107}$$

$$\left(\mathbf{D}_B^{ET}\right)^0 = \frac{1}{3}\bar{\mathbf{Q}}_B^{\text{cont}}\,\bar{\boldsymbol{\zeta}}_B\left[\left(-\frac{h_5-h_3}{2}\right)^3-\left(\frac{h_5-h_3}{2}\right)^3\right]_{\rfloor}^{\lceil} = \frac{1}{12}\bar{\mathbf{Q}}_B^{\text{cont}}\,\bar{\boldsymbol{\zeta}}_B\left(h_3-h_5\right)^3 \tag{108}$$

$$\left(\mathbf{A}_B^{MT}\right)^0 = \bar{\mathbf{Q}}_B^{\text{cont}}\,\bar{\boldsymbol{\Psi}}_B\left[-\frac{h_5-h_3}{2}-\frac{h_5-h_3}{2}\right]_{\rfloor}^{\lceil} = \bar{\mathbf{Q}}_B^{\text{cont}}\,\bar{\boldsymbol{\Psi}}_B\left(h_3-h_5\right) \tag{109}$$

$$\left(\mathbf{B}_B^{MT}\right)^0 = -\frac{1}{2}\bar{\mathbf{Q}}_B^{\text{cont}}\,\bar{\boldsymbol{\Psi}}_B\left[\left(-\frac{h_5-h_3}{2}\right)^2-\left(\frac{h_5-h_3}{2}\right)^2\right]_{\rfloor}^{\lceil} = 0 \tag{110}$$

$$\left(\mathbf{D}_B^{MT}\right)^0 = \frac{1}{3}\bar{\mathbf{Q}}_B^{\text{cont}}\,\bar{\boldsymbol{\Psi}}_B\left[\left(-\frac{h_5-h_3}{2}\right)^3-\left(\frac{h_5-h_3}{2}\right)^3\right]_{\rfloor}^{\lceil} = \frac{1}{12}\bar{\mathbf{Q}}_B^{\text{cont}}\,\bar{\boldsymbol{\Psi}}_B\left(h_3-h_5\right)^3 \tag{111}$$

Shifting these terms to the midplane of the face sheet, which serves as the reference plane for the panel, using eqs. (48, 49) with $\Delta z = \dfrac{h_5+h_3}{2}$ yields,

$$\left(\mathbf{A}_B^E\right)^{\text{cont}} = \bar{\mathbf{Q}}_B^{\text{cont}}\,\bar{\mathbf{e}}_B\left(h_3-h_5\right) \tag{112}$$

$$\left(\mathbf{B}_B^E\right)^{\text{cont}} = \frac{h_3+h_5}{2}\bar{\mathbf{Q}}_B^{\text{cont}}\,\bar{\mathbf{e}}_B\left(h_3-h_5\right) = \frac{1}{2}\bar{\mathbf{Q}}_B^{\text{cont}}\,\bar{\mathbf{e}}_B\left(h_3^2-h_5^2\right) \tag{113}$$

$$\left(\mathbf{A}_B^M\right)^{\text{cont}} = \bar{\mathbf{Q}}_B^{\text{cont}}\,\bar{\mathbf{q}}_B\left(h_3 - h_5\right) \tag{114}$$

$$\left(\mathbf{B}_B^M\right)^{\text{cont}} = \frac{h_3 + h_5}{2}\bar{\mathbf{Q}}_B^{\text{cont}}\,\bar{\mathbf{q}}_B\left(h_3 - h_5\right) = \frac{1}{2}\bar{\mathbf{Q}}_B^{\text{cont}}\,\bar{\mathbf{q}}_B\left(h_3^2 - h_5^2\right) \tag{115}$$

$$\left(\mathbf{A}_B^{ET}\right)^{\text{cont}} = \bar{\mathbf{Q}}_B^{\text{cont}}\,\bar{\boldsymbol{\zeta}}_B\left(h_3 - h_5\right) \tag{116}$$

$$\left(\mathbf{B}_B^{ET}\right)^{\text{cont}} = \frac{h_3 + h_5}{2}\bar{\mathbf{Q}}_B^{\text{cont}}\,\bar{\boldsymbol{\zeta}}_B\left(h_3 - h_5\right) = \frac{1}{2}\bar{\mathbf{Q}}_B^{\text{cont}}\,\bar{\boldsymbol{\zeta}}_B\left(h_3^2 - h_5^2\right) \tag{117}$$

$$\left(\mathbf{D}_B^{ET}\right)^{\text{cont}} = \frac{1}{12}\bar{\mathbf{Q}}_B^{\text{cont}}\,\bar{\boldsymbol{\zeta}}_B\left(h_3 - h_5\right)^3 + \left(\frac{h_3 + h_5}{2}\right)^2\bar{\mathbf{Q}}_B^{\text{cont}}\,\bar{\boldsymbol{\zeta}}_B\left(h_3 - h_5\right) = \frac{1}{3}\bar{\mathbf{Q}}_B^{\text{cont}}\,\bar{\boldsymbol{\alpha}}_B\left(h_3^3 - h_5^3\right) \tag{118}$$

$$\left(\mathbf{A}_B^{MT}\right)^{\text{cont}} = \bar{\mathbf{Q}}_B^{\text{cont}}\,\bar{\boldsymbol{\Psi}}_B\left(h_3 - h_5\right) \tag{119}$$

$$\left(\mathbf{B}_B^{MT}\right)^{\text{cont}} = \frac{h_3 + h_5}{2}\bar{\mathbf{Q}}_B^{\text{cont}}\,\bar{\boldsymbol{\Psi}}_B\left(h_3 - h_5\right) = \frac{1}{2}\bar{\mathbf{Q}}_B^{\text{cont}}\,\bar{\boldsymbol{\Psi}}_B\left(h_3^2 - h_5^2\right) \tag{120}$$

$$\left(\mathbf{D}_B^{MT}\right)^{\text{cont}} = \frac{1}{12}\bar{\mathbf{Q}}_B^{\text{cont}}\,\bar{\boldsymbol{\Psi}}_B\left(h_3 - h_5\right)^3 + \left(\frac{h_3 + h_5}{2}\right)^2\bar{\mathbf{Q}}_B^{\text{cont}}\,\bar{\boldsymbol{\Psi}}_B\left(h_3 - h_5\right) = \frac{1}{3}\bar{\mathbf{Q}}_B^{\text{cont}}\,\bar{\boldsymbol{\alpha}}_B\left(h_3^3 - h_5^3\right) \tag{121}$$

Then, as discussed in section 3, the contributions of the blade and the face sheet to the panel electric, magnetic, thermo-electric, and thermo-magnetic ABD terms can be added to yield the corresponding effective panel ABD terms (since the blade and face sheet terms are now known with respect to the same reference plane). Thus,

$$\mathbf{A}_{\text{panel}}^E = \mathbf{A}_{\text{FS}}^E + \bar{\mathbf{Q}}_B^{\text{cont}}\,\bar{\mathbf{e}}_B\left(h_3 - h_5\right) \tag{122}$$

$$\mathbf{B}_{\text{panel}}^E = \mathbf{B}_{\text{FS}}^E + \frac{1}{2}\bar{\mathbf{Q}}_B^{\text{cont}}\,\bar{\mathbf{e}}_B\left(h_3^2 - h_5^2\right) \tag{123}$$

$$\mathbf{A}_{\text{panel}}^M = \mathbf{A}_{\text{FS}}^M + \bar{\mathbf{Q}}_B^{\text{cont}}\,\bar{\mathbf{q}}_B\left(h_3 - h_5\right) \tag{124}$$

$$\mathbf{B}_{\text{panel}}^M = \mathbf{B}_{\text{FS}}^M + \frac{1}{2}\bar{\mathbf{Q}}_B^{\text{cont}}\,\bar{\mathbf{q}}_B\left(h_3^2 - h_5^2\right) \tag{125}$$

$$\mathbf{A}_{\text{panel}}^{ET} = \mathbf{A}_{\text{FS}}^{ET} + \bar{\mathbf{Q}}_B^{\text{cont}}\,\bar{\boldsymbol{\zeta}}_B\left(h_3 - h_5\right) \tag{126}$$

$$\mathbf{B}_{\text{panel}}^{ET} = \mathbf{B}_{\text{FS}}^{ET} + \frac{1}{2}\bar{\mathbf{Q}}_B^{\text{cont}}\,\bar{\boldsymbol{\zeta}}_B\left(h_3^2 - h_5^2\right) \tag{127}$$

$$\mathbf{D}_{\text{panel}}^{ET} = \mathbf{D}_{\text{FS}}^{ET} + \frac{1}{3}\bar{\mathbf{Q}}_B^{\text{cont}}\,\bar{\zeta}_B\left(h_3^3 - h_5^3\right) \tag{128}$$

$$\mathbf{A}_{\text{panel}}^{MT} = \mathbf{A}_{\text{FS}}^{MT} + \bar{\mathbf{Q}}_B^{\text{cont}}\,\bar{\Psi}_B\left(h_3 - h_5\right) \tag{129}$$

$$\mathbf{B}_{\text{panel}}^{MT} = \mathbf{B}_{\text{FS}}^{MT} + \frac{1}{2}\bar{\mathbf{Q}}_B^{\text{cont}}\,\bar{\Psi}_B\left(h_3^2 - h_5^2\right) \tag{130}$$

$$\mathbf{D}_{\text{panel}}^{MT} = \mathbf{D}_{\text{FS}}^{MT} + \frac{1}{3}\bar{\mathbf{Q}}_B^{\text{cont}}\,\bar{\Psi}_B\left(h_3^3 - h_5^3\right) \tag{131}$$

where $\mathbf{A}_{\text{FS}}^{\bullet}$, $\mathbf{B}_{\text{FS}}^{\bullet}$, and $\mathbf{D}_{\text{FS}}^{\bullet}$ are the face sheet laminate electric, magnetic, thermo-electric, and thermo-magnetic ABD matrices.

It should be noted that if the blade stiffened panel includes a bottom face sheet, its contribution can be included by simply shifting its mechanical, thermal, electric, magnetic, thermo-electric, and thermo-magnetic ABD terms to the face sheet midplane according to eqs. (9) to (11), (21), (23), (27), (48), and (49) and adding these shifted terms to the corresponding panel ABD terms.

5. Analysis of Panels with Flanged Stiffeners

Considering a flanged stiffened panel, as shown in figure 4, the outlined region is referred to as "Segment 8". Comparing figure 4 to figure 3, it is clear that the only difference between the flanged stiffened panel and the blade stiffened panel is the presence of the flange. Thus, the development of effective ABD terms for the flanged stiffened panel necessitates only the additional analysis of Segment 8. As shown in figure 5, Segment 8 is composed of two other segments, Segments 1 and 6.

In the *x*-direction, which is the direction of the stiffener (and thus the strong direction), iso-strain and iso-curvature conditions are employed. It is further assumed that the homogenized Segment 8 *x*-direction force and moment resultants are the sum of the volume-weighted *x*-direction force and moment resultants of the constituent segments (Segment 1 and 6). This is analogous to the "mechanics of materials" micromechanics approach presented by Herakovich (ref. 28) that homogenizes continuous fiber composites to obtain effective properties. The conditions employed for the stiffener direction are,

$$\left(\varepsilon_{xx}^0\right)^1 = \left(\varepsilon_{xx}^0\right)^6 = \left(\varepsilon_{xx}^0\right)^8 \tag{132}$$

$$\left(\kappa_{xx}\right)^1 = \left(\kappa_{xx}\right)^6 = \left(\kappa_{xx}\right)^8 \tag{133}$$

$$\left(N_{xx}\right)^8 = \frac{1}{S_x}\left[\left(FWNT\right)\left(N_{xx}\right)^1 + \left(WNT\right)\left(N_{xx}\right)^6\right] \tag{134}$$

$$\left(M_{xx}\right)^8 = \frac{1}{S_x}\left[\left(FWNT\right)\left(M_{xx}\right)^1 + \left(WNT\right)\left(M_{xx}\right)^6\right] \tag{135}$$

where *Sx* is the stiffener spacing, *FWNT* is the distance between flanges, and *WNT* is the flange width.

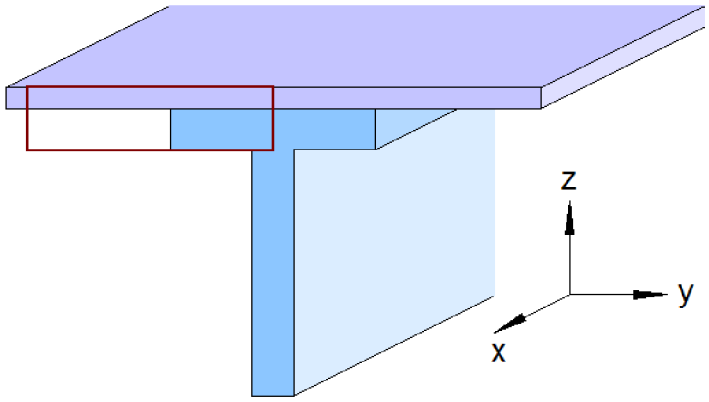

Figure 4.—A flanged stiffened panel with the segment 8 region outlined.

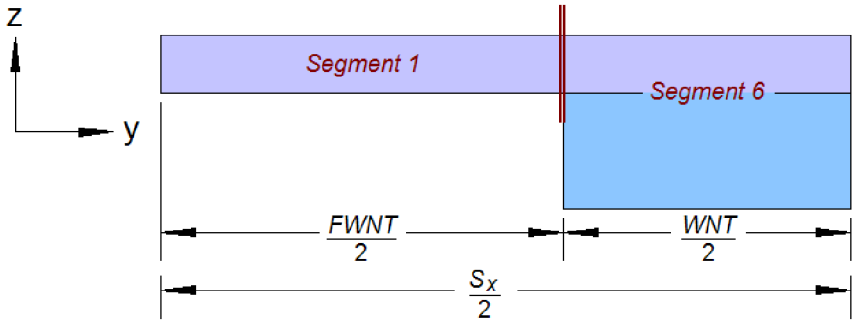

Figure 5.—The Segment 8 region divided into Segments 1 and 6.

In the *y*-direction and for the in plane shear effect (*xy*-components), the converse assumptions are employed. That is, iso-force and moment resultant conditions are imposed, along with volume-weighted summing for the strain and curvature components. These conditions are,

$$\left(N_{yy}\right)^1 = \left(N_{yy}\right)^6 = \left(N_{yy}\right)^8 \tag{136}$$

$$\left(N_{xy}\right)^1 = \left(N_{xy}\right)^6 = \left(N_{xy}\right)^8 \tag{137}$$

$$\left(M_{yy}\right)^1 = \left(M_{yy}\right)^6 = \left(M_{yy}\right)^8 \tag{138}$$

$$\left(M_{xy}\right)^1 = \left(M_{xy}\right)^6 = \left(M_{xy}\right)^8 \tag{139}$$

$$\left(\varepsilon^0_{yy}\right)^8 = \frac{1}{S_x}\left[(FWNT)\left(\varepsilon^0_{yy}\right)^1 + (WNT)\left(\varepsilon^0_{yy}\right)^6\right] \tag{140}$$

$$\left(\gamma^0_{xy}\right)^8 = \frac{1}{S_x}\left[(FWNT)\left(\gamma^0_{xy}\right)^1 + (WNT)\left(\gamma^0_{xy}\right)^6\right] \tag{141}$$

$$(\kappa_{xx})^8 = \frac{1}{S_x}\left[(FWNT)(\kappa_{xx})^1 + (WNT)(\kappa_{xx})^6\right] \tag{142}$$

$$(\kappa_{xy})^8 = \frac{1}{S_x}\left[(FWNT)(\kappa_{xy})^1 + (WNT)(\kappa_{xy})^6\right] \tag{143}$$

The constitutive equation for each segment is given by,

$$\begin{bmatrix} N_{xx} \\ N_{yy} \\ N_{xy} \\ M_{xx} \\ M_{yy} \\ M_{xy} \end{bmatrix} = \begin{bmatrix} \mathbf{A} & \mathbf{B} \\ \mathbf{B}^{\mathrm{T}} & \mathbf{D} \end{bmatrix} \begin{bmatrix} \varepsilon^0_{xx} \\ \varepsilon^0_{yy} \\ \gamma^0_{xy} \\ \kappa_{xx} \\ \kappa_{yy} \\ \kappa_{xy} \end{bmatrix} - \begin{bmatrix} \mathbf{A}^{\alpha} & \mathbf{B}^{\alpha} \\ \mathbf{B}^{\alpha} & \mathbf{D}^{\alpha} \end{bmatrix} \begin{bmatrix} \Delta T \\ -\Delta G \end{bmatrix} - \begin{bmatrix} \mathbf{A}^{E} \\ \mathbf{B}^{E} \end{bmatrix} \begin{bmatrix} E_1 \\ E_2 \\ E_3 \end{bmatrix} - \begin{bmatrix} \mathbf{A}^{M} \\ \mathbf{B}^{M} \end{bmatrix} \begin{bmatrix} H_1 \\ H_2 \\ H_3 \end{bmatrix} - \begin{bmatrix} \mathbf{A}^{ET} & \mathbf{B}^{ET} \\ \mathbf{B}^{ET} & \mathbf{D}^{ET} \end{bmatrix} \begin{bmatrix} \Delta T \\ -\Delta G \end{bmatrix} - \begin{bmatrix} \mathbf{A}^{MT} & \mathbf{B}^{MT} \\ \mathbf{B}^{MT} & \mathbf{D}^{MT} \end{bmatrix} \begin{bmatrix} \Delta T \\ -\Delta G \end{bmatrix} \tag{144}$$

where $\mathbf{B}^{\mathrm{T}}$ is the transpose of the **B** matrix, which is necessary because the **B** matrix itself is typically asymmetric for Segment 8 (although the ABD matrix remains symmetric). The equations are rearranged such that all components that fall under the iso-assumptions appear on the left hand side,

$$\begin{bmatrix} \varepsilon^0_{xx} \\ N_{yy} \\ N_{xy} \\ \kappa_{xx} \\ M_{yy} \\ M_{xy} \end{bmatrix} = \left[\hat{\mathbf{C}}\right] \begin{bmatrix} N_{xx} \\ \varepsilon^0_{yy} \\ \gamma^0_{xy} \\ M_{xx} \\ \kappa_{yy} \\ \kappa_{xy} \end{bmatrix} - \left[\hat{\mathbf{C}}^{\alpha}\right] \begin{bmatrix} \Delta T \\ -\Delta G \end{bmatrix} - \left[\hat{\mathbf{C}}^{E}\right] \begin{bmatrix} E_1 \\ E_2 \\ E_3 \end{bmatrix} - \left[\hat{\mathbf{C}}^{M}\right] \begin{bmatrix} H_1 \\ H_2 \\ H_3 \end{bmatrix} - \left[\hat{\mathbf{C}}^{ET}\right] \begin{bmatrix} \Delta T \\ -\Delta G \end{bmatrix} - \left[\hat{\mathbf{C}}^{MT}\right] \begin{bmatrix} \Delta T \\ -\Delta G \end{bmatrix} \tag{145}$$

or, in simplified notation,

$$(\mathbf{R_A}) = \left[\hat{\mathbf{C}}\right](\mathbf{R_B}) - \left[\hat{\mathbf{C}}^{\alpha}\right] \begin{bmatrix} \Delta T \\ -\Delta G \end{bmatrix} - \left[\hat{\mathbf{C}}^{E}\right] \begin{bmatrix} E_1 \\ E_2 \\ E_3 \end{bmatrix} - \left[\hat{\mathbf{C}}^{M}\right] \begin{bmatrix} H_1 \\ H_2 \\ H_3 \end{bmatrix} - \left[\hat{\mathbf{C}}^{ET}\right] \begin{bmatrix} \Delta T \\ -\Delta G \end{bmatrix} - \left[\hat{\mathbf{C}}^{MT}\right] \begin{bmatrix} \Delta T \\ -\Delta G \end{bmatrix} \tag{146}$$

where the hatted matrices represent ABD matrices altered via the rearrangement required in forming eq. (145) from eq. (144). Solving eq. (146) for $\mathbf{R_B}$ yields,

$$(\mathbf{R_B}) = \left[\hat{\mathbf{C}}\right]^{-1}\left\{(\mathbf{R_A}) + \left[\hat{\mathbf{C}}^{\alpha}\right]\begin{bmatrix}\Delta T\\ -\Delta G\end{bmatrix} + \left[\hat{\mathbf{C}}^{E}\right]\begin{bmatrix}E_1\\ E_2\\ E_3\end{bmatrix} + \left[\hat{\mathbf{C}}^{M}\right]\begin{bmatrix}H_1\\ H_2\\ H_3\end{bmatrix} + \left[\hat{\mathbf{C}}^{ET}\right]\begin{bmatrix}\Delta T\\ -\Delta G\end{bmatrix} + \left[\hat{\mathbf{C}}^{MT}\right]\begin{bmatrix}\Delta T\\ -\Delta G\end{bmatrix}\right\} \tag{147}$$

Now, employing the above simplified notation, all of the iso-assumptions can be expressed as,

$$(\mathbf{R_A})^1 = (\mathbf{R_A})^6 = (\mathbf{R_A})^8 \tag{148}$$

while all of the volume-weighted summation assumptions can be expressed as,

$$(\mathbf{R_B})^8 = \frac{1}{S_x}\left[(FWNT)(\mathbf{R_B})^1 + (WNT)(\mathbf{R_B})^6\right] \tag{149}$$

The $\mathbf{R_B}$ vector for each segment in eq. (149) can be replaced with the expression from eq. (147),

$$\begin{aligned} S_x\left[\hat{\mathbf{C}}^8\right]^{-1}\Bigg\{&(\mathbf{R_A}) + \left[\hat{\mathbf{C}}^{\alpha 8}\right]\begin{bmatrix}\Delta T\\ -\Delta G\end{bmatrix} + \left[\hat{\mathbf{C}}^{E8}\right]\begin{bmatrix}E_1\\ E_2\\ E_3\end{bmatrix} + \left[\hat{\mathbf{C}}^{M8}\right]\begin{bmatrix}H_1\\ H_2\\ H_3\end{bmatrix} + \left[\hat{\mathbf{C}}^{ET8}\right]\begin{bmatrix}\Delta T\\ -\Delta G\end{bmatrix} \\ &+ \left[\hat{\mathbf{C}}^{MT8}\right]\begin{bmatrix}\Delta T\\ -\Delta G\end{bmatrix}\Bigg\} = (FWNT)\left[\hat{\mathbf{C}}^1\right]^{-1}\Bigg\{(\mathbf{R_A}) + \left[\hat{\mathbf{C}}^{\alpha 1}\right]\begin{bmatrix}\Delta T\\ -\Delta G\end{bmatrix} + \left[\hat{\mathbf{C}}^{E1}\right]\begin{bmatrix}E_1\\ E_2\\ E_3\end{bmatrix} + \left[\hat{\mathbf{C}}^{M1}\right]\begin{bmatrix}H_1\\ H_2\\ H_3\end{bmatrix} \\ &+ \left[\hat{\mathbf{C}}^{ET1}\right]\begin{bmatrix}\Delta T\\ -\Delta G\end{bmatrix} + \left[\hat{\mathbf{C}}^{MT1}\right]\begin{bmatrix}\Delta T\\ -\Delta G\end{bmatrix}\Bigg\} + (WNT)\left[\hat{\mathbf{C}}^6\right]^{-1}\Bigg\{(\mathbf{R_A}) + \left[\hat{\mathbf{C}}^{\alpha 6}\right]\begin{bmatrix}\Delta T\\ -\Delta G\end{bmatrix} + \left[\hat{\mathbf{C}}^{E6}\right]\begin{bmatrix}E_1\\ E_2\\ E_3\end{bmatrix} \\ &+ \left[\hat{\mathbf{C}}^{M6}\right]\begin{bmatrix}H_1\\ H_2\\ H_3\end{bmatrix} + \left[\hat{\mathbf{C}}^{ET6}\right]\begin{bmatrix}\Delta T\\ -\Delta G\end{bmatrix} + \left[\hat{\mathbf{C}}^{MT6}\right]\begin{bmatrix}\Delta T\\ -\Delta G\end{bmatrix}\Bigg\} \end{aligned} \tag{150}$$

Each effect present in eq. (150) can be isolated by considering the case when only it is active. That is, if we assume that the panel has only mechanical loading and no thermal, electric, or magnetic loading, eq. (150) simplifies to,

$$S_x\left[\hat{\mathbf{C}}^8\right]^{-1}(\mathbf{R_A}) = (FWNT)\left[\hat{\mathbf{C}}^1\right]^{-1}(\mathbf{R_A}) + (WNT)\left[\hat{\mathbf{C}}^6\right]^{-1}(\mathbf{R_A}) \tag{151}$$

or,

$$\left[\hat{\mathbf{C}}^8\right]^{-1} = \frac{1}{S_x}\left\{(FWNT)\left[\hat{\mathbf{C}}^1\right]^{-1} + (WNT)\left[\hat{\mathbf{C}}^6\right]^{-1}\right\} \tag{152}$$

Then, inverting eq. (151) provides $\hat{\mathbf{C}}^8$, and rearranging the terms (see below) provides the homogenized ABD matrix for Segment 8.

For the thermal, electric, magnetic, thermo-electric, and thermo-magnetic terms appearing in eq. (150), we have,

Thermal

$$S_x\left[\hat{\mathbf{C}}^8\right]^{-1}\left[\hat{\mathbf{C}}^{\alpha 8}\right]\begin{bmatrix}\Delta T\\ -\Delta G\end{bmatrix}=(FWNT)\left[\hat{\mathbf{C}}^1\right]^{-1}\left[\hat{\mathbf{C}}^{\alpha 1}\right]\begin{bmatrix}\Delta T\\ -\Delta G\end{bmatrix}+(WNT)\left[\hat{\mathbf{C}}^6\right]^{-1}\left[\hat{\mathbf{C}}^{\alpha 6}\right]\begin{bmatrix}\Delta T\\ -\Delta G\end{bmatrix} \tag{153}$$

or

$$\left[\hat{\mathbf{C}}^{\alpha 8}\right]=\frac{1}{S_x}\left[\hat{\mathbf{C}}^8\right]\left\{(FWNT)\left[\hat{\mathbf{C}}^1\right]^{-1}\left[\hat{\mathbf{C}}^{\alpha 1}\right]+(WNT)\left[\hat{\mathbf{C}}^6\right]^{-1}\left[\hat{\mathbf{C}}^{\alpha 6}\right]\right\} \tag{154}$$

Electric

$$S_x\left[\hat{\mathbf{C}}^8\right]^{-1}\left[\hat{\mathbf{C}}^{E8}\right]\begin{bmatrix}E_1\\ E_2\\ E_3\end{bmatrix}=(FWNT)\left[\hat{\mathbf{C}}^1\right]^{-1}\left[\hat{\mathbf{C}}^{E1}\right]\begin{bmatrix}E_1\\ E_2\\ E_3\end{bmatrix}+(WNT)\left[\hat{\mathbf{C}}^6\right]^{-1}\left[\hat{\mathbf{C}}^{E6}\right]\begin{bmatrix}E_1\\ E_2\\ E_3\end{bmatrix} \tag{155}$$

or

$$\left[\hat{\mathbf{C}}^{E8}\right]=\frac{1}{S_x}\left[\hat{\mathbf{C}}^8\right]\left\{(FWNT)\left[\hat{\mathbf{C}}^1\right]^{-1}\left[\hat{\mathbf{C}}^{E1}\right]+(WNT)\left[\hat{\mathbf{C}}^6\right]^{-1}\left[\hat{\mathbf{C}}^{E6}\right]\right\}\frac{1}{2} \tag{156}$$

Magnetic

$$S_x\left[\hat{\mathbf{C}}^8\right]^{-1}\left[\hat{\mathbf{C}}^{M8}\right]\begin{bmatrix}H_1\\ H_2\\ H_3\end{bmatrix}=(FWNT)\left[\hat{\mathbf{C}}^1\right]^{-1}\left[\hat{\mathbf{C}}^{M1}\right]\begin{bmatrix}H_1\\ H_2\\ H_3\end{bmatrix}+(WNT)\left[\hat{\mathbf{C}}^6\right]^{-1}\left[\hat{\mathbf{C}}^{M6}\right]\begin{bmatrix}H_1\\ H_2\\ H_3\end{bmatrix} \tag{157}$$

or

$$\left[\hat{\mathbf{C}}^{M8}\right]=\frac{1}{S_x}\left[\hat{\mathbf{C}}^8\right]\left\{(FWNT)\left[\hat{\mathbf{C}}^1\right]^{-1}\left[\hat{\mathbf{C}}^{M1}\right]+(WNT)\left[\hat{\mathbf{C}}^6\right]^{-1}\left[\hat{\mathbf{C}}^{M6}\right]\right\} \tag{158}$$

Thermoelectric

$$S_x\left[\hat{\mathbf{C}}^8\right]^{-1}\left[\hat{\mathbf{C}}^{ET8}\right]\begin{bmatrix}\Delta T\\ -\Delta G\end{bmatrix}=(FWNT)\left[\hat{\mathbf{C}}^1\right]^{-1}\left[\hat{\mathbf{C}}^{ET1}\right]\begin{bmatrix}\Delta T\\ -\Delta G\end{bmatrix}+(WNT)\left[\hat{\mathbf{C}}^6\right]^{-1}\left[\hat{\mathbf{C}}^{ET6}\right]\begin{bmatrix}\Delta T\\ -\Delta G\end{bmatrix} \tag{159}$$

or

$$\left[\hat{\mathbf{C}}^{ET8}\right]=\frac{1}{S_x}\left[\hat{\mathbf{C}}^8\right]\left\{(FWNT)\left[\hat{\mathbf{C}}^1\right]^{-1}\left[\hat{\mathbf{C}}^{ET1}\right]+(WNT)\left[\hat{\mathbf{C}}^6\right]^{-1}\left[\hat{\mathbf{C}}^{ET6}\right]\right\} \tag{160}$$

Thermomagnetic

$$S_x\left[\hat{\mathbf{C}}^8\right]^{-1}\left[\hat{\mathbf{C}}^{MT8}\right]\begin{bmatrix}\Delta T\\ -\Delta G\end{bmatrix}=(FWNT)\left[\hat{\mathbf{C}}^1\right]^{-1}\left[\hat{\mathbf{C}}^{MT1}\right]\begin{bmatrix}\Delta T\\ -\Delta G\end{bmatrix}+(WNT)\left[\hat{\mathbf{C}}^6\right]^{-1}\left[\hat{\mathbf{C}}^{MT6}\right]\begin{bmatrix}\Delta T\\ -\Delta G\end{bmatrix} \tag{161}$$

or

$$\left[\hat{\mathbf{C}}^{MT8}\right]=\frac{1}{S_x}\left[\hat{\mathbf{C}}^8\right]\left\{(FWNT)\left[\hat{\mathbf{C}}^1\right]^{-1}\left[\hat{\mathbf{C}}^{MT1}\right]+(WNT)\left[\hat{\mathbf{C}}^6\right]^{-1}\left[\hat{\mathbf{C}}^{MT6}\right]\right\} \tag{162}$$

By rearranging each of eqs. (152), (154), (156), (158), (160), and (162), the Segment 8 thermal, electric, magnetic, thermoelectric, and thermomagnetic ABD matrices can be determined. However, for this to be accomplished, all of the hatted matrices for each segment must be determined. This is done by separating the segment constitutive equation as,

$$\begin{aligned}\begin{bmatrix}N_{yy}\\ N_{xy}\\ M_{yy}\\ M_{xy}\end{bmatrix}=&\begin{bmatrix}A_{22}&A_{23}&B_{22}&B_{23}\\ A_{23}&A_{33}&B_{32}&B_{33}\\ B_{22}&B_{32}&D_{22}&D_{23}\\ B_{23}&B_{33}&D_{32}&D_{33}\end{bmatrix}\begin{bmatrix}\varepsilon^0_{yy}\\ \gamma^0_{xy}\\ \kappa_{yy}\\ \kappa_{xy}\end{bmatrix}+\begin{bmatrix}A_{12}&B_{21}\\ A_{13}&B_{31}\\ B_{12}&D_{12}\\ B_{13}&D_{13}\end{bmatrix}\begin{bmatrix}\varepsilon^0_{xx}\\ \kappa_{xx}\end{bmatrix}\\ &-\begin{bmatrix}A^\alpha_2&B^\alpha_2\\ A^\alpha_3&B^\alpha_3\\ B^\alpha_2&D^\alpha_2\\ B^\alpha_3&D^\alpha_3\end{bmatrix}\begin{bmatrix}\Delta T\\ -\Delta G\end{bmatrix}-\begin{bmatrix}A^E_{21}&A^E_{22}&A^E_{23}\\ A^E_{31}&A^E_{32}&A^E_{33}\\ B^E_{21}&B^E_{22}&B^E_{23}\\ B^E_{31}&B^E_{32}&B^E_{33}\end{bmatrix}\begin{bmatrix}E_1\\ E_2\\ E_3\end{bmatrix}-\begin{bmatrix}A^M_{21}&A^M_{22}&A^M_{23}\\ A^M_{31}&A^M_{32}&A^M_{33}\\ B^M_{21}&B^M_{22}&B^M_{23}\\ B^M_{31}&B^M_{32}&B^M_{33}\end{bmatrix}\begin{bmatrix}H_1\\ H_2\\ H_3\end{bmatrix}\\ &-\begin{bmatrix}A^{ET}_2&B^{ET}_2\\ A^{ET}_3&B^{ET}_3\\ B^{ET}_2&D^{ET}_2\\ B^{ET}_3&D^{ET}_3\end{bmatrix}\begin{bmatrix}\Delta T\\ -\Delta G\end{bmatrix}-\begin{bmatrix}A^{MT}_2&B^{MT}_2\\ A^{MT}_3&B^{MT}_3\\ B^{MT}_2&D^{MT}_2\\ B^{MT}_3&D^{MT}_3\end{bmatrix}\begin{bmatrix}\Delta T\\ -\Delta G\end{bmatrix}\end{aligned} \tag{163}$$

or, employing simplified notation,

$$\mathbf{v}_1=\mathbf{S}_{11}\mathbf{u}_1+\mathbf{S}_{12}\mathbf{u}_2-\mathbf{S}^\alpha_1\Delta\mathbf{T}-\mathbf{S}^E_1\mathbf{E}-\mathbf{S}^M_1\mathbf{H}-\mathbf{S}^{ET}_1\Delta\mathbf{T}-\mathbf{S}^{MT}_1\Delta\mathbf{T} \tag{164}$$

and

$$\begin{bmatrix} N_{xx} \\ M_{xx} \end{bmatrix} = \begin{bmatrix} A_{12} & A_{13} & B_{12} & B_{13} \\ B_{21} & B_{31} & D_{12} & D_{13} \end{bmatrix} \begin{bmatrix} \varepsilon^0_{yy} \\ \gamma^0_{xy} \\ \kappa_{yy} \\ \kappa_{xy} \end{bmatrix} + \begin{bmatrix} A_{11} & B_{11} \\ B_{11} & D_{11} \end{bmatrix} \begin{bmatrix} \varepsilon^0_{xx} \\ \kappa_{xx} \end{bmatrix}$$
$$- \begin{bmatrix} A^{\alpha}_1 & B^{\alpha}_1 \\ B^{\alpha}_1 & D^{\alpha}_1 \end{bmatrix} \begin{bmatrix} \Delta T \\ -\Delta G \end{bmatrix} - \begin{bmatrix} A^{E}_{11} & A^{E}_{12} & A^{E}_{13} \\ B^{E}_{11} & B^{E}_{12} & B^{E}_{13} \end{bmatrix} \begin{bmatrix} E_1 \\ E_2 \\ E_3 \end{bmatrix} - \begin{bmatrix} A^{M}_{11} & A^{M}_{12} & A^{M}_{13} \\ B^{M}_{11} & B^{M}_{12} & B^{M}_{13} \end{bmatrix} \begin{bmatrix} H_1 \\ H_2 \\ H_3 \end{bmatrix} \tag{165}$$
$$- \begin{bmatrix} A^{ET}_1 & B^{ET}_1 \\ B^{ET}_1 & D^{ET}_1 \end{bmatrix} \begin{bmatrix} \Delta T \\ -\Delta G \end{bmatrix} - \begin{bmatrix} A^{MT}_1 & B^{MT}_1 \\ B^{MT}_1 & D^{MT}_1 \end{bmatrix} \begin{bmatrix} \Delta T \\ -\Delta G \end{bmatrix}$$

or, employing simplified notation,

$$\mathbf{v}_2 = \mathbf{S}_{21}\mathbf{u}_1 + \mathbf{S}_{22}\mathbf{u}_2 - \mathbf{S}^{\alpha}_2\Delta\mathbf{T} - \mathbf{S}^{E}_2\mathbf{E} - \mathbf{S}^{M}_2\mathbf{H} - \mathbf{S}^{ET}_2\Delta\mathbf{T} - \mathbf{S}^{MT}_2\Delta\mathbf{T} \tag{166}$$

Equations (164) and (166) can be rearranged and combined as,

$$\begin{bmatrix} \mathbf{v}_1 \\ \mathbf{u}_2 \end{bmatrix} = \begin{bmatrix} \hat{\mathbf{S}}_{11} & \hat{\mathbf{S}}_{12} \\ \hat{\mathbf{S}}_{21} & \hat{\mathbf{S}}_{22} \end{bmatrix} \begin{bmatrix} \mathbf{u}_1 \\ \mathbf{v}_2 \end{bmatrix} - \begin{bmatrix} \hat{\mathbf{S}}^{\alpha}_1 \\ \hat{\mathbf{S}}^{\alpha}_2 \end{bmatrix} \Delta\mathbf{T} - \begin{bmatrix} \hat{\mathbf{S}}^{E}_1 \\ \hat{\mathbf{S}}^{E}_2 \end{bmatrix} \mathbf{E} - \begin{bmatrix} \hat{\mathbf{S}}^{M}_1 \\ \hat{\mathbf{S}}^{M}_2 \end{bmatrix} \mathbf{H} - \begin{bmatrix} \hat{\mathbf{S}}^{ET}_1 \\ \hat{\mathbf{S}}^{ET}_2 \end{bmatrix} \Delta\mathbf{T} - \begin{bmatrix} \hat{\mathbf{S}}^{MT}_1 \\ \hat{\mathbf{S}}^{MT}_2 \end{bmatrix} \Delta\mathbf{T} \tag{167}$$

where now all components subjected to the iso-conditions appear on the left hand side. Solving eq. (166) for $\mathbf{u}_2$ yields,

$$\mathbf{u}_2 = [\mathbf{S}_{22}]^{-1} \left\{ \mathbf{v}_2 - \mathbf{S}_{21}\mathbf{u}_1 + \mathbf{S}^{\alpha}_2\Delta\mathbf{T} + \mathbf{S}^{E}_2\mathbf{E} + \mathbf{S}^{M}_2\mathbf{H} + \mathbf{S}^{ET}_2\Delta\mathbf{T} + \mathbf{S}^{MT}_2\Delta\mathbf{T} \right\} \tag{168}$$

and substituting for $\mathbf{u}_2$ in eq. (164) using eq. (168) yields,

$$\begin{aligned} \mathbf{v}_1 = {} & \mathbf{S}_{11}\mathbf{u}_1 + \mathbf{S}_{12}[\mathbf{S}_{22}]^{-1} \left\{ \mathbf{v}_2 - \mathbf{S}_{21}\mathbf{u}_1 + \mathbf{S}^{\alpha}_2\Delta\mathbf{T} + \mathbf{S}^{E}_2\mathbf{E} + \mathbf{S}^{M}_2\mathbf{H} + \mathbf{S}^{ET}_2\Delta\mathbf{T} + \mathbf{S}^{MT}_2\Delta\mathbf{T} \right\} \\ & - \mathbf{S}^{\alpha}_1\Delta\mathbf{T} - \mathbf{S}^{E}_1\mathbf{E} - \mathbf{S}^{M}_1\mathbf{H} - \mathbf{S}^{ET}_1\Delta\mathbf{T} - \mathbf{S}^{MT}_1\Delta\mathbf{T} \end{aligned} \tag{169}$$

or, with terms grouped,

$$\begin{aligned} \mathbf{v}_1 = {} & \left\{ \mathbf{S}_{11} - \mathbf{S}_{12}[\mathbf{S}_{22}]^{-1}\mathbf{S}_{21} \right\} \mathbf{u}_1 + \mathbf{S}_{12}[\mathbf{S}_{22}]^{-1}\mathbf{v}_2 - \left\{ \mathbf{S}^{\alpha}_1 - \mathbf{S}_{12}[\mathbf{S}_{22}]^{-1}\mathbf{S}^{\alpha}_2 \right\} \Delta\mathbf{T} \\ & - \left\{ \mathbf{S}^{E}_1 - \mathbf{S}_{12}[\mathbf{S}_{22}]^{-1}\mathbf{S}^{E}_2 \right\} \mathbf{E} \quad - \left\{ \mathbf{S}^{M}_1 - \mathbf{S}_{12}[\mathbf{S}_{22}]^{-1}\mathbf{S}^{M}_2 \right\} \mathbf{H} - \left\{ \mathbf{S}^{ET}_1 - \mathbf{S}_{12}[\mathbf{S}_{22}]^{-1}\mathbf{S}^{ET}_2 \right\} \Delta\mathbf{T} \\ & - \left\{ \mathbf{S}^{MT}_1 - \mathbf{S}_{12}[\mathbf{S}_{22}]^{-1}\mathbf{S}^{MT}_2 \right\} \Delta\mathbf{T} \end{aligned} \tag{170}$$

Comparing eqs. (170) and (168) with eq. (167) allows the identification of the following hatted terms,

Mechanical

$$\hat{\mathbf{S}}_{11} = \mathbf{S}_{11} - \mathbf{S}_{12}[\mathbf{S}_{22}]^{-1}\mathbf{S}_{21} \tag{171}$$

$$\hat{\mathbf{S}}_{12} = \mathbf{S}_{12}\left[\mathbf{S}_{22}\right]^{-1} \tag{172}$$

$$\hat{\mathbf{S}}_{21} = -\left[\mathbf{S}_{22}\right]^{-1}\mathbf{S}_{21} \tag{173}$$

$$\hat{\mathbf{S}}_{22} = \left[\mathbf{S}_{22}\right]^{-1} \tag{174}$$

Thermal

$$\hat{\mathbf{S}}_1^{\alpha} = \mathbf{S}_1^{\alpha} - \mathbf{S}_{12}\left[\mathbf{S}_{22}\right]^{-1}\mathbf{S}_2^{\alpha} \tag{175}$$

$$\hat{\mathbf{S}}_2^{\alpha} = -\left[\mathbf{S}_{22}\right]^{-1}\mathbf{S}_2^{\alpha} \tag{176}$$

Electric

$$\hat{\mathbf{S}}_1^{E} = \mathbf{S}_1^{E} - \mathbf{S}_{12}\left[\mathbf{S}_{22}\right]^{-1}\mathbf{S}_2^{E} \tag{177}$$

$$\hat{\mathbf{S}}_2^{E} = -\left[\mathbf{S}_{22}\right]^{-1}\mathbf{S}_2^{E} \tag{178}$$

Magnetic

$$\hat{\mathbf{S}}_1^{M} = \mathbf{S}_1^{M} - \mathbf{S}_{12}\left[\mathbf{S}_{22}\right]^{-1}\mathbf{S}_2^{M} \tag{179}$$

$$\hat{\mathbf{S}}_2^{M} = -\left[\mathbf{S}_{22}\right]^{-1}\mathbf{S}_2^{M} \tag{180}$$

Thermoelectric

$$\hat{\mathbf{S}}_1^{ET} = \mathbf{S}_1^{ET} - \mathbf{S}_{12}\left[\mathbf{S}_{22}\right]^{-1}\mathbf{S}_2^{ET} \tag{181}$$

$$\hat{\mathbf{S}}_2^{ET} = -\left[\mathbf{S}_{22}\right]^{-1}\mathbf{S}_2^{ET} \tag{182}$$

Thermomagnetic

$$\hat{\mathbf{S}}_1^{MT} = \mathbf{S}_1^{MT} - \mathbf{S}_{12}\left[\mathbf{S}_{22}\right]^{-1}\mathbf{S}_2^{MT} \tag{183}$$

$$\hat{\mathbf{S}}_2^{MT} = -\left[\mathbf{S}_{22}\right]^{-1}\mathbf{S}_2^{MT} \tag{184}$$

The equivalence between the $\hat{\mathbf{S}}^{\bullet}$ matrix terms in eqs. (171) to (184) and the $\hat{\mathbf{C}}^{\bullet}$ matrix terms from eqs. (152), (154), (156), (158), (160), and (162) is,

$$\hat{\mathbf{C}} = \begin{bmatrix} \hat{S}_{22}(1,1) & \hat{S}_{21}(1,1) & \hat{S}_{21}(1,2) & \hat{S}_{22}(1,2) & \hat{S}_{21}(1,3) & \hat{S}_{21}(1,4) \\ \hat{S}_{12}(1,1) & \hat{S}_{11}(1,1) & \hat{S}_{11}(1,2) & \hat{S}_{12}(2,1) & \hat{S}_{11}(1,3) & \hat{S}_{11}(1,4) \\ \hat{S}_{12}(2,1) & \hat{S}_{11}(2,1) & \hat{S}_{11}(2,2) & \hat{S}_{12}(2,2) & \hat{S}_{11}(2,3) & \hat{S}_{11}(2,4) \\ \hat{S}_{22}(2,1) & \hat{S}_{21}(2,1) & \hat{S}_{21}(2,2) & \hat{S}_{22}(2,2) & \hat{S}_{21}(1,3) & \hat{S}_{21}(1,4) \\ \hat{S}_{12}(3,1) & \hat{S}_{11}(3,1) & \hat{S}_{11}(3,2) & \hat{S}_{12}(3,2) & \hat{S}_{11}(3,3) & \hat{S}_{11}(3,4) \\ \hat{S}_{12}(4,1) & \hat{S}_{11}(4,1) & \hat{S}_{11}(4,2) & \hat{S}_{12}(4,2) & \hat{S}_{11}(4,3) & \hat{S}_{11}(4,4) \end{bmatrix} \tag{185}$$

$$\hat{\mathbf{C}}^{\alpha} = \begin{bmatrix} \hat{S}_2^{\alpha}(1,1) & \hat{S}_2^{\alpha}(1,2) \\ \hat{S}_1^{\alpha}(1,1) & \hat{S}_1^{\alpha}(1,2) \\ \hat{S}_1^{\alpha}(2,1) & \hat{S}_1^{\alpha}(2,2) \\ \hat{S}_2^{\alpha}(2,1) & \hat{S}_2^{\alpha}(2,2) \\ \hat{S}_1^{\alpha}(3,1) & \hat{S}_1^{\alpha}(3,2) \\ \hat{S}_1^{\alpha}(4,1) & \hat{S}_1^{\alpha}(4,1) \end{bmatrix} \tag{186}$$

$$\hat{\mathbf{C}}^{E} = \begin{bmatrix} \hat{S}_2^{E}(1,1) & \hat{S}_2^{E}(1,2) & \hat{S}_2^{E}(1,3) \\ \hat{S}_1^{E}(1,1) & \hat{S}_1^{E}(1,2) & \hat{S}_1^{E}(1,3) \\ \hat{S}_1^{E}(2,1) & \hat{S}_1^{E}(2,2) & \hat{S}_1^{E}(2,3) \\ \hat{S}_2^{E}(2,1) & \hat{S}_2^{E}(2,2) & \hat{S}_2^{E}(2,3) \\ \hat{S}_1^{E}(3,1) & \hat{S}_1^{E}(3,2) & \hat{S}_1^{E}(3,3) \\ \hat{S}_1^{E}(4,1) & \hat{S}_1^{E}(4,2) & \hat{S}_1^{E}(4,3) \end{bmatrix} \tag{187}$$

$$\hat{\mathbf{C}}^{M} = \begin{bmatrix} \hat{S}_2^{M}(1,1) & \hat{S}_2^{M}(1,2) & \hat{S}_2^{M}(1,3) \\ \hat{S}_1^{M}(1,1) & \hat{S}_1^{M}(1,2) & \hat{S}_1^{M}(1,3) \\ \hat{S}_1^{M}(2,1) & \hat{S}_1^{M}(2,2) & \hat{S}_1^{M}(2,3) \\ \hat{S}_2^{M}(2,1) & \hat{S}_2^{M}(2,2) & \hat{S}_2^{M}(2,3) \\ \hat{S}_1^{M}(3,1) & \hat{S}_1^{M}(3,2) & \hat{S}_1^{M}(3,3) \\ \hat{S}_1^{M}(4,1) & \hat{S}_1^{M}(4,2) & \hat{S}_1^{M}(4,3) \end{bmatrix} \tag{188}$$

$$\hat{\mathbf{C}}^{ET} = \begin{bmatrix} \hat{S}_2^{ET}(1,1) & \hat{S}_2^{ET}(1,2) \\ \hat{S}_1^{ET}(1,1) & \hat{S}_1^{ET}(1,2) \\ \hat{S}_1^{ET}(2,1) & \hat{S}_1^{ET}(2,2) \\ \hat{S}_2^{ET}(2,1) & \hat{S}_2^{ET}(2,2) \\ \hat{S}_1^{ET}(3,1) & \hat{S}_1^{ET}(3,2) \\ \hat{S}_1^{ET}(4,1) & \hat{S}_1^{ET}(4,1) \end{bmatrix} \tag{189}$$

$$\hat{\mathbf{C}}^{MT} = \begin{bmatrix} \hat{S}_2^{MT}(1,1) & \hat{S}_2^{MT}(1,2) \\ \hat{S}_1^{MT}(1,1) & \hat{S}_1^{MT}(1,2) \\ \hat{S}_1^{MT}(2,1) & \hat{S}_1^{MT}(2,2) \\ \hat{S}_2^{MT}(2,1) & \hat{S}_2^{MT}(2,2) \\ \hat{S}_1^{MT}(3,1) & \hat{S}_1^{MT}(3,2) \\ \hat{S}_1^{MT}(4,1) & \hat{S}_1^{MT}(4,1) \end{bmatrix} \tag{190}$$

where the parenthetical indices refer to the indices of the components within each $\hat{S}_{ij}^{\bullet}$ and $\hat{S}_{k}^{\bullet}$ matrix.

Using eqs. (152), (154), (156), (158), (160), and (162), we can now determine the hatted quantities for Segment 8 from the hatted quantities of Segments 1 and 6 given by eqs. (171) to (190). In order to then determine the non-hatted quantities for Segment 8, the reverse of the procedure embodied by eqs. (164) to (190) are employed, resulting in equations of identical form of eqs. (171) to (184), but with the rolls of hatted and unhatted quantities reversed. That is,

Mechanical

$$\mathbf{S}_{11} = \hat{\mathbf{S}}_{11} - \hat{\mathbf{S}}_{12}\left[\hat{\mathbf{S}}_{22}\right]^{-1}\hat{\mathbf{S}}_{21} \tag{191}$$

$$\mathbf{S}_{12} = \hat{\mathbf{S}}_{12}\left[\hat{\mathbf{S}}_{22}\right]^{-1} \tag{192}$$

$$\mathbf{S}_{21} = -\left[\hat{\mathbf{S}}_{22}\right]^{-1}\hat{\mathbf{S}}_{21} \tag{193}$$

$$\mathbf{S}_{22} = \left[\hat{\mathbf{S}}_{22}\right]^{-1} \tag{194}$$

Thermal

$$\mathbf{S}_1^{\alpha} = \hat{\mathbf{S}}_1^{\alpha} - \hat{\mathbf{S}}_{12}\left[\hat{\mathbf{S}}_{22}\right]^{-1}\hat{\mathbf{S}}_2^{\alpha} \tag{195}$$

$$\mathbf{S}_2^{\alpha} = -\left[\hat{\mathbf{S}}_{22}\right]^{-1}\hat{\mathbf{S}}_2^{\alpha} \tag{196}$$

Electric

$$\mathbf{S}_1^{E} = \hat{\mathbf{S}}_1^{E} - \hat{\mathbf{S}}_{12}\left[\hat{\mathbf{S}}_{22}\right]^{-1}\hat{\mathbf{S}}_2^{E} \tag{197}$$

$$\mathbf{S}_2^{E} = -\left[\hat{\mathbf{S}}_{22}\right]^{-1}\hat{\mathbf{S}}_2^{E} \tag{198}$$

Magnetic

$$\mathbf{S}_1^{M} = \hat{\mathbf{S}}_1^{M} - \hat{\mathbf{S}}_{12}\left[\hat{\mathbf{S}}_{22}\right]^{-1}\hat{\mathbf{S}}_2^{M} \tag{199}$$

$$\mathbf{S}_2^M = -\left[\hat{\mathbf{S}}_{22}\right]^{-1} \hat{\mathbf{S}}_2^M \tag{200}$$

Thermoelectric

$$\mathbf{S}_1^{ET} = \hat{\mathbf{S}}_1^{ET} - \hat{\mathbf{S}}_{12}\left[\hat{\mathbf{S}}_{22}\right]^{-1} \hat{\mathbf{S}}_2^{ET} \tag{201}$$

$$\mathbf{S}_2^{ET} = -\left[\hat{\mathbf{S}}_{22}\right]^{-1} \hat{\mathbf{S}}_2^{ET} \tag{202}$$

Thermomagnetic

$$\mathbf{S}_1^{MT} = \hat{\mathbf{S}}_1^{MT} - \hat{\mathbf{S}}_{12}\left[\hat{\mathbf{S}}_{22}\right]^{-1} \hat{\mathbf{S}}_2^{MT} \tag{203}$$

$$\mathbf{S}_2^{MT} = -\left[\hat{\mathbf{S}}_{22}\right]^{-1} \hat{\mathbf{S}}_2^{MT} \tag{204}$$

Finally, the form of the equivalence between the S matrix terms and the **C** matrix terms is identical to the form of the equivalence between the $\hat{\mathbf{S}}$ matrix terms and the $\hat{\mathbf{C}}$ matrix terms given in eqs. (185) to (190).

6. The Thermal Analogy

It is clear from the preceding development that an analogy exists between the thermal treatment of the material/laminate and each of the piezoelectric, piezomagnetic, thermoelectric, and thermomagnetic treatments of the material laminate. That is, the piezoelectric, piezomagnetic, thermoelectric, and thermomagnetic effects are each incorporated into the overall theory in a way that is analogous to the treatment of thermal effects. Therefore, it is possible to utilize the thermo-electro-magnetic terms within the theory to mimic thermal behavior, and conversely, it is possible to utilize the thermal terms within the theory to mimic the piezoelectric, piezomagnetic, thermoelectric, and thermomagnetic effects. This thermal analogy can be used to verify the thermo-electro-magnetic implementation vs. an established thermal implementation or to perform a piezoelectric, piezomagnetic, thermoelectric, and thermomagnetic analysis using an established thermal implementation. Côté et al. (ref. 30) employed the latter approach to simulate the dynamic response of composite beam with an embedded piezoelectric actuator.

6.1 Material Level Thermo-Electro-Magnetic Terms Mimicking Thermal Response

The general thermo-piezo-electro-magnetic constitutive equation for a material is given by,

$$\begin{bmatrix}\sigma_{11}\\ \sigma_{22}\\ \sigma_{33}\\ \sigma_{23}\\ \sigma_{13}\\ \sigma_{12}\end{bmatrix} = \begin{bmatrix} C_{11} & C_{12} & C_{13} & C_{14} & C_{15} & C_{16}\\ C_{12} & C_{22} & C_{23} & C_{24} & C_{25} & C_{26}\\ C_{13} & C_{23} & C_{33} & C_{34} & C_{35} & C_{36}\\ C_{14} & C_{24} & C_{34} & C_{44} & C_{45} & C_{46}\\ C_{15} & C_{25} & C_{35} & C_{45} & C_{55} & C_{56}\\ C_{16} & C_{25} & C_{36} & C_{46} & C_{56} & C_{66}\end{bmatrix}\begin{bmatrix}\varepsilon_{11}-\alpha_{11}\Delta T\\ \varepsilon_{22}-\alpha_{22}\Delta T\\ \varepsilon_{33}-\alpha_{33}\Delta T\\ 2\varepsilon_{23}-2\alpha_{23}\Delta T\\ 2\varepsilon_{13}-2\alpha_{13}\Delta T\\ 2\varepsilon_{12}-2\alpha_{12}\Delta T\end{bmatrix} - \begin{bmatrix} e_{11} & e_{21} & e_{31}\\ e_{12} & e_{22} & e_{32}\\ e_{13} & e_{23} & e_{33}\\ e_{14} & e_{24} & e_{34}\\ e_{15} & e_{25} & e_{35}\\ e_{16} & e_{26} & e_{36}\end{bmatrix}\begin{bmatrix}E_1+\zeta_1\Delta T\\ E_2+\zeta_2\Delta T\\ E_3+\zeta_3\Delta T\end{bmatrix} - \begin{bmatrix} q_{11} & q_{21} & q_{31}\\ q_{12} & q_{22} & q_{32}\\ q_{13} & q_{23} & q_{33}\\ q_{14} & q_{24} & q_{34}\\ q_{15} & q_{25} & q_{35}\\ q_{16} & q_{26} & q_{36}\end{bmatrix}\begin{bmatrix}H_1+\psi_1\Delta T\\ H_2+\psi_2\Delta T\\ H_3+\psi_3\Delta T\end{bmatrix} \tag{205}$$

This equation can be written in matrix form as,

$$\boldsymbol{\sigma} = \mathbf{C}\left[\boldsymbol{\varepsilon} - \boldsymbol{\alpha}\Delta T\right] - \mathbf{e}\left[\mathbf{E} + \boldsymbol{\zeta}\Delta T\right] - \mathbf{q}\left[\mathbf{H} + \boldsymbol{\psi}\Delta T\right] \tag{206}$$

or

$$\boldsymbol{\sigma} = \mathbf{C}\left[\boldsymbol{\varepsilon} - \boldsymbol{\alpha}\Delta T - \mathbf{C}^{-1}\mathbf{e}\mathbf{E} - \mathbf{C}^{-1}\mathbf{e}\boldsymbol{\zeta}\Delta T - \mathbf{C}^{-1}\mathbf{q}\mathbf{H} - \mathbf{C}^{-1}\mathbf{q}\,\boldsymbol{\psi}\Delta T\right] \tag{207}$$

Thus, in order to mimic the material level thermal effects using the piezoelectric terms, we seek a "Fake" piezoelectric coefficient matrix such that $\boldsymbol{\alpha}\Delta T = \mathbf{C}^{-1}\mathbf{e}^{\text{Fake}}\mathbf{E}$.

Assuming orthotropic behavior,

$$\begin{bmatrix}\alpha_1\\ \alpha_2\\ \alpha_3\\ 0\\ 0\\ 0\end{bmatrix}\Delta T = \begin{bmatrix} C_{11} & C_{12} & C_{13} & 0 & 0 & 0\\ C_{12} & C_{22} & C_{23} & 0 & 0 & 0\\ C_{13} & C_{23} & C_{33} & 0 & 0 & 0\\ 0 & 0 & 0 & C_{44} & 0 & 0\\ 0 & 0 & 0 & 0 & C_{55} & 0\\ 0 & 0 & 0 & 0 & 0 & C_{66}\end{bmatrix}^{-1}\begin{bmatrix} e_{11} & e_{21} & e_{31}\\ e_{12} & e_{22} & e_{32}\\ e_{13} & e_{23} & e_{33}\\ e_{14} & e_{24} & e_{34}\\ e_{15} & e_{25} & e_{35}\\ e_{16} & e_{26} & e_{36}\end{bmatrix}^{\text{Fake}}\begin{bmatrix}E_1\\ E_2\\ E_3\end{bmatrix} \tag{208}$$

Now, by setting $E_1 = \Delta T,\ E_2 = 0,\ E_3 = 0$, we have,

$$\begin{bmatrix}\alpha_1\\ \alpha_2\\ \alpha_3\\ 0\\ 0\\ 0\end{bmatrix}\Delta T=\begin{bmatrix}C_{11} & C_{12} & C_{13} & 0 & 0 & 0\\ C_{12} & C_{22} & C_{23} & 0 & 0 & 0\\ C_{13} & C_{23} & C_{33} & 0 & 0 & 0\\ 0 & 0 & 0 & C_{44} & 0 & 0\\ 0 & 0 & 0 & 0 & C_{55} & 0\\ 0 & 0 & 0 & 0 & 0 & C_{66}\end{bmatrix}^{-1}\begin{bmatrix}e_{11} & e_{21} & e_{31}\\ e_{12} & e_{22} & e_{32}\\ e_{13} & e_{23} & e_{33}\\ e_{14} & e_{24} & e_{34}\\ e_{15} & e_{25} & e_{35}\\ e_{16} & e_{26} & e_{36}\end{bmatrix}^{\text{Fake}}\begin{bmatrix}\Delta T\\ 0\\ 0\end{bmatrix} \tag{209}$$

or

$$\begin{bmatrix}C_{11} & C_{12} & C_{13} & 0 & 0 & 0\\ C_{12} & C_{22} & C_{23} & 0 & 0 & 0\\ C_{13} & C_{23} & C_{33} & 0 & 0 & 0\\ 0 & 0 & 0 & C_{44} & 0 & 0\\ 0 & 0 & 0 & 0 & C_{55} & 0\\ 0 & 0 & 0 & 0 & 0 & C_{66}\end{bmatrix}\begin{bmatrix}\alpha_1\\ \alpha_2\\ \alpha_3\\ 0\\ 0\\ 0\end{bmatrix}\Delta T=\begin{bmatrix}e_{11}\\ e_{12}\\ e_{13}\\ e_{14}\\ e_{15}\\ e_{16}\end{bmatrix}^{\text{Fake}}\Delta T \tag{210}$$

which gives,

$$\begin{aligned}e_{11}^{\text{Fake}} &= C_{11}\alpha_1 + C_{12}\alpha_2 + C_{13}\alpha_3\\ e_{12}^{\text{Fake}} &= C_{12}\alpha_1 + C_{22}\alpha_2 + C_{23}\alpha_3\\ e_{13}^{\text{Fake}} &= C_{13}\alpha_1 + C_{23}\alpha_2 + C_{33}\alpha_3\\ e_{14}^{\text{Fake}} &= 0\\ e_{15}^{\text{Fake}} &= 0\\ e_{16}^{\text{Fake}} &= 0\end{aligned} \tag{211}$$

Thus, by utilizing the fake piezoelectric coefficients indicated by eq. (211), along with $E_1 = \Delta T$, $E_2 = 0$, $E_3 = 0$ (and then also utilizing fake thermal expansion coefficients, $\boldsymbol{\alpha}^{\text{Fake}} = 0$), it is possible to determine the thermal behavior of a material through the piezoelectric terms. This can be used to verify the piezoelectric implementation.

Similarly, to verify the piezomagnetic effects, we set $H_1 = \Delta T$, $H_2 = 0$, $H_3 = 0$, and

$$\begin{aligned}q_{11}^{\text{Fake}} &= C_{11}\alpha_1 + C_{12}\alpha_2 + C_{13}\alpha_3\\ q_{12}^{\text{Fake}} &= C_{12}\alpha_1 + C_{22}\alpha_2 + C_{23}\alpha_3\\ q_{13}^{\text{Fake}} &= C_{13}\alpha_1 + C_{23}\alpha_2 + C_{33}\alpha_3\\ q_{14}^{\text{Fake}} &= 0\\ q_{15}^{\text{Fake}} &= 0\\ q_{16}^{\text{Fake}} &= 0\end{aligned} \tag{212}$$

For the thermo-electric effects, what we have $\boldsymbol{\alpha}\,\Delta T = \mathbf{C}^{-1}\mathbf{e}^{\text{Fake}}\,\boldsymbol{\zeta}^{\text{Fake}}\,\Delta T$. Again, assuming orthotropic material behavior,

$$\begin{bmatrix} C_{11} & C_{12} & C_{13} & 0 & 0 & 0 \\ C_{12} & C_{22} & C_{23} & 0 & 0 & 0 \\ C_{13} & C_{23} & C_{33} & 0 & 0 & 0 \\ 0 & 0 & 0 & C_{44} & 0 & 0 \\ 0 & 0 & 0 & 0 & C_{55} & 0 \\ 0 & 0 & 0 & 0 & 0 & C_{66} \end{bmatrix} \begin{bmatrix} \alpha_1 \\ \alpha_2 \\ \alpha_3 \\ 0 \\ 0 \\ 0 \end{bmatrix} = \begin{bmatrix} e_{11} & e_{21} & e_{31} \\ e_{12} & e_{22} & e_{32} \\ e_{13} & e_{23} & e_{33} \\ e_{14} & e_{24} & e_{34} \\ e_{15} & e_{25} & e_{35} \\ e_{16} & e_{26} & e_{36} \end{bmatrix}^{\text{Fake}} \begin{bmatrix} \zeta_1 \\ \zeta_2 \\ \zeta_3 \end{bmatrix}^{\text{Fake}} \tag{213}$$

Setting $\zeta_1^{\text{Fake}} = 1,\ \zeta_2^{\text{Fake}} = 0,\ \zeta_3^{\text{Fake}} = 0$, we have

$$\begin{bmatrix} C_{11} & C_{12} & C_{13} & 0 & 0 & 0 \\ C_{12} & C_{22} & C_{23} & 0 & 0 & 0 \\ C_{13} & C_{23} & C_{33} & 0 & 0 & 0 \\ 0 & 0 & 0 & C_{44} & 0 & 0 \\ 0 & 0 & 0 & 0 & C_{55} & 0 \\ 0 & 0 & 0 & 0 & 0 & C_{66} \end{bmatrix} \begin{bmatrix} \alpha_1 \\ \alpha_2 \\ \alpha_3 \\ 0 \\ 0 \\ 0 \end{bmatrix} = \begin{bmatrix} e_{11} & e_{21} & e_{31} \\ e_{12} & e_{22} & e_{32} \\ e_{13} & e_{23} & e_{33} \\ e_{14} & e_{24} & e_{34} \\ e_{15} & e_{25} & e_{35} \\ e_{16} & e_{26} & e_{36} \end{bmatrix}^{\text{Fake}} \begin{bmatrix} 1 \\ 0 \\ 0 \end{bmatrix} = \begin{bmatrix} e_{11} \\ e_{12} \\ e_{13} \\ e_{14} \\ e_{15} \\ e_{16} \end{bmatrix}^{\text{Fake}} \tag{214}$$

resulting in,

$$\begin{aligned} e_{11}^{\text{Fake}} &= C_{11}\alpha_1 + C_{12}\alpha_2 + C_{13}\alpha_3 \\ e_{12}^{\text{Fake}} &= C_{12}\alpha_1 + C_{22}\alpha_2 + C_{23}\alpha_3 \\ e_{13}^{\text{Fake}} &= C_{13}\alpha_1 + C_{23}\alpha_2 + C_{33}\alpha_3 \\ e_{14}^{\text{Fake}} &= 0 \\ e_{15}^{\text{Fake}} &= 0 \\ e_{16}^{\text{Fake}} &= 0 \end{aligned} \tag{215}$$

Similarly, for the thermo-magnetic terms, we set $\psi_1 = 1,\ \psi_2 = 0,\ \psi_3 = 0$ and obtain,

$$\begin{aligned} q_{11}^{\text{Fake}} &= C_{11}\alpha_1 + C_{12}\alpha_2 + C_{13}\alpha_3 \\ q_{12}^{\text{Fake}} &= C_{12}\alpha_1 + C_{22}\alpha_2 + C_{23}\alpha_3 \\ q_{13}^{\text{Fake}} &= C_{13}\alpha_1 + C_{23}\alpha_2 + C_{33}\alpha_3 \\ q_{14}^{\text{Fake}} &= 0 \\ q_{15}^{\text{Fake}} &= 0 \\ q_{16}^{\text{Fake}} &= 0 \end{aligned} \tag{216}$$

6.2 Material Level Thermal Terms Mimicking Thermo-Electro-Magnetic Response

In order to mimic the material piezoelectric behavior using the thermal terms, we again begin with eqs. (205) to (207). Setting $\boldsymbol{\alpha}^{\text{Fake}}\,\Delta T^{\text{Fake}} = \mathbf{C}^{-1}\mathbf{e}\,\mathbf{E}$ and retaining anisotropic behavior,

$$\begin{bmatrix}\alpha_1\\ \alpha_2\\ \alpha_3\\ \alpha_4\\ \alpha_5\\ \alpha_6\end{bmatrix}^{\text{Fake}} \Delta T^{\text{Fake}} = \begin{bmatrix} C_{11} & C_{12} & C_{13} & C_{14} & C_{15} & C_{16}\\ C_{21} & C_{22} & C_{23} & C_{24} & C_{25} & C_{26}\\ C_{31} & C_{32} & C_{33} & C_{34} & C_{35} & C_{36}\\ C_{41} & C_{42} & C_{43} & C_{44} & C_{45} & C_{46}\\ C_{51} & C_{52} & C_{53} & C_{54} & C_{55} & C_{56}\\ C_{61} & C_{62} & C_{63} & C_{64} & C_{65} & C_{66}\end{bmatrix}^{-1} \begin{bmatrix} e_{11} & e_{21} & e_{31}\\ e_{12} & e_{22} & e_{32}\\ e_{13} & e_{23} & e_{33}\\ e_{14} & e_{24} & e_{34}\\ e_{15} & e_{25} & e_{35}\\ e_{16} & e_{26} & e_{36}\end{bmatrix} \begin{bmatrix}E_1\\ E_2\\ E_3\end{bmatrix} \tag{217}$$

Setting $\Delta T^{\text{Fake}} = E_1,\ E_2 = 0,\ E_3 = 0$, we have,

$$\begin{bmatrix}\alpha_1\\ \alpha_2\\ \alpha_3\\ \alpha_4\\ \alpha_5\\ \alpha_6\end{bmatrix}^{\text{Fake}} E_1 = \begin{bmatrix} C_{11} & C_{12} & C_{13} & C_{14} & C_{15} & C_{16}\\ C_{21} & C_{22} & C_{23} & C_{24} & C_{25} & C_{26}\\ C_{31} & C_{32} & C_{33} & C_{34} & C_{35} & C_{36}\\ C_{41} & C_{42} & C_{43} & C_{44} & C_{45} & C_{46}\\ C_{51} & C_{52} & C_{53} & C_{54} & C_{55} & C_{56}\\ C_{61} & C_{62} & C_{63} & C_{64} & C_{65} & C_{66}\end{bmatrix}^{-1} \begin{bmatrix} e_{11} & e_{21} & e_{31}\\ e_{12} & e_{22} & e_{32}\\ e_{13} & e_{23} & e_{33}\\ e_{14} & e_{24} & e_{34}\\ e_{15} & e_{25} & e_{35}\\ e_{16} & e_{26} & e_{36}\end{bmatrix} \begin{bmatrix}E_1\\ 0\\ 0\end{bmatrix} \tag{218}$$

or

$$\begin{bmatrix}\alpha_1\\ \alpha_2\\ \alpha_3\\ \alpha_4\\ \alpha_5\\ \alpha_6\end{bmatrix}^{\text{Fake}} E_1 = \begin{bmatrix} C_{11} & C_{12} & C_{13} & C_{14} & C_{15} & C_{16}\\ C_{21} & C_{22} & C_{23} & C_{24} & C_{25} & C_{26}\\ C_{31} & C_{32} & C_{33} & C_{34} & C_{35} & C_{36}\\ C_{41} & C_{42} & C_{43} & C_{44} & C_{45} & C_{46}\\ C_{51} & C_{52} & C_{53} & C_{54} & C_{55} & C_{56}\\ C_{61} & C_{62} & C_{63} & C_{64} & C_{65} & C_{66}\end{bmatrix}^{-1} \begin{bmatrix} e_{11}\\ e_{12}\\ e_{13}\\ e_{14}\\ e_{15}\\ e_{16}\end{bmatrix} E_1 \tag{219}$$

so

$$\begin{bmatrix}\alpha_1\\ \alpha_2\\ \alpha_3\\ \alpha_4\\ \alpha_5\\ \alpha_6\end{bmatrix}^{\text{Fake}} = \begin{bmatrix} C_{11} & C_{12} & C_{13} & C_{14} & C_{15} & C_{16}\\ C_{21} & C_{22} & C_{23} & C_{24} & C_{25} & C_{26}\\ C_{31} & C_{32} & C_{33} & C_{34} & C_{35} & C_{36}\\ C_{41} & C_{42} & C_{43} & C_{44} & C_{45} & C_{46}\\ C_{51} & C_{52} & C_{53} & C_{54} & C_{55} & C_{56}\\ C_{61} & C_{62} & C_{63} & C_{64} & C_{65} & C_{66}\end{bmatrix}^{-1} \begin{bmatrix} e_{11}\\ e_{12}\\ e_{13}\\ e_{14}\\ e_{15}\\ e_{16}\end{bmatrix} \tag{220}$$

Generally, for any single applied electric field component, E_i, set $\Delta T^{\text{Fake}} = E_i$ and $E_j = 0$ ($j \neq i$) along with,

$$\begin{bmatrix} \alpha_1 \\ \alpha_2 \\ \alpha_3 \\ \alpha_4 \\ \alpha_5 \\ \alpha_6 \end{bmatrix}^{\text{Fake}} = \begin{bmatrix} C_{11} & C_{12} & C_{13} & C_{14} & C_{15} & C_{16} \\ C_{21} & C_{22} & C_{23} & C_{24} & C_{25} & C_{26} \\ C_{31} & C_{32} & C_{33} & C_{34} & C_{35} & C_{36} \\ C_{41} & C_{42} & C_{43} & C_{44} & C_{45} & C_{46} \\ C_{51} & C_{52} & C_{53} & C_{54} & C_{55} & C_{56} \\ C_{61} & C_{62} & C_{63} & C_{64} & C_{65} & C_{66} \end{bmatrix}^{-1} \begin{bmatrix} e_{i1} \\ e_{i2} \\ e_{i3} \\ e_{i4} \\ e_{i5} \\ e_{i6} \end{bmatrix} \tag{221}$$

Similarly, to mimic the piezomagnetic effects using the thermal terms, set $\Delta T^{\text{Fake}} = H_i$ and $H_j = 0$ ($j \neq i$) along with,

$$\begin{bmatrix} \alpha_1 \\ \alpha_2 \\ \alpha_3 \\ \alpha_4 \\ \alpha_5 \\ \alpha_6 \end{bmatrix}^{\text{Fake}} = \begin{bmatrix} C_{11} & C_{12} & C_{13} & C_{14} & C_{15} & C_{16} \\ C_{21} & C_{22} & C_{23} & C_{24} & C_{25} & C_{26} \\ C_{31} & C_{32} & C_{33} & C_{34} & C_{35} & C_{36} \\ C_{41} & C_{42} & C_{43} & C_{44} & C_{45} & C_{46} \\ C_{51} & C_{52} & C_{53} & C_{54} & C_{55} & C_{56} \\ C_{61} & C_{62} & C_{63} & C_{64} & C_{65} & C_{66} \end{bmatrix}^{-1} \begin{bmatrix} q_{i1} \\ q_{i2} \\ q_{i3} \\ q_{i4} \\ q_{i5} \\ q_{i6} \end{bmatrix} \tag{222}$$

In order to mimic the thermo-electric effects, we set $\boldsymbol{\alpha}^{\text{Fake}} \Delta T^{\text{Fake}} = \mathbf{C}^{-1}\mathbf{e}\boldsymbol{\zeta}\Delta T$. Retaining anisotropic material behavior and setting $\Delta T^{\text{Fake}} = \Delta T$,

$$\begin{bmatrix} \alpha_1 \\ \alpha_2 \\ \alpha_3 \\ \alpha_4 \\ \alpha_5 \\ \alpha_6 \end{bmatrix}^{\text{Fake}} = \begin{bmatrix} C_{11} & C_{12} & C_{13} & C_{14} & C_{15} & C_{16} \\ C_{21} & C_{22} & C_{23} & C_{24} & C_{25} & C_{26} \\ C_{31} & C_{32} & C_{33} & C_{34} & C_{35} & C_{36} \\ C_{41} & C_{42} & C_{43} & C_{44} & C_{45} & C_{46} \\ C_{51} & C_{52} & C_{53} & C_{54} & C_{55} & C_{56} \\ C_{61} & C_{62} & C_{63} & C_{64} & C_{65} & C_{66} \end{bmatrix}^{-1} \begin{bmatrix} e_{11} & e_{21} & e_{31} \\ e_{12} & e_{22} & e_{32} \\ e_{13} & e_{23} & e_{33} \\ e_{14} & e_{24} & e_{34} \\ e_{15} & e_{25} & e_{35} \\ e_{16} & e_{26} & e_{36} \end{bmatrix} \begin{bmatrix} \zeta_1 \\ \zeta_2 \\ \zeta_3 \end{bmatrix} \tag{223}$$

In order to mimic the thermo-magnetic effects, we set $\Delta T^{\text{Fake}} = \Delta T$, along with,

$$\begin{bmatrix}\alpha_1\\ \alpha_2\\ \alpha_3\\ \alpha_4\\ \alpha_5\\ \alpha_6\end{bmatrix}^{\text{Fake}} = \begin{bmatrix} C_{11} & C_{12} & C_{13} & C_{14} & C_{15} & C_{16}\\ C_{21} & C_{22} & C_{23} & C_{24} & C_{25} & C_{26}\\ C_{31} & C_{32} & C_{33} & C_{34} & C_{35} & C_{36}\\ C_{41} & C_{42} & C_{43} & C_{44} & C_{45} & C_{46}\\ C_{51} & C_{52} & C_{53} & C_{54} & C_{55} & C_{56}\\ C_{61} & C_{62} & C_{63} & C_{64} & C_{65} & C_{66}\end{bmatrix}^{-1} \begin{bmatrix} q_{11} & q_{21} & q_{31}\\ q_{12} & q_{22} & q_{32}\\ q_{13} & q_{23} & q_{33}\\ q_{14} & q_{24} & q_{34}\\ q_{15} & q_{25} & q_{35}\\ q_{16} & q_{26} & q_{36}\end{bmatrix} \begin{bmatrix}\zeta_1\\ \zeta_2\\ \zeta_3\end{bmatrix} \tag{224}$$

It is thus possible to mimic the piezoelectric or piezomagnetic behavior of a material in response to a single electric or magnetic field component by using the fake coefficients of thermal expansion given by eqs. (221) and (222). The thermo-electric and thermo-magnetic behavior can be mimicked by using the fake coefficients of thermal expansion given by eqs. (223) and (224).

6.3 Panel Level Thermal Terms Mimicking Thermo-Electro-Magnetic Response

A simple thermal analogy is also in effect on the panel and laminate level. The laminate or stiffened panel constitutive equation is given by,

$$\begin{bmatrix}\mathbf{N}\\ \mathbf{M}\end{bmatrix} = \begin{bmatrix}\mathbf{A} & \mathbf{B}\\ \mathbf{B} & \mathbf{D}\end{bmatrix}\begin{bmatrix}\boldsymbol{\varepsilon}^0\\ \boldsymbol{\kappa}^0\end{bmatrix} - \begin{bmatrix}\mathbf{A}^{\alpha} & \mathbf{B}^{\alpha}\\ \mathbf{B}^{\alpha} & \mathbf{D}^{\alpha}\end{bmatrix}\begin{bmatrix}\Delta T\\ -\Delta G\end{bmatrix} - \begin{bmatrix}\mathbf{A}^{E}\\ \mathbf{B}^{E}\end{bmatrix}\begin{bmatrix}E_x\\ E_y\\ E_z\end{bmatrix} - \begin{bmatrix}\mathbf{A}^{M}\\ \mathbf{B}^{M}\end{bmatrix}\begin{bmatrix}H_x\\ H_y\\ H_z\end{bmatrix} - \begin{bmatrix}\mathbf{A}^{ET} & \mathbf{B}^{ET}\\ \mathbf{B}^{ET} & \mathbf{D}^{ET}\end{bmatrix}\begin{bmatrix}\Delta T\\ -\Delta G\end{bmatrix} - \begin{bmatrix}\mathbf{A}^{MT} & \mathbf{B}^{MT}\\ \mathbf{B}^{MT} & \mathbf{D}^{MT}\end{bmatrix}\begin{bmatrix}\Delta T\\ -\Delta G\end{bmatrix} \tag{225}$$

Equating fake thermal terms with the piezoelectric terms gives,

$$\begin{bmatrix}\mathbf{A}^{\alpha} & \mathbf{B}^{\alpha}\\ \mathbf{B}^{\alpha} & \mathbf{D}^{\alpha}\end{bmatrix}^{\text{Fake}}\begin{bmatrix}\Delta T\\ -\Delta G\end{bmatrix}^{\text{Fake}} = \begin{bmatrix}\mathbf{A}^{E}\\ \mathbf{B}^{E}\end{bmatrix}\begin{bmatrix}E_x\\ E_y\\ E_z\end{bmatrix} \tag{226}$$

or,

$$\begin{bmatrix} A_1^{\alpha} & B_1^{\alpha}\\ A_2^{\alpha} & B_2^{\alpha}\\ A_3^{\alpha} & B_3^{\alpha}\\ B_1^{\alpha} & D_1^{\alpha}\\ B_2^{\alpha} & D_2^{\alpha}\\ B_3^{\alpha} & D_3^{\alpha}\end{bmatrix}^{\text{Fake}}\begin{bmatrix}\Delta T\\ -\Delta G\end{bmatrix}^{\text{Fake}} = \begin{bmatrix} A_{11}^{E} & A_{12}^{E} & A_{13}^{E}\\ A_{21}^{E} & A_{22}^{E} & A_{23}^{E}\\ A_{31}^{E} & A_{32}^{E} & A_{33}^{E}\\ B_{11}^{E} & B_{12}^{E} & B_{13}^{E}\\ B_{21}^{E} & B_{22}^{E} & B_{23}^{E}\\ B_{31}^{E} & B_{32}^{E} & B_{33}^{E}\end{bmatrix}\begin{bmatrix}E_x\\ E_y\\ E_z\end{bmatrix} \tag{227}$$

Applying a single electric field component, E_i, we have,

$$\begin{bmatrix} A_1^{\alpha} & B_1^{\alpha} \\ A_2^{\alpha} & B_2^{\alpha} \\ A_3^{\alpha} & B_3^{\alpha} \\ B_1^{\alpha} & D_1^{\alpha} \\ B_2^{\alpha} & D_2^{\alpha} \\ B_3^{\alpha} & D_3^{\alpha} \end{bmatrix}^{\text{Fake}} \begin{bmatrix} \Delta T \\ -\Delta G \end{bmatrix}^{\text{Fake}} = \begin{bmatrix} A_{1i}^{E} \\ A_{2i}^{E} \\ A_{3i}^{E} \\ B_{1i}^{E} \\ B_{2i}^{E} \\ B_{3i}^{E} \end{bmatrix} E_i \tag{228}$$

Setting $\Delta T^{\text{Fake}} = E_i$ and $\Delta G^{\text{Fake}} = 0$ gives,

$$\begin{bmatrix} A_1^{\alpha} \\ A_2^{\alpha} \\ A_3^{\alpha} \\ B_1^{\alpha} \\ B_2^{\alpha} \\ B_3^{\alpha} \end{bmatrix}^{\text{Fake}} E_i = \begin{bmatrix} A_{1i}^{E} \\ A_{2i}^{E} \\ A_{3i}^{E} \\ B_{1i}^{E} \\ B_{2i}^{E} \\ B_{3i}^{E} \end{bmatrix} E_i \tag{229}$$

or,

$$\begin{bmatrix} A_1^{\alpha} \\ A_2^{\alpha} \\ A_3^{\alpha} \\ B_1^{\alpha} \\ B_2^{\alpha} \\ B_3^{\alpha} \end{bmatrix}^{\text{Fake}} = \begin{bmatrix} A_{1i}^{E} \\ A_{2i}^{E} \\ A_{3i}^{E} \\ B_{1i}^{E} \\ B_{2i}^{E} \\ B_{3i}^{E} \end{bmatrix} \tag{230}$$

Similarly, to determine fake thermal terms that mimic the panel/laminate piezomagnetic response, we set $\Delta T^{\text{Fake}} = H_i$ and $\Delta G^{\text{Fake}} = 0$ along with,

$$\begin{bmatrix} A_1^{\alpha} \\ A_2^{\alpha} \\ A_3^{\alpha} \\ B_1^{\alpha} \\ B_2^{\alpha} \\ B_3^{\alpha} \end{bmatrix}^{\text{Fake}} = \begin{bmatrix} A_{1i}^{M} \\ A_{2i}^{M} \\ A_{3i}^{M} \\ B_{1i}^{M} \\ B_{2i}^{M} \\ B_{3i}^{M} \end{bmatrix} \tag{231}$$

These results are useful because they enable the analysis of piezoelectric and piezomagnetic shells within NASTRAN using the software's thermal analysis capabilities. NASTRAN accepts thermal ABD matrices for the shell materials. Thus, by providing NASTRAN with the appropriate fake thermal terms, the software will solve a thermal problem that is analogous to a desired piezoelectric or piezomagnetic problem. An even simpler analogy exists between the panel level thermal terms and the thermo-electric or thermo-magnetic terms. Simply setting,

$$\begin{bmatrix} \mathbf{A}^{\alpha} & \mathbf{B}^{\alpha} \\ \mathbf{B}^{\alpha} & \mathbf{D}^{\alpha} \end{bmatrix}^{\text{Fake}} = \begin{bmatrix} \mathbf{A}^{ET} & \mathbf{B}^{ET} \\ \mathbf{B}^{ET} & \mathbf{D}^{ET} \end{bmatrix} \tag{232}$$

or

$$\begin{bmatrix} \mathbf{A}^{\alpha} & \mathbf{B}^{\alpha} \\ \mathbf{B}^{\alpha} & \mathbf{D}^{\alpha} \end{bmatrix}^{\text{Fake}} = \begin{bmatrix} \mathbf{A}^{MT} & \mathbf{B}^{MT} \\ \mathbf{B}^{MT} & \mathbf{D}^{MT} \end{bmatrix} \tag{233}$$

will enable the thermal capabilities to mimic the thermo-electric or thermo-magnetic response. However, these analogies are less useful because their use assumes that the panel or laminate only reacts to the applied thermal loading through the thermo-electric or thermo-magnetic terms, and not through the standard thermal expansion terms. That is, these analogies would only be valid for the case in which the panel/laminate coefficients of thermal expansion are zero.

7. Results and Discussion

To verify the thermo-electro-magneto-elastic implementation within HyperSizer, we consider a bonded facesheet-flange combination, which is identical to the HyperSizer section 8 shown in figures 4 and 5. The geometry of this problem is shown in figure 6. Within HyperSizer, this case corresponds to a T-stiffened panel (see fig. 4) with an infinitesimal web. The facesheet is composed of PZT-7A zirconium lead titanate piezoelectric material with a through-thickness poling direction, while the flange is composed of aluminum. The material properties employed for these materials are given in tables 1 and 2. As indicated in figure 6, a voltage difference of 1×10^5 V is applied through the thickness of the face sheet. This corresponds to an electric field of $(1\times10^5 \text{ V})/(0.00229 \text{ m}) = 43.67$ MV/m. This problem has also been analyzed using the ABAQUS finite element analysis package, employing the finite element mesh shown in figure 7, consisting of a total of 21,200 elements. The facesheet is composed of CPE4E piezoelectric plane strain continuum elements, while the flange and adhesive are composed of CPE4R reduced integration plane strain continuum elements.

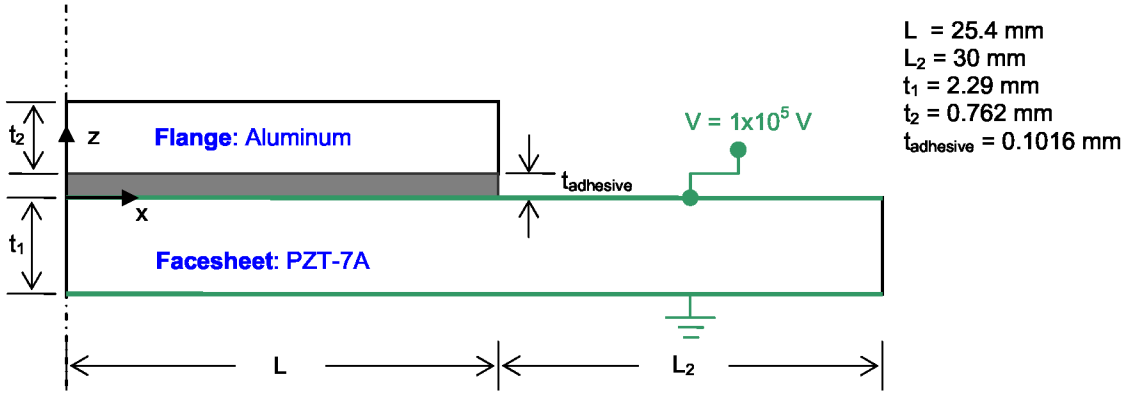

Figure 6.—ABAQUS solution domain for a facesheet-adhesive-flange combination.

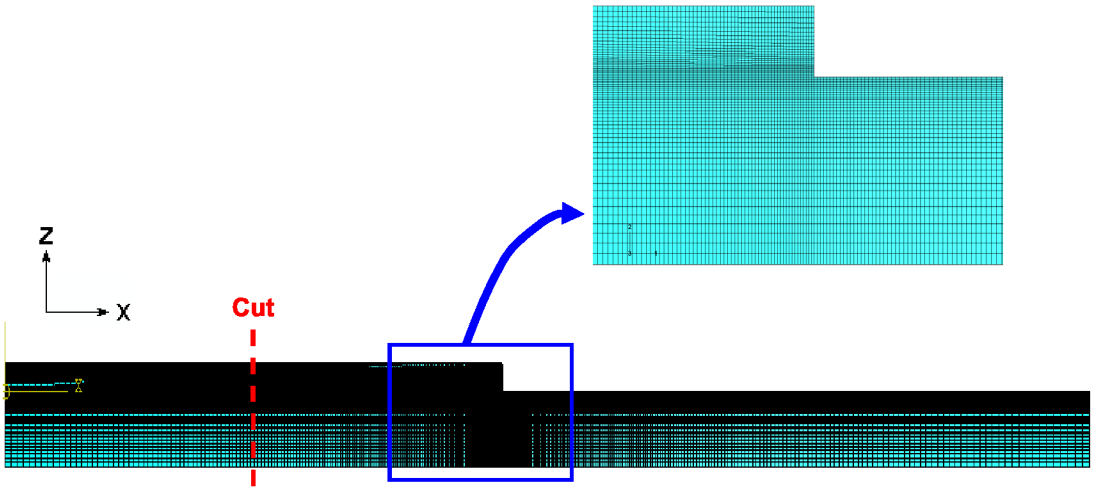

Figure 7.—ABAQUS mesh for the bonded doubler joint.

TABLE 1.—ELASTIC CONSTANTS OF THE MATERIALS USED IN THE ANALYSES (REFS. 3 AND 4)

	E_{11} (GPa)	E_{22} (GPa)	E_{33} (GPa)	V_{12}	v_{13}	v_{23}	G_{12} (GPa)	G_{13} (GPa)	G_{23} (GPa)
Aluminum	68.95	68.95	68.95	0.30	0.30	0.30	26.52	26.52	26.52
PZT-7A	94.97	81.90	94.97	0.384	0.323	0.331	25.40	25.40	35.90

TABLE 2.—PIEZOELECTRIC PROPERTIES (REF. 4) OF THE MATERIALS USED IN THE ANALYSES

	e_{222} (C/m^2)	e_{233} (C/m^2)	e_{211} (C/m^2)	e_{323} (C/m^2)	e_{112} (C/m^2)	k_{22} (10^{-9} C/V m)	k_{33} (10^{-9} C/V m)	k_{11} (10^{-9} C/V m)
PZT-7A	12.25	–2.1	–2.1	9.2	9.2	2.07	4.07	4.07

The normal stresses in the plane defined by the facesheet (*x-y* plane) arising due to the applied voltage along the cut shown in figure 7 are plotted in figures 8 and 9. The original ABAQUS solution (labeled "ABAQUS Fully Coupled") agrees reasonably well with the HyperSizer solution, but some deviation is evident. This deviation is caused by the fact that HyperSizer's formulation is based on the ability to apply constant panel (or laminate) level electric field components. In contrast, the ABAQUS continuum solution involves the application of electric potential at boundaries along with solution of a boundary value problem for the electric potential throughout the model. As will be shown, the ABAQUS solution does not result in constant electric field components.

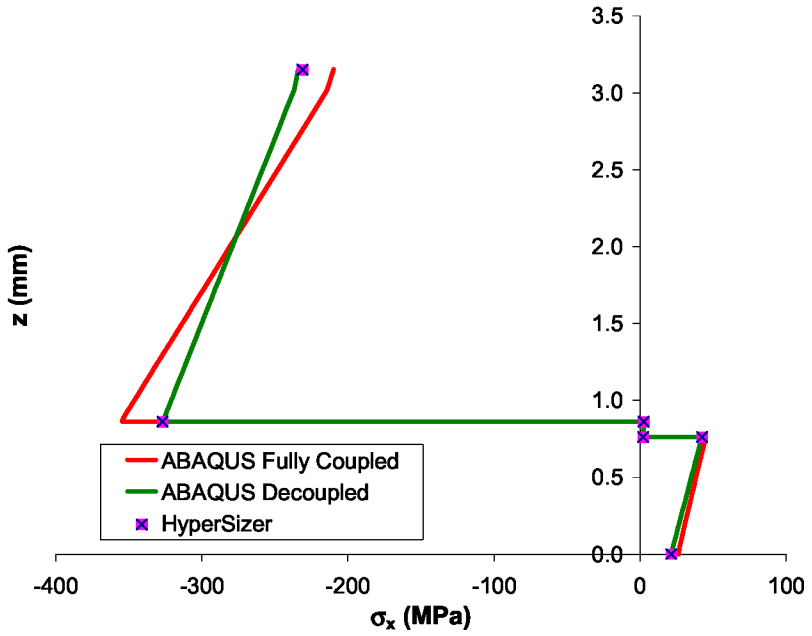

Figure 8.—Stress component (σ_x) along the cut through the flange adhesive and facesheet defined in figure 7 as predicted by HyperSizer and ABAQUS both with fully coupled and decoupled electric field components.

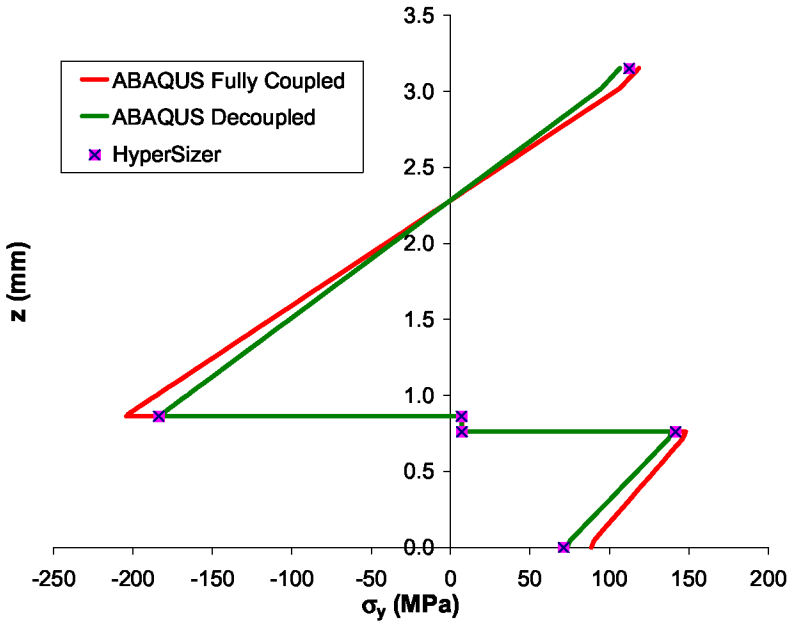

Figure 9.—Stress component (σ_y) along the cut through the flange adhesive and facesheet defined in figure 7 as predicted by HyperSizer and ABAQUS both with fully coupled and decoupled electric field components.

In order to provide the ABAQUS solution with constant electric field components, which mimics the HyperSizer formulation, it is possible to employ artificially large dielectric constants (κ_{ij}) for the PZT-7A material. This, in effect, decouples the electric field components (E_i) in the piezoelectric material constitutive equation,

$$\begin{bmatrix} \sigma_{11} \\ \sigma_{22} \\ \sigma_{33} \\ \sigma_{23} \\ \sigma_{13} \\ \sigma_{12} \\ D_1 \\ D_2 \\ D_3 \end{bmatrix} = \begin{bmatrix} C_{11} & C_{12} & C_{13} & 0 & 0 & 0 & e_{11} & 0 & 0 \\ C_{12} & C_{22} & C_{23} & 0 & 0 & 0 & e_{12} & 0 & 0 \\ C_{13} & C_{23} & C_{33} & 0 & 0 & 0 & e_{13} & 0 & 0 \\ 0 & 0 & 0 & C_{44} & 0 & 0 & 0 & 0 & 0 \\ 0 & 0 & 0 & 0 & C_{55} & 0 & 0 & 0 & e_{35} \\ 0 & 0 & 0 & 0 & 0 & C_{66} & 0 & e_{26} & 0 \\ e_{11} & e_{12} & e_{13} & 0 & 0 & 0 & \kappa_{11} & 0 & 0 \\ 0 & 0 & 0 & 0 & 0 & e_{26} & 0 & \kappa_{22} & 0 \\ 0 & 0 & 0 & 0 & e_{35} & 0 & 0 & 0 & \kappa_{33} \end{bmatrix} \begin{bmatrix} \varepsilon_{11} \\ \varepsilon_{22} \\ \varepsilon_{33} \\ \gamma_{23} \\ \gamma_{13} \\ \gamma_{12} \\ E_1 \\ E_2 \\ E_3 \end{bmatrix} \tag{234}$$

where D_i are the electric displacement components and an x_1 poling direction has been assumed. By making the dielectric constants large, the stress, strain, and electric displacement components will depend on the electric field components, but the electric field components will not depend on the stress, strain, or electric displacement components. This condition is analogous to specifying constant electric field components, as is done in HyperSizer, such that they cannot vary due to the other field components.

To accomplish the decoupling of the electric field components described above, the dielectric constants given in table 2 were increased by a factor of 10^5. Results for this case, labeled "ABAQUS Decoupled", in figures 8 and 9 now agree extremely well with the HyperSizer solution. Figures 10 to 13 provide further comparisons between the ABAQUS results with and without fully electric field coupling. Figure 10 indicates a slight difference in the von Mises stress field between the two cases. Likewise figure 11 shows only a small difference between the electric potential solution between the fully coupled and decoupled cases. However, the spatial derivatives of the electric potential, which are the electric field components in the two directions, do show significant differences. In figure 12(a), in the region of the facesheet directly beneath the flange, a through-thickness electric field gradient has arisen due to stress, strain, and electric displacement components that arise in the region due to the presence of the flange. In figure 12(b) on the other hand, the decoupling has eliminated this variation in the E_z electric field component, and a constant E_z value of 43.67 MV/m results in the facesheet, identical to the value applied in HyperSizer. The variation in E_z evident in figure 12(a) is approximately ±8 percent with respect to the constant decoupled value, which is not excessively large, but clearly is large enough to have an effect. In figure 13(a), a gradient in the E_x electric field component has arisen near the free edge of the adhesive bond within the facesheet. This is due to γ_{xz} shear strain that arises in this region which, thanks to a non-zero e_{26} (see eq. (234)), gives rise to an electric displacement and field. In figure 13(b), the decoupling of the electric field components has eliminated this gradient, and a constant E_x field results with a value of zero. Again, this is identical to the condition imposed in the HyperSizer solution.

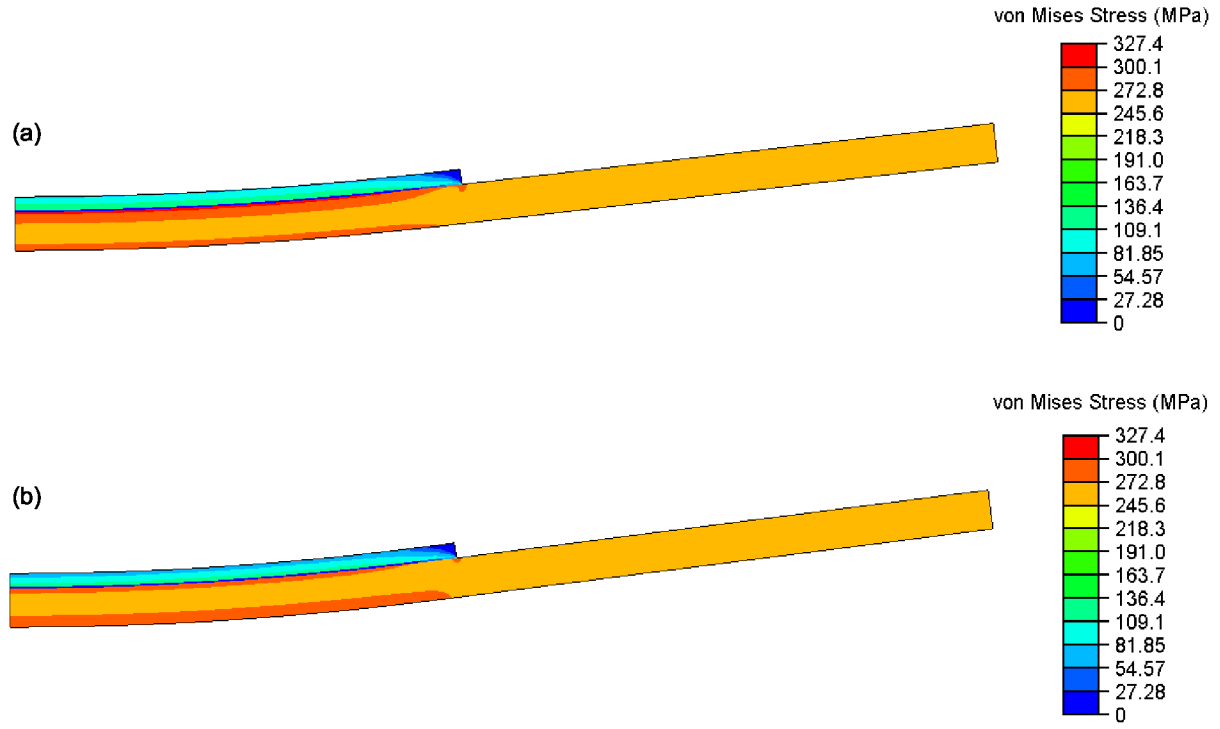

Figure 10.—Von Mises stress field predicted by ABAQUS with (a) fully coupled and (b) decoupled electric field components.

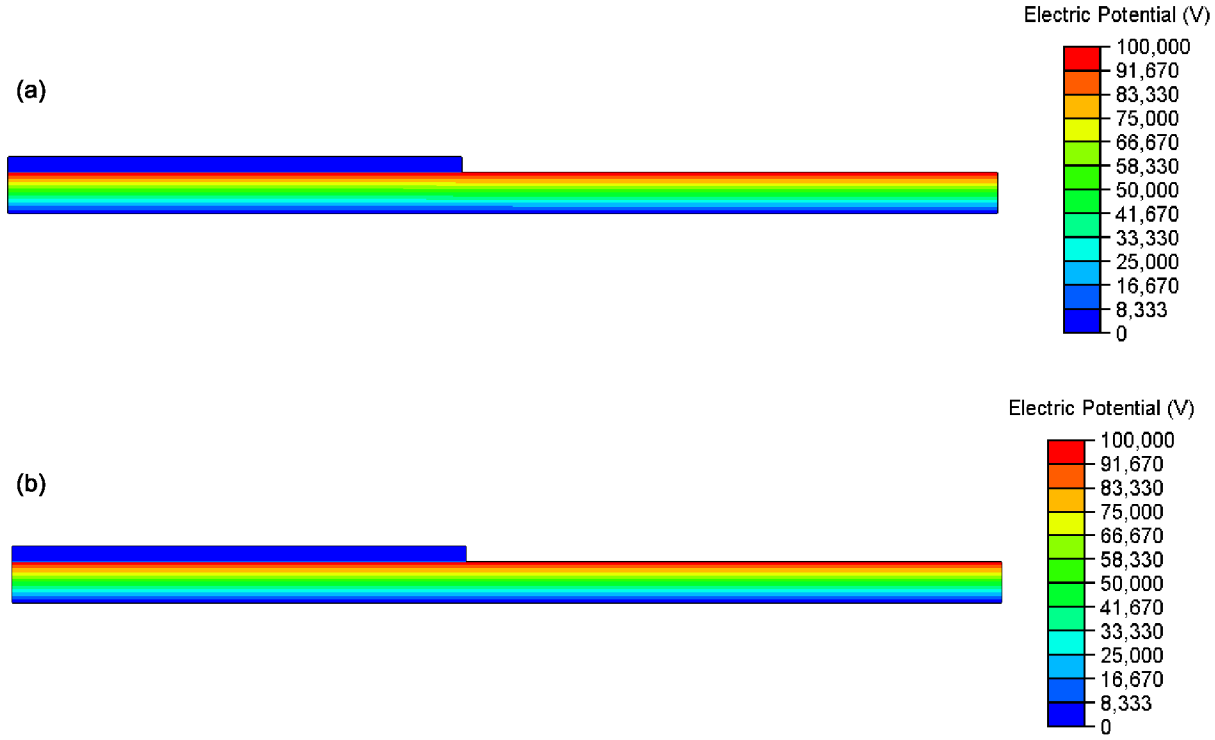

Figure 11.—Electric potential field predicted by ABAQUS with (a) fully coupled and (b) decoupled electric field components.

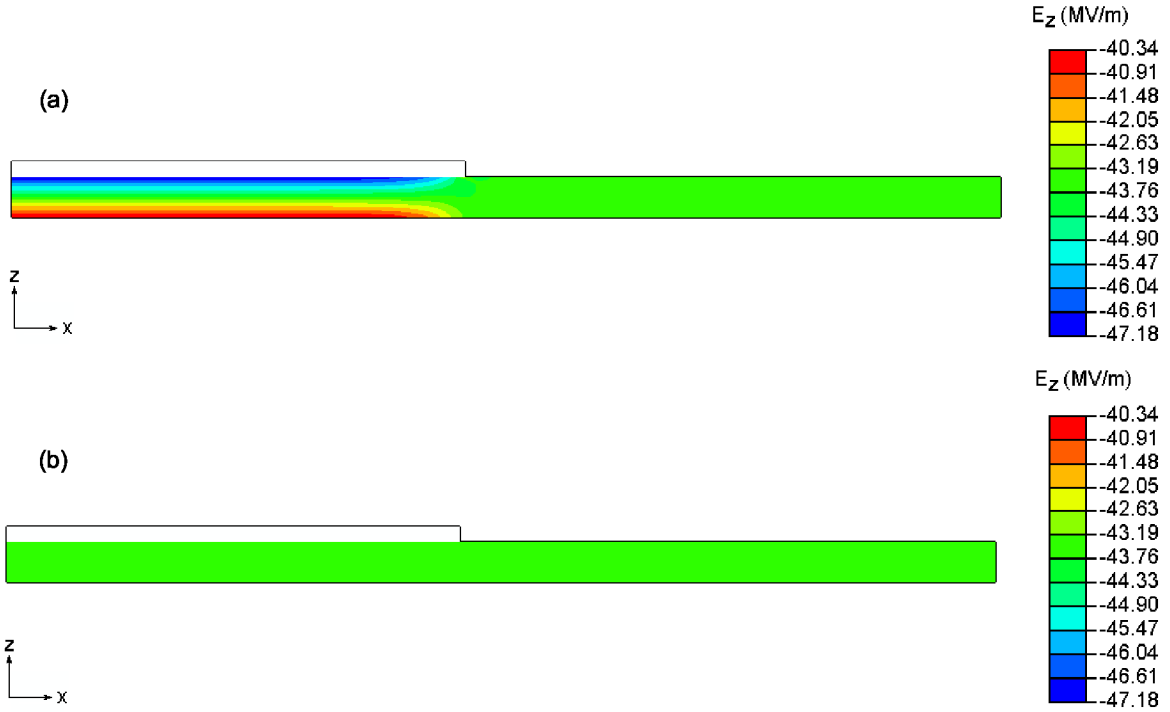

Figure 12.—Electric field component E_z predicted by ABAQUS with (a) fully coupled and (b) decoupled electric field components.

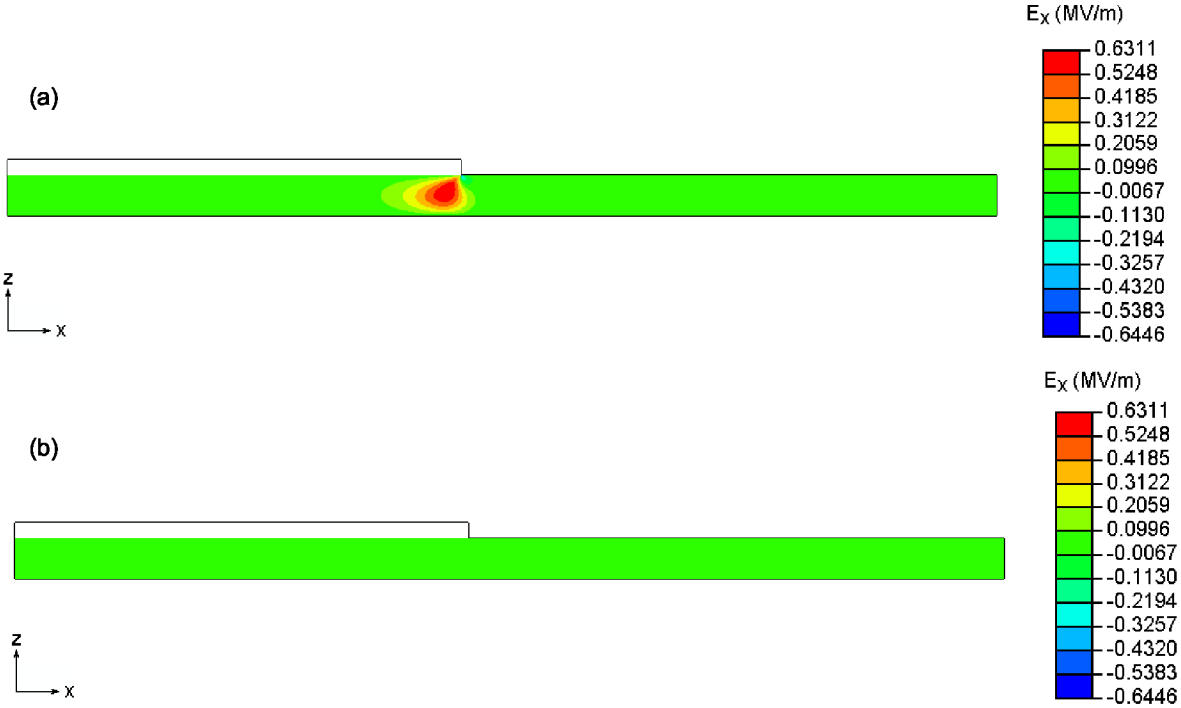

Figure 13.—Electric field component E_x predicted by ABAQUS with (a) fully coupled and (b) decoupled electric field components.

8. Conclusion

The methods employed within HyperSizer to analyze composite stiffened panels with thermo-electro-magneto-elastic coupling have been presented. Starting on the level of the laminate, classical lamination theory is employed, and new electric, magnetic, thermo-electric, and thermo-magnetic ABD terms have been identified. Homogenization techniques have been presented for blade and flanged stiffeners that result in stiffened panel level constitutive equations that are analogous to thermo-electro-magnetic laminate constitutive equations. These allow the stiffened panel to be included in a higher scale structural model via methods that accept laminate constitutive equation terms such as MSC/NASTRAN. While MSC/NASTRAN does not presently accept the newly developed thermo-electro-magnetic terms, the ability to calculate these terms allows the easy quantification and analysis of a new class of smart stiffened panels.

The analogy between standard lamination theory thermal expansion effects and the newly developed thermo-electro-magnetic effect was also discussed. This thermal analogy can be used to model the response of smart structure through a method's existing thermal capabilities, or to model a thermal response of a structure through a method's electro-magnetic material capabilities. The former is useful for generating results for comparison with a known method, while the latter is useful for verifying a thermo-electro-magnetic method by generating known thermal results. In both cases, the coefficients needed to take advantage of the thermal analogy have been identified.

Verification results have been presented that compare HyperSizer piezoelectric results with ABAQUS piezoelectric finite results for a facesheet-adhesive-flange combination. Because the ABAQUS capabilities are limited to piezoelectric materials, the new piezomagnetic, thermo-electric, and thermo-magnetic capabilities of HyperSizer were not compared. The results indicated generally good agreement between HyperSizer and ABAQUS. However, because ABAQUS solves a piezoelectric boundary value problem subject to prescribed electric potential, the electric field components can vary spatially within the model. The HyperSizer implementation, on the other hand, is based on classical lamination theory with prescribed spatially constant electric field components. This limitation leads to some discrepancy in the results. By decoupling the electric field components within the ABAQUS solution by significantly increasing the piezoelectric material dielectric constants, the electric field components are forced to remain constant. ABAQUS results in this decoupled condition match the HyperSizer results nearly exactly, serving to verify the HyperSizer piezoelectric implementation.

References

1. Gandhi, M.V. and Thompson, B.S. (1992) *Smart Materials and Structures*. Chapman & Hall, New York.
2. Uchino, K. (1997) *Piezoelectric Actuators and Ultrasonic Motors*. Kluwer Academic Publishers, Hingham, MA.
3. Parton, V.Z. and Krudryavtsev, B.A. (1988) *Electromagnetoelasticity Piezoelectrics and Electrically Conductive Solids*. Taylor & Francis, New York.
4. Krudryavtsev, B.A., Parton, V.Z., and Senik, N.A. (1990) "Magnetothermoelasticity" in *Applied Mechanics: Soviet Reviews Volume 2: Electromagnetoelasticity*, G.K. Mikhailov and V.Z. Parton, eds., Hemisphere Publishing Corp., New York.
5. Bednarcyk, B.A. and Arnold, S.M. (2002a) "MAC/GMC 4.0 User's Manual, Volume 2: Keywords Manual" NASA/TM—2002-212077/VOL2, 2002 and "Volume 2: Keywords Manual" TM 2002-212077/Vol 2.
6. Bednarcyk, B.A. and Arnold, S.M. (2002b) "MAC/GMC 4.0 User's Manual, Volume 2: Keywords Manual" NASA/TM—2002-212077/VOL2, 2002 and "Volume 3: Example Problem Manual" NASA/TM—2002-212077/VOL3.
7. Collier Research Corp. (1998) *HyperSizer Structural Sizing Software*. Hampton, VA.

8. Lee, C.K. "Theory of Laminated Piezoelectric Plates for the Design of Distributed Sensors/Actuators. Part I: Governing Equations and Reciprocal Relationships" *Journal of the Acoustical Society of America*, 87, 1145–1158.
9. Crawley, E.F. and Lazarus, K.B. (1991) "Induced Strain Actuation of Isotropic and Anisotropic Plates" *AIAA Journal*, 29, 944–951.
10. Tauchert, T.R. (1992) "Piezothermoelastic Behavior of a Laminated Plate" *Journal of Thermal Stresses*, 15, 25–37.
11. Tzou, H.S. (1993) *Piezoelectric Shells: Distributed Sensing and Control of Continua*, Kluwer Academic, Norwell, MA.
12. Jonnalagadda, K.D., Blanford, G.E., and Tauchert, T.R. (1994) "Piezothermoelastic Composite Plate Analysis Using a First-Order Shear Deformation Theory" *Computers and Structures*, 51, 79–89.
13. Carrera, E. (1997) "An Improved Reissner-Mindlin-type Model for the Electromechanical Analysis of Multilayered Plates Including Piezo-layers" *Journal of Intelligent Material Systems and Structures*, 8, 232–248.
14. Saravanos, D.A. and Heyliger, P.R. (1999) "Mechanics and Computational Models for Laminated Piezoelectric Beams, Plates, and Shells" *Applied Mechanics Reviews*, 52, 305–320.
15. Gopinathan, S.V., Varadan, V.V., and Varadan, V.K. (2000) "A Review and Critique of Theories for Piezoelectric Laminates" *Smart Materials and Structures*, 9, 24–48.
16. Schultz, M.R. and Hyer, M.W. (2003) "Snap-through of Unsymmetric Cross-ply Laminates using Piezoceramic Actuators" *Journal of Intelligent Material Systems and Structures*, 14, 795–814.
17. Fernandes, A. and Pouget, J. (2004) "Analytical and Numerical Modelling of Laminated Composites with Piezoelectric Elements" *Journal of Intelligent Material Systems and Structures*, 15, 753–761.
18. Robbins, D.H. and Reddy, J.N. (1993) "Modelling of Thick Composites Using a Layerwise Laminate Theory" *International Journal for Numerical Methods in Engineering*, 36, 655–677.
19. Saravanos, D.A., Heyliger, P.R., and Hopkins, D.A. (1997) "Layerwise Mechanics and Finite Element for the Dynamic Analysis of Piezoelectric Composite Plates" *International Journal of Solids and Structures*, 34, 359–378.
20. Lee, H.J. and Saravanos, D.A. (1997) "Generalized Finite Element Formulation for Smart Multi-Layered Thermal Piezoelectric Composite Plates" *International Journal of Solids and Structures*, 34, 3355–3371.
21. Lee, H.J. and Saravanos, D.A. (2000) "A Mixed Multi-Field Finite Element Formulation for Thermopiezoelectric Composite Shells" *International Journal of Solids and Structures*, 37, 4949–4967.
22. Bansal, A. and Ramaswamy, A. (2002) "FE Analysis of Piezo-laminate Composites Under Thermal Loads" *Journal of Intelligent Material Systems and Structures*, 13, 291–301.
23. Pan, E. (2001) "Exact Solution for Simply-Supported and Multilayered Magneto-Electro-Elastic Plates" *Journal of Applied Mechanics*, 68, 608–618.
24. Pan, E. and Heyliger, P.R. (2003) "Exact Solutions for Magnetoelectroelastic Laminates in Cylindrical Bending" *International Journal of Solids and Structures* 40, 6859–6876.
25. Heyliger, P.R., Ramirez, F., and Pan, E. (2004) "Two-dimensional Static Fields in Magnetoelectroelastic Laminates" *Journal of Intelligent Material Systems and Structures*, 15, 689–709.
26. Bednarcyk, B.A. (2003) "An Inelastic Micro/Macro Theory for Hybrid Smart/Metal Composites" *Composites: Part B*, 34, 175–197.
27. Jones, R.M. (1975) *Mechanics of Composite Materials*. Hemisphere, New York.
28. Herakovich, C.T. (1998) *Mechanics of Fibrous Composites*. John Wiley & Sons, New York.
29. Collier, C.S. (1993) "Stiffness, Thermal Expansion, and Thermal Bending Formulation of Stiffened, Fiber- Reinforced Composite Panels" AIAA Paper No. 1993–1569.
30. Côté, F., Masson, P., Mrad, N., and Cotoni, V. (2004) "Dynamic and Static Modeling of Piezoelectric Composite Structures Using a Thermal Analogy with NSC/NASTRAN" *Composite Structures*, 65, 2004.

REPORT DOCUMENTATION PAGE		Form Approved OMB No. 0704-0188

1. REPORT DATE *(DD-MM-YYYY)*	2. REPORT TYPE	3. DATES COVERED *(From - To)*
01-07-2009	Final Contractor Report	

4. TITLE AND SUBTITLE
Coupled Thermo-Electro-Magneto-Elastic Response of Smart Stiffened Panels

5a. CONTRACT NUMBER

5b. GRANT NUMBER

5c. PROGRAM ELEMENT NUMBER

6. AUTHOR(S)
Bednarcyk, Brett, A.; Yarrington, Phillip, W.

5d. PROJECT NUMBER
NCC3-878

5e. TASK NUMBER

5f. WORK UNIT NUMBER
WBS 645846.02.07.03.03.02

7. PERFORMING ORGANIZATION NAME(S) AND ADDRESS(ES)
Ohio Aerospace Institute
22800 Cedar Point Road
Brook Park, Ohio 44142

8. PERFORMING ORGANIZATION REPORT NUMBER
E-16540

9. SPONSORING/MONITORING AGENCY NAME(S) AND ADDRESS(ES)
National Aeronautics and Space Administration
Washington, DC 20546-0001

10. SPONSORING/MONITOR'S ACRONYM(S)
NASA

11. SPONSORING/MONITORING REPORT NUMBER
NASA/CR-2009-215269

12. DISTRIBUTION/AVAILABILITY STATEMENT
Unclassified-Unlimited
Subject Category: 39
Available electronically at http://gltrs.grc.nasa.gov
This publication is available from the NASA Center for AeroSpace Information, 443-757-5802

13. SUPPLEMENTARY NOTES

14. ABSTRACT
This report documents the procedures developed for incorporating smart laminate and panel analysis capabilities within the HyperSizer aerospace structural sizing software package. HyperSizer analyzes stiffened panels composed of arbitrary composite laminates through stiffener homogenization, or "smearing", techniques. The result is an effective constitutive equation for the stiffened panel that is suitable for use in a full vehicle-scale finite element analysis via MSC/NASTRAN. The existing thermo-elastic capabilities of HyperSizer have herein been extended to include coupled thermo-electro-magneto-elastic analysis capabilities. This represents a significant step toward realization of design tools capable of guiding the development of the next generation of smart aerospace structures. Verification results are presented that compare the developed smart HyperSizer capability with an ABAQUS piezoelectric finite element solution for a facesheet-flange combination. These results show good agreement between HyperSizer and ABAQUS, but highlight a limitation of the HyperSizer formulation in that constant electric field components are assumed.

15. SUBJECT TERMS
Smart structures; Panels; Composite structures; Piezoelectricity; Laminates; Smart materials; Structural design; Constitutive equations; Electric fields

16. SECURITY CLASSIFICATION OF:			17. LIMITATION OF ABSTRACT	18. NUMBER OF PAGES	19a. NAME OF RESPONSIBLE PERSON
a. REPORT	b. ABSTRACT	c. THIS PAGE			STI Help Desk (email:help@sti.nasa.gov)
U	U	U	UU	55	19b. TELEPHONE NUMBER *(include area code)* 443-757-5802